Investigation of experimental cell lines and non-invasive online sensor technologies in a 3D bioreactor system for extracorporeal liver support therapy

vorgelegt von
Diplom-Ingenieur
Marco Richter
geb. in Leipzig

Von der Fakultät III – Prozesswissenschaften
der Technischen Universität Berlin
zur Erlangung des akademischen Grades

Doktor der Ingenieurwissenschaften
-Dr.-Ing-

genehmigte Dissertation

Promotionsausschuss:
Vorsitzender: Prof. Dr. Peter Neubauer
Berichter: Prof. Dr. rer. nat. Roland Lauster
Berichter: Dr. vet. med. Katrin Zeilinger
Berichter: Prof. Dr. Jens Kurreck

Tag der wissenschaftlichen Aussprache: 11.07.2016

Berlin 2016

Acknowledgments

The work presented was accomplished during the period of September 2011 till April 2016 at the Bioreactor Group (BCRT, Charité). The studies were performed within the EU project d-Liver, which was funded by the European Community's FP7 Research Framework Programme under the grant agreement number 287596.

I am very grateful to have joined the research group of Dr. Katrin Zeilinger and want to say: "Thank you" that I had the opportunity to contribute to the interesting research of 3D bioreactor technology with the focus on the liver. It made my time in your group very exciting, working in such a field close to the clinical application. I thank you for your guidance, your knowledge and motivation during my work, be it in laboratory issues, writing this thesis or personal matters. The trust and the freedom as well as the encouragement to make own decisions you have given, was what I cherish the most since I believe this formed me to a responsible researcher and will strengthen my further career.

I am very grateful to my colleagues in the group providing a cosy atmosphere in the lab. I admire your motivation, be it your own work involved or the work of somebody else, your cooperativeness and scientific input was outstanding. Additionally the friendly talks during lunch and the fun we had beside work, made going to work an enjoyable part and I miss it already. For the time invested in proof reading I would like to say "Thank you" to Dr. Fanny Knöspel and Nora Freyer. You are the best!

Special thanks I want to say to Dr. Emma Fairhall of Professor Matthew Wright´s group at University Newcastle with whom I performed my first B-13 bioreactor experiments and with her expertise in pancreatic progenitor cells this project mainly resulted in success. She also provided this study with the experimental human B-13 equivalent cell line (H-14), which was investigated during the pilot study using up-scaled clinical bioreactor. Furthermore, I would like to thank Professor Matthew Wright for his scientific advice, his English proofreading and his friendly discussions during project meetings.

I also thank Susanne Tröbs, who performed her Bachelor thesis and her Project work for the Master degree under my supervision. Susanne Tröbs helped to establish multi-parametric sensor monitoring in the analytical-scale bioreactor. She also participated in the upscaling process for the pilot study using HPAC-derived H-14 (genetic modified) cells.

Acknowledgments go to the d-Liver consortium, especially to Herbert Schuck of Fraunhofer IBMT for his expertise in impedance measurement and support during impedance signal analysis during experiments. Likewise, I would like to thank Marie-Line Cosnier and Cédric Goyer of CEA-Leti-France for their support regarding ammonia sensor integration and signal analysis. I would like to thank Stem Cell Systems, especially Frank Schubert for their technical support and scientific input during the project time.

For the kind provision of rat tissue (liver and pancreas) received from Dr. Julia Frühwald of Pharmacelsus I am very grateful.

I would like to thank Professor Roland Lauster for being my doctoral supervisor and for the assessment of this work.

Finally I would like to thank my family for their constant support and motivation fulfilling this task. I would like to dedicate this thesis to my fiancée who has always been at my side at good and bad days during this period. Your encouragement, guidance and also preventing me from getting lost in unnecessary details helped me to bring this work to a success. Thank you so much! You are my role model and I never want to be without you anymore.

Declaration of Authorship

I certify that the work presented here is, to the best of my knowledge and belief, original and the result of my own investigations, except as acknowledged. The present work has not been submitted, either in part or whole, for a degree at this or any other University. Parts of this work have been published under the following titles:

Richter, M., Fairhall, E.A., Hoffmann, S.A., Tröbs, S., Knöspel, F., Probert, P.M.E., Oakley, F., Stroux, A., Wright, M.C., Zeilinger, K. Pancreatic progenitor-derived hepatocytes are viable and functional in a 3D high density bioreactor culture system. Toxicology Research 2016, 5 (**1**), 278-290, DOI: 10.1039/C5TX00187K; http://pubs.rsc.org/en/Content/ArticleLanding/2016/TX/C5TX00187K#!divAbstract.

Richter, M., Tröbs, S., Cosnier, M-L., Schuck, H., Freyer, N., Schubert, F., Wright, M.C., Zeilinger, K. Integration of multi-parametric sensor systems in bioartificial liver support system. 41st Annual Congress of the European Society for Artificial Organs (ESAO), September 17-20 2014, Rom, Italy (Oral presentation).

Richter, M., Fairhall E.A., Hoffmann, S.A., Schubert, F., Wright, M.C., Zeilinger, K. Hepatic trans-differentiation of pancreatic hepatocyte-progenitor cells (B-13) in a 3D high-density culture system. German Association for the study of the Liver (GASL), January 24-25 2014, Tübingen, Germany (Oral presentation).

Richter, M., Fairhall, E.A., Hoffmann, S.A., Frühwald, J., Wright, M.C., Zeilinger, K. Dexamethasone induced hepatic differentiation of rat pancreatic progenitor cells (B-13) in a 3D multi-compartment bioreactor system. European Association for the study of the liver (EASL), April 24-28 2013, Amsterdam, Netherland (Poster).

Berlin, 28. April 2016

Marco Richter

Abstract

Liver transplantation is currently the only successful treatment to cure acute or acute-on-chronic liver failure. However, the number of patients waiting for a donor organ is constantly rising due to scarcity of organ donations. To overcome this bottleneck different bio-artificial liver technologies are under investigation, which may take over functions of the diseased liver until a suitable donor organ can be transplanted or the diseased liver has recovered and regained its functions. A drawback so far is the lack of an effective cell source compensating human liver functions *in vivo* during extracorporeal liver support therapy. To be used in extracorporeal liver support therapy, cells need to be available in sufficient numbers, and they should be of human origin to minimize immunologic complications and safety risks for the patient.

In this study, a novel cell source and sensor-based online monitoring methods were investigated using a multi-compartment hollow-fibre bioreactor technology developed at the Charité in Berlin for application in clinical extracorporeal liver support therapy.

In the first part of the study, the rat pancreatic progenitor cell line (AR42J-B-13) was investigated as a model cell source for use in the bioreactor system. The ability of B-13 cells to trans-differentiate to liver-like cells (B-13/H cells) and the maintenance of hepatic functions were determined by means of metabolic parameters in addition to gene expression and histological analyses. Experiments revealed successful trans-differentiation in the bioreactor system. Bioreactor cultures showed increasing liver-specific functions, namely production of albumin and urea as well as cytochrome P450 activity. In contrast, secretion of amylase, typical for undifferentiated B-13 cells, declined over the culture period. Metabolic observations were confirmed by data from gene expression and protein analysis. Immune histochemical staining showed the expression of hepatic markers (CYP2E1, albumin, CK18, CEBP-β and MRP2) in B-13/H cells after hepatic trans-differentiation in the bioreactor system.

In the second part of the study, the integration of multi-parametric sensors into the bioreactor system was investigated to allow for cell culture surveillance in real-time. For this purpose oxygen and pH sensors (PreSens-Precision Sensing GmbH), as well as ammonia sensors and impedance sensors developed by the cooperation partners CEA-Leti-France and Fraunhofer IBMT, respectively, were integrated in an analytical-scale bioreactor for evaluation. In order to evaluate the ability of sensor-based methods to detect cell injury, the toxic drug methapyrilene was applied to B-13/H cells trans-differentiated in the bioreactor system. Online measurement of ammonia concentrations

showed results comparable to offline values measured in samples from the culture medium. However, further optimisation concerning sterilisation, sensitivity, minimization of noise detection and sensor leakage is needed before using the technology in clinical applications. Impedance measurement enabled safe, sensitive and non-invasive detection of changes in the culture condition with a distinct response to toxic stress. To evaluate the bio-artificial liver system in a clinical setting, primary porcine liver cells (ppL) were investigated in the bioreactor system. As a model for toxic plasma exposure during clinical liver support sessions, the effect of the hepatotoxic drug acetaminophen (APAP) was evaluated. The response of the cells to toxic drug exposure was successfully monitored by sensor-based measurements, confirming the results from B-13/H cultures. Based on the results a procedure for culture prediction and decision-making conceived for extracorporeal liver support in a clinical setting was established.

In the third part of the work, an up-scaled version of the bioreactor system was used in a pilot study to investigate the efficiency of cell culture and sensor-based monitoring in a clinical setting. As a cell source the H-14 cells developed by the cooperation partner Newcastle University were used as an experimental human equivalent of the B-13 cell line. The results of the pilot study indicate the feasibility of sensor-based monitoring during cell culture in the large-scale bioreactor. However, additional work has to be conducted to ensure sufficient cell numbers and to optimize sensor techniques for extracorporeal liver support in clinical application.

In conclusion, the B-13 cell line represents a suitable model cell source in combination with the four-compartment bioreactor system for *in vitro* and clinical research. The integration of non-invasive online sensors enables sensitive culture surveillance and culture prediction. Finally, the genetically modified HPAC cell line H-14 might be a vital step towards the establishment of a human cell source in sufficient quality and quantity for extracorporeal liver support.

Zusammenfassung

Die Lebertransplantation stellt derzeit die einzige kurative Behandlungsmethode bei chronischen und akuten Leberversagen dar. Aufgrund des ständig steigenden Bedarfs bei gleichzeitigem Mangel an Spenderorganen versterben viele Patienten auf der Warteliste für die Transplantation. Dieser Engpass hat dazu geführt, dass verschiedene bioartifizielle Technologien entwickelt wurden, welche die Leberfunktionen temporär übernehmen können, um die Wartezeit bis zur Transplantation zu überbrücken bzw. die regenerative Fähigkeit der Leber bis zu ihrer Genesung zu unterstützen. Eine derzeitige Hürde ist in der Erschließung einer effektiven Zellquelle für die extrakorporale Leberunterstützungstherapie zu sehen. Diese sollte leberspezifische Funktionen ausüben, in ausreichend großen Mengen zur Verfügung stehen und von humanem Ursprung sein, um immunologische Komplikationen in der Klinik zu vermeiden.

In dieser Studie wurden eine neuartige Zellquelle, sowie sensorbasierte Methoden zur Echtzeitüberwachung von Funktionsparametern für die extrakorporale Leberunterstützung in einer an der Charité entwickelten 3D-Hohlfaser-Bioreaktortechnologie untersucht.

Im ersten Teil dieser Arbeit wurde als Modellzellquelle die aus Rattenpankreas stammende Vorläuferzellline AR42J-B-13 hinsichtlich ihrer Transdifferenzierung zu leberähnlichen Zellen (B-13/H Zellen) in dem 3D-Bioreaktorsystem untersucht. Der Differenzierungserfolg und der Erhalt leberspezifischer Funktionen wurden anhand des Metabolismus, der Genexpression und histologischen Analysen bestimmt. Die durchgeführten Experimente zeigten eine erfolgreiche Transdifferenzierung der B-13 Zellen mit einem Anstieg leberähnlicher Funktionen wie Albumin- und Harnstoffproduktion sowie Cytochrom P450-Enzymaktivitäten. Gleichzeitig konnte eine Abnahme der Amylasesekretion, charakteristisch für undifferenzierte B-13 Zellen, nachgewiesen werden. Dies konnte ebenfalls mittels Genexpression und Proteinanalyse bestätigt werden. Immunhistologische Färbungen zeigten eine Expression leberspezifischer Proteine (CYP2E1, Albumin, CK18, CEBP-β und MRP2) in dem Bioreaktorsystem nach erfolgter hepatischer Transdifferenzierung.

Ein weiteres Ziel dieser Studie war die Integrierung eines sensorbasierten Online-Detektionssystems zur Überwachung des Zellverhaltens, sowie deren Funktionalität und Vitalität in der 3D-Bioreaktorkultur. Zu diesem Zweck wurden Sauerstoff- und pH-Sensoren (PreSens-Precision Sensing GmbH) sowie von den Kooperationspartnern CEA-Leti-France und Fraunhofer IBMT entwickelte online Sensoren für Ammoniak-

und Impedanzmessungen in einer Laborvariante des Bioreaktorkultursystems untersucht. Zur Analyse der Effektivität und Sensitivität der Sensoren wurde durch Zugabe der toxischen Substanz Methapyrilen ein Zellstress induziert. Der integrierte Ammoniaksensor zeigte gute Übereinstimmungen mit Werten aus offline gemessenen Proben. Jedoch zeigte sich ein Verbesserungsbedarf für die klinische Anwendung hinsichtlich des Sterilisationsverfahrens, der Sensitivität und der Sensordichtigkeit. Der Impedanzsensor ermöglichte eine sichere, sensitive und nicht-invasive Detektion und konnte die aktuellen Zellkonditionen aufzeigen. Für die Evaluierung des bioartifiziellen Lebersystems unter kliniknahen Bedingungen wurden primäre porzine Leberzellen verwendet. Als Modell für die Perfusion mit toxischem Plasma wurde der Effekt des hepatotoxischen Medikamentes Acetaminophen untersucht. Die induzierte Toxizität konnte erfolgreich mittels integrierter Sensoren identifiziert werden und bestätigte die Ergebnisse der zuvor untersuchten B-13/H Zellkulturen. Auf der Basis der Ergebnisse konnte ein Schema erarbeitet werden, welches eine Prognose über die Kulturqualität im Bioreaktor ermöglicht und im Hinblick auf die klinische Anwendung eine zeitnahe Entscheidung über die klinische Anwendung des Systems ermöglicht.

Im dritten Teil dieser Arbeit wurde eine Pilotstudie zur Evaluierung der Zellkultivierung und der Online-Sensorsysteme in einer Bioreaktorvariante im Klinikmaßstab durchgeführt. Hierfür wurde die experimentelle H-14 Zelllinie verwendet, welche von der Universität Newcastle als humanes Äquivalent für die B-13 Zelllinie generiert wurde. Die Ergebnisse der Pilotstudie zeigten die Machbarkeit einer sensorbasierten Überwachung des Zellverhaltens. Jedoch sind noch weitere Experimente erforderlich, um eine ausreichende Zellmenge für die extrakorporale Anwendung sicherzustellen, sowie die Sensortechnologie zu optimieren.

Die Ergebnisse lassen den Schluss zu, dass B-13 Zellen in Kombination mit dem Vier-Kompartiment Bioreaktorsystem eine geeignete Modellzelllinie für die *in vitro* oder klinische Forschung darstellen. Die Integration nicht-invasiver Online-Sensoren ermöglicht eine sensitive Überwachung der Zellkultur. Die genetisch modifizierte HPAC-Zelllinie H-14 könnte einen wichtigen Schritt zur Generierung einer humanen funktionellen Zellquelle in ausreichender Qualität und Quantität für die Anwendung zur extrakorporalen Leberunterstützung darstellen.

Table of contents

Abbreviations

ACLF	acute-on-chronic liver failure
ALF	acute liver failure
ALT	alanine aminotransferase
AMC-BAL	Academic Medical Centre Bio-artificial Liver Device
APAP	acetaminophen
AST	aspartate aminotransferase
B-13	AR42J-B-13
B-13/H	trans-differentiated B-13 cell showing hepatocyte characteristic
BAL	bio-artificial liver
BLSS	Bio-artificial Liver Support System
BSA	bovine serum albumin
C3A	subclone of the human hepatoma-derived HepG2 cell line
CEA-Leti	Commissariat à l'énergie atomique et aux énergies alternatives – Laboratoire d'Electronique et de Technologie de l'Information
CEBP-β	CCAAT/enhancer-binding protein
CK	cytokeratin
CPS-1	carbamoyl phosphate synthetase
CYP	cytochrome P450
Disp-FTC-HP8-S	disposable optical-chemical flow-through cell for pH measurement
Disp-FTC-PSt3	disposable optical-chemical flow-through cell for oxygen measurement
DMEM	Dulbecco's modified Eagle's medium
EDTA	ethylenediaminetetraacetic acid
EGTA	ethyleneglycol-bis(2-amino-ethylether)-N,N,N',N'-tetraacetic acid
ELAD	extracorporeal liver assist device

ELISA	enzyme-linked immunosorbent assay
EROD	ethoxyresorufin-O-deethylase
EtOH	ethanol
FCS	foetal calf serum
FPSA	fractionated plasma separation and adsorption
Fraunhofer IBMT	Fraunhofer Institut für Biomedizinische Technik
Gal	galactosyltransferase
GCP	good clinical practices
GLDH	glutamate dehydrogenase
GMP	good manufacturing practices
H-14	genetic modified HPAC
HBV	hepatitis B virus
HCC	hepatocellular carcinoma
HCV	hepatitis C virus
HepaRG	cell line derived from a human hepatocellular carcinoma
HepatAssist 2000	extracorporeal bio-artificial liver device
HNF	hepatocyte nuclear factor
HPAC	human pancreatic acinar cells
HRP	horse-radish peroxidase
LAGESO	Landesamt für Gesundheit und Soziales
LDH	lactate dehydrogenase
LED	light-emitting diode
MANOVA	multivariate analysis of variance
MARS®	Molecular Adsorbent Recirculating System
MRP2	multidrug resistance-associated protein 2
NAFLD	non-alcoholic fatty liver disease
NOD/SCID	non-obese diabetic/severe combined immunodeficient
P2HEMA	poly-2-hydroxyethylmethacrylate
PBS	phosphate buffered saline
PCR	polymerase chain reaction

PERV	porcine endogenous retrovirus
ppL	primary porcine liver cells
PVC	polyvinyl chloride
SEM	standard error of the mean
TMB	3,3’,5,5’-tetramethylbenzidine
WNT	signalling pathways of a group of signal transduction pathways

1 Introduction

1.1 Liver injury

The liver is a complex and highly specialized organ of the human body. The liver is not only responsible for the production of proteins, such as albumin, which is a major blood protein, it also takes part in many other metabolic processes, like regulation of amino acids, carbohydrates and fatty acids, necessary for the functionality of the body. Furthermore, the ability to detoxify harmful endogenous substances such as ammonium and to convert exogenous compounds, e.g. drugs or chemicals, in non-toxic metabolites makes this organ unique and vital for the organism. For that reason, liver failure is a life-threatening disease with great impact on mortality. In the United Kingdom, liver disease is among the five most frequent causes for death. Rates increase even further in comparison to other major causes of death.[1] Primary liver cancer and liver cirrhosis are characteristic for liver disease and describe the typical liver pathology at end-stage liver failure.

Primary liver cancer, mainly hepatocellular carcinoma (HCC), is responsible for approx. 47,000 deaths in Europe,[2] and there are approx. 550,000 new patients diagnosed with HCC worldwide every year.[3,4] Liver cirrhosis causes approx. 170,000 deaths per year (1.8% of all deaths) in Europe.[5] Excessive alcohol abuse represents a major risk factor for liver cirrhosis.[6–8] In 2010, a number of 500,000 people worldwide died due to alcoholic cirrhosis, and further 80,000 deaths occurred as a result of alcohol related hepatocellular cancer.[9,10]

Another major cause leading to liver cirrhosis or hepatocellular cancer is infection with hepatitis B virus (HBV) or hepatitis C virus (HCV). Chronic infection with HBV is associated with a 20-30% risk to develop liver cirrhosis[11] and a 10% risk of hepatocellular carcinoma in Europe/USA.[12] Both HBV and HCV remain often undiagnosed for a long time,[13] and HBV was therefore called a “silent killer”.[2,12] While there is to date no causal therapy of HBV infection, an efficient drug therapy for treatment of HCV was recently shown.[14–16] However, despite this breakthrough in HCV therapy, there are still many patients, who have no access to these drugs, or suffer from irreversible liver damage. Other hepatitis virus infections, e.g. hepatitis delta virus coinfection or hepatitis E virus infection cause a more acute form of hepatitis. Compared to chronic HBV infection, patients show early progression to liver cirrhosis, a rapid hepatic decompensation and death, and causal therapy is not possible so far.[17–19]

The enhanced emergence of non-alcoholic fatty liver disease (NAFLD) is mainly caused by the excessive lifestyle in the industrialized countries. Overweight or obesity

are associated with an increased risk of liver steatosis. NAFLD describes the accumulation of liver fat in more than 5% of hepatocytes and is among the most frequent liver diseases in the world.[20] Beginning with steatosis of the organ, steatohepatitis and finally liver cirrhosis may develop in consequence.[21,22] People suffering from diabetes mellitus type 2 are at an increased risk to develop NAFLD, and the combination of both diseases goes along with a more aggressive disease progression compared to patients suffering from NAFLD alone.[23,24]

Less frequent forms of liver diseases include haemochromatosis, autoimmune hepatitis, primary biliary cirrhosis and primary sclerosing cholangitis. These diseases typically show characteristics of chronic liver disease. Some of them, e.g. haemochromatosis show an increasing incidence and the resulting clinical symptoms dramatically reduce the quality of life.[25] Patients suffering from chronic liver disease have a high risk of liver failure, the so called acute-on-chronic liver failure (ACLF), which goes along with encephalopathy progressing towards coma and multiple organ failure.[26] Similar symptoms are observed in acute liver failure (ALF), which can be caused either by drug intoxication, e.g. acetaminophen (Paracetamol) overdosing or by acute viral hepatitis.

Since 1963, when liver transplantation was successfully performed for the first time by Thomas E. Starzl,[27] it became an essential treatment for irreversible ACLF or ALF[28] and has become a routine procedure with survival rates between 83% and 90%.[2,29] In Europe approx. 5,500 liver transplantations are performed per year.[2] However, due to the scarcity of donor organs the number of transplantations is limited.[30,31] The introduction of procedures like split-liver transplantation or living related liver transplantation, accounting for approx. 11% of all procedures today,[2,20,21] cannot overcome organ shortage, which remains the major limitation of liver transplantation. In 2011, a number of 1,199 liver transplantations were performed in Germany, while 1,792 liver disease patients were added to the waiting list,[29] emphasizing the discrepancy between patients in need and available donor organs. Another limitation is the high cost of liver transplantation. According to Milliman *et al.* (2008 & 2014) more than 700,000 US dollars are required for liver transplantation and postoperative treatments in one patient during the first year.[32,33] Thus, there is a rising demand to develop new strategies to overcome these limitations.[2,34] Extracorporeal liver support systems for temporary bridging of the failing liver represent one possible solution to solve these problems. This approach could be used to support the liver function until liver transplantation or until the patient´s own organ recovers, making use of the self-regeneration capacity of the liver. Moreover, complications due to liver failure could be reduced and the quality of life of liver disease patients could be improved by extracorporeal liver support therapy.[35–38] Two different types of extracorporeal liver support systems are available: artificial devices based on chemical-mechanical detoxification of the patient´s blood

plasma, and bio-artificial devices based on liver cell culture in an extracorporeal circuit for plasma detoxification and substitution of metabolic products.

1.2 Artificial liver support

The working principle of artificial liver support systems is the removal of accumulated toxins in the body, which cannot be achieved by the patient's liver anymore due to continuous progression of liver disease or the occurrence of liver failure. The blood plasma of such patients contains high levels of ammonia, fatty acids, conjugated bilirubin and other nitrogenous waste compounds, which are thought to be responsible for the development of life-threatening conditions.[39] Intentions to eliminate these potentially harmful substances resulted in the attempt to filter them out of the system, simulating the filtration ability of the kidney. In 1956 the group of Kiley *et al.* could demonstrate the successful clearance of ammonia in four patients by treating them with haemodialysis. Their positive results further encouraged other researchers to use this separation technique to treat patients suffering from liver failure.[40] The principle of haemodialysis is based on a concentration exchange between two flowing solutions separated by a partially permeable membrane (osmosis). During clinical use, blood of the patient is pumped through the fibres of a dialyzer, whereas a dialysis solution is pumped in opposite direction around the fibres, resulting in a high concentration gradient of the substances contained in blood and dialysis liquid. The walls of the fibres prevent passage of blood cells and large proteins, while they are permeable for smaller and water soluble substances (e.g. urea, ammonia and exogenous toxic compounds). Another possibility to filter toxic substances out of the blood stream is called hemofiltration. Similar to haemodialysis, blood is separated by a partially permeable membrane, but no dialysis solution is used. By adjusting a positive hydrostatic pressure, water including dissolved substances is drained from the blood. Using this procedure, toxic substances are removed by convection, in contrast to diffusion applied for haemodialysis. The so called ultrafiltrate is discarded and liquid volume withdrawn is replaced by a defined substitution solution to ensure a constant blood volume. In hemofiltration also larger solutes are removed via convection which is in contrast to haemodialysis where mostly small molecules are removed due to the slow speed of larger molecules during diffusion. Both principles can be combined to optimise removal of large and small solutes. Despite some positive effects of these mechanical techniques, the clearance of blood from toxins in the case of hepatic failure is still inefficient. The low toxin clearance is owned to the fact that many toxic substances are bound to proteins and only low concentrations of free toxic substances are present in the plasma.[41] Albumin, which is the main protein of human blood plasma, binds a majority of endogenous toxins, e.g. bilirubin or bile acids. It is an important transporter for

endogenous and exogenous substances like intermediates and end products of metabolism and drugs. The accumulation of toxins in the blood leads to organ failure shown in patients suffering from acute hepatic failure.[42,43] Exchanging the toxic plasma with fresh frozen plasma from blood donors could be an alternative option, but its high costs due to the large volume of fresh plasma needed and the risk of infection restrict this method.[44,45] Furthermore, the side-effects of coagulation imbalance and citrate load can be problematic for patients with severe liver failure, if not carefully implemented.[46,47] In order to improve toxin removal from the plasma, albumin dialysis was introduced as an additional method.[48,49] Furthermore, chemical adsorption techniques, e.g. anion exchange chromatography, charcoal or neutral resin filtration, can improve clearance of patient blood containing toxic compounds.[50]

In the following, two artificial liver support systems currently used in clinical application are described, the Molecular Adsorbent Recirculating System (MARS®) and the Fractionated Plasma Separation Adsorption and Dialysis system known as Prometheus®.

1.2.1 MARS®

Since its introduction in 1993 the MARS® device has been used in several clinical studies to temporarily replace the detoxification function of the organ in patients suffering from severe liver disease.[51,52] The device is based on haemodialysis and uses albumin as a scavenger molecule to remove lipophilic toxic compounds, which accumulate in the blood during liver failure.[53,54] Albumin is added to the dialysis solution to compete with toxin-bound albumin in the blood stream.[55] The dialysis solution is regenerated and is used again in a closed loop circle (secondary circuit). Small water-soluble compounds as well as toxins dissociated from albumin binding at the blood site are able to pass through the membrane due to concentration gradients. In the dialysis solution of the secondary circuit toxins are bound due to albumin, while water soluble substances in the secondary circuit are removed via conventional low-flux single pass dialysis. Albumin bound to toxins is regenerated by passing through different adsorbers, e.g. a charcoal and an anion exchange column. Thereafter, albumin solution is reused in the detoxification process until columns are saturated.[49,56–58]

Clinical studies investigating the efficiency of MARS® treatment in patients with ALF or ACLF showed improvement of encephalopathy after removal of albumin-bound toxins as well as improvement of kidney and liver function.[54,59–62] However, a significant effect on the survival rate was not observed.

1.2.2 Prometheus®

Since only unbound fractions of toxins can pass the membranes in the MARS® device, which limits the detoxification of albumin-bound compounds,[63] the Fractionated Plasma

Separation and Adsorption (FPSA) technique evolved in 1999.[63,64] FPSA is combined with haemodialysis in the Prometheus® system introduced by Fresenius Medical Care (Bad Homburg, Germany). Similar to the MARS® device, it is based on pumping the patient´s blood through a dialyser with a partially permeable membrane. The membrane prevents passage of blood cells and larger proteins, like e.g. fibrinogen, but enables albumin and other smaller molecules to enter the dialysis circuit.[65,66] The resulting "fractionated" plasma, which is enriched with albumin-bound toxins, is pumped through a neutral resin filter, followed by an anion exchange chromatography column. Protein-bound toxins are bound to these adsorbers, whereas albumin is regenerated and can be reincorporated in the blood flow. In a second step, water-soluble substances are removed via conventional haemodialysis.

Successful application of the Prometheus® device in patients with acute liver failure in association with multi-organ failure was described by Kramer *et al.* after severe ecstasy/cocaine abuse.[67] Improved clearance of ammonia, known to be closely related to hepatic encephalopathy, and also of bilirubin and bile acids could be demonstrated in patients treated with the Prometheus® device.[68–70] Furthermore a study involving 77 patients suffering from ACLF showed an improvement of serum levels of bilirubin when treated with the Prometheus® system.[71] However, similar to the results from MARS®, the probability of survival was not increased.[52,72]

These results implicate that successful detoxification alone is not sufficient to effectively support liver regeneration. Further liver-specific functions, namely metabolic regulation and protein synthesis, seem to be of great importance to this process too.[52,73]

1.3 Bio-artificial liver support

Cell-based bio-artificial liver support systems offer the option to overcome the limitations of artificial liver support systems by compensating the synthesis of proteins, e.g. albumin or coagulation factors, and regulating carbohydrate, fat and amino acid metabolism, in addition to plasma detoxification.[74]

1.3.1 Cell sources

A critical issue in bio-artificial liver support systems is the cell source and the associated high functional requirements to the cells in a clinical setting: Cells need to be functionally equivalent to human hepatocytes, free of pathogens, non-tumorigenic and they should not evoke immunological side-effects in the patient. In addition, sufficient and flexible cell availability and processing according to GMP/GCP conditions are essential.

Primary human hepatocytes represent the preferred choice of cells for *in vitro* liver research as well as for clinical bio-artificial liver support because they provide the typical functions of the organ. Besides, liver support systems using this cell source would benefit of the biosafety and provision of homologous biologically active substances.[35,75] However, the lack of suitable donor tissue for cell isolation and the occurrence of de-differentiation of the cells *in vitro*, resulting in a loss of hepatic function,[76,77] restrict their use in liver support systems. Hepatocyte proliferation is observed *in vivo* during liver regeneration and growth, but has not yet been achieved under *in vitro* cell culture conditions because they fail to undergo mitosis.[78–81] Primary porcine hepatocytes have the advantage of abundant availability, low cost and well-established isolation methods.[35] However, the metabolic performance of porcine liver cells shows some differences to those of human liver cells due to species-dependent differences in metabolic pathways. In addition, the use of primary porcine liver cells (ppL) is associated with a risk of hypersensitivity reaction due to xenogeneic antigen presentation when using these cells in bio-artificial liver support systems.[82,83] This risk can be minimized using filter techniques to prevent direct contact of immunoglobulins contained in the patient blood with the cells immobilized in the bio-artificial liver device.[84] Use of Gal gene knockout pigs would minimize the probability of xenogenous immune reactions even further.[85] Another risk could be infection with porcine endogenous retrovirus (PERV), although no infection in patients treated with bio-artificial liver support therapy has been reported so far.[86–89]

Established hepatoma cell lines provide an unlimited cell source due to their proliferative ability, but they exhibit altered hepatocyte-specific metabolic functions due to transformation.[26,90–92] The cell line C3A derived from a clone of the HepG2 cell line is to date the only cell line used in clinical trials of liver support systems.[35,92–94] However, this cell line lacks the ability to metabolise ammonia via the urea cycle and therefore shows restrictions in nitrogen elimination.[94] The HepaRG cell line represents another promising cell line for bio-artificial liver support due to its ability to differentiate into hepatocytes and biliary cells when treated with dimethyl-sulfoxide (DMSO).[95] Investigations of this cell line in different bio-artificial bioreactor types showed a number of liver-specific functions of the cells, including ammonia elimination, urea production and cytochrome P450 (CYP) dependent metabolism.[96–99] Although human cell lines are an attractive cell source in extracorporeal liver support because of their abundant availability and easy logistics, safety risks due to possible tumour development by the cells have to be considered, if cells are rinsed into the blood stream of the patient. This is especially dangerous for patients living under immunosuppressive conditions.[39] A suitable precaution would be the usage of filter

techniques to prevent cell transfer into the patient´s blood, which is generally accepted.[92]

Hepatic cells generated from human adult or pluripotent stem cells were proposed to solve the problem of scarce availability of human liver cells.[100,101] In addition, the use of autologous stem cells would prevent immunological complications.[102] However, the functionality of stem cell-derived hepatocytes obtained with current differentiation protocols is not equivalent to that of primary hepatocytes and so they are still insufficient for clinical use in liver support systems.

1.3.2 AR42J-B-13 cell line as an alternative

The liver and the pancreas are closely related in their development, since both tissues are derived from the embryonic endoderm.[103,104] Investigations in rodents revealed that hepatocytes engraft in the pancreas after induced cell damage, e.g. via copper-deficient diet, cadmium exposure[105,106] or overexpression of growth factors, e.g. keratinocyte growth factor.[107] Furthermore, exposure to elevated glucocorticoid concentrations was reported to induce the trans-differentiation of acinar cells into hepatocytes *in vitro*.[108] Glucocorticoids are steroid hormones primarily secreted from the adrenal gland. They are involved in the regulation of multiple metabolic processes, e.g. hepatic gluconeogenesis.[109,110] Short-term administration of glucocorticoids (dexamethasone-21-phosphate) to rats resulted in hepatic marker expression in acinar cells *in vivo* without any damage to the tissue.[111] Furthermore, in a transgenic mouse model trans-differentiation of exocrine pancreas into liver-like tissue by elevated levels of endogenous glucocorticoids was observed describing a pathophysiological process.[112,113] These observations were encouraged by the finding that elevation of glucocorticoids resulted in a transient suppression of WNT3a expression during trans-differentiation of acinar cells into hepatocytes.[114] WNT signalling is known to be involved in liver development and regulation of zonal hepatocyte gene expression in adult liver cells.[115,116]

A similar pathophysiological process can be observed during trans-differentiation of the AR42J-B13 (B-13) cell line to hepatocyte-like cells (B-13/H).[117,118] The B-13 cell line, a subclone isolated from the rat AR42J pancreatic cell line, is related to pancreatic ductal progenitor cells.[76,113,119,120] Upon glucocorticoid treatment, a majority (85 – 95%) of treated B-13 cells exhibited immunoreactivity for hepatocyte markers such as albumin, cytokeratin (CK) 8 and transferrin.[119] Furthermore, expression of hepatic CYP enzymes and oxidative metabolism of testosterone were demonstrated in B-13/H cells.[118,120,121] B-13/H cells remain differentiated for several weeks on plastic substrates in contrast to primary hepatocytes, which rapidly de-differentiate in conventional two-dimensional (2D) culture systems resulting in a loss of liver-specific functions.[76] In

addition, B-13 cells show no growth in soft agar, maintaining anchorage-dependent growth and they respond to factors which prevent uncontrolled cell growth in contrast to other hepatic cell lines (e.g. HepG2). Fairhall *et al.* showed that injection of B-13 cells into NOD/SCID mice did not result in tumour formation, which is an important advantage in potential clinical settings. Cells only engrafted in the pancreas and in the liver of mice, and they trans-differentiated to B-13/H cells in the liver expressing hepatic-specific markers, e.g. CYP2E1.[118] Since B-13 cells rapidly proliferate under standard cell culture conditions and can easily be trans-differentiated by glucocorticoid addition, they provide a renewable, cost-effective source of functional hepatocyte-like cells and could be used in *in vitro* studies such as preclinical drug testing or liver disease research.

The engineering of a human cell line with equivalent characteristics to the B-13 cell line would solve the problem of scarce availability and dysfunction of current cell sources in clinical liver support strategies. In case of successful demonstration of the liver-specific functionality of such a cell line, sufficient functional hepatocytes at low production costs could be generated for bio-artificial liver devices. In addition, results from *in vitro* research could be used to develop new clinical cell transplantation approaches, if the clinical safety of the cells can be shown.

1.3.3 Hollow fibre bioreactor systems and their clinical evaluation

Studies on primary hepatocytes have shown an improved maintenance of cell viability and liver-specific functions like drug metabolism, disposition and toxicity when using models simulating a 3D environment, like e.g. sandwich cultures (reviewed by Swift *et al.* 2010).[122] Especially polarisation of hepatocytes, known to form distinct apical and basolateral domains in native tissue, seems to have a crucial impact on cell viability and function.[123] For that reason models are of interest, which support cell adhesion, cell communication and cell-matrix interaction by simulating the *in vivo* tissue architecture.[92,124–127] Furthermore, nutrient supply, metabolite removal and oxygenation are of major importance to enable long-term maintenance of cell functionality and prevent de-differentiation of the cultured cells. With regard to efficient extracorporeal liver support these systems have to be suitable for hosting and sustaining high cell numbers to ensure sufficient substitution of the failing liver. It is suggested that 150-300 g liver cells are needed to compensate the impaired liver function in patients with ALF.[128,129] This would represent 10-20% of an adult human liver, which contains approx. 1.5×10^{11} hepatocytes.[130] It has to be considered that the cell function in extracorporeal liver devices is not completely the same as that of native liver *in vivo*, due to *in vitro* cell culture conditions and/or use of xenobiotic cells or cell lines. Thus, higher cell numbers would be likely advisable.

A number of different bioreactor configurations were conceived to provide suitable culture conditions and enable a scale-up in a three-dimensional (3D) architecture. The most common bioreactor configurations used for extracorporeal liver support in clinical application are hollow fibre systems.[26,35,37,90,91,131] In most systems, hollow fibres made out of partially permeable membranes are packed in cylindrical columns providing a scaffold as an anchorage for the liver cells.[35,132] The cells are usually seeded outside the fibres in the extra-capillary space and the perfusate (e.g. plasma or blood) is pumped through the capillaries providing nutrient supply and substance mass transfer across the membrane. However, many individual modifications were made to improve bio-artificial performance.[35]

Extracorporeal liver devices used in clinical trials:

The extracorporeal liver assist device (ELAD) developed by Sussman *et al*. (1992)[133] is based on a modified dialysis cartridge. The ELAD uses the human hepatoblastoma cell line C3A, which is grown to confluence in the extra-capillary space of the dialysis cartridge. One cartridge houses approx. 100 g of C3A cells.[93] Up to four cartridges are combined in a single device for extracorporeal liver support treatment. The ultrafiltrate is generated from the blood drawn from the patient and pumped through the lumen of the hollow fibres. Heparin is used to prevent blood coagulation in the system. Glucose and oxygen are added to the recirculation circuit of the ELAD cartridges to provide adequate nutrient and oxygen supply to the immobilized cells. The risk of escaping cells from the ELAD circuit entering the patient blood circuit is prevented using filters prior to the ultrafiltrate entry in patient blood circuit. In clinical applications of ELAD, no acute complications of the liver support therapy such as hemodynamic instability or complement activation were observed.[134] Furthermore, the patient status improved with respect to encephalopathy and patients could be successfully bridged until liver transplantation.[90,93]

Another similar system represents the Bioartificial Liver Support System (BLSS) by Excorp Medical, Inc..[135] In the BLSS primary porcine hepatocytes are mixed with 20% collagen and seeded into the extra-capillary space of the device. Blood of the patient is oxygenized in an oxygenator and pumped through the capillary lumen allowing plasma compounds to diffuse between the blood and the cell compartment. First clinical use of the BLSS showed successful treatment of patients with ALF and demonstrated clinical safety.[88,136] Clinically a reduction in ammonia, lactate and total bilirubin could be achieved.[35,88,137]

Further extracorporeal liver support systems using primary porcine cells are the HepatAssist 2000 and the Academic Medical Centre Bioartificial Liver Device (AMC-BAL). The HepatAssisst 2000 device uses cryopreserved cells, which are seeded in the extra-capillary space of the cartridge and hollow fibres are perfused with patient plasma

following plasma detoxification by a charcoal column.[138] The HepatAssist 2000 device participated in several Phase I clinical trials and was successfully used as bridging device in patients waiting for liver transplantation.[35,139] The neurological status of patients improved[140] and a reduction in ammonia, bilirubin and transaminase levels was achieved during treatment. In a study with 39 patients six patients suffering from ALF, mostly due to acetaminophen (APAP) overdosing, recovered spontaneously after HepatAssist 2000 treatment.[141] Although the survival rate, with regard to entire patient population, was not increased in a randomized trial involving a total of 171 patients, a significant increase in survival was observed in HepatAssist 2000 treated patients suffering from fulminant/sub-fulminant hepatic failure as compared to the control group receiving standard medical treatment.[139]

In the AMC-BAL a nonwoven hydrophilic polyester matrix is spirally wound around a massive core. Primary porcine hepatocytes attach to this matrix in a 3D configuration. Hollow fibres responsible for on-site gas exchange are placed between accrued layers in a longitudinal direction.[142] Plasma pumped through the device has direct contact with the cultured cells providing optimal mass transfer and oxygenation.[35,88] Six patients suffering from ALF were successfully treated with the AMC-BAL device and were transplanted afterwards. Similar to previously described systems the encephalopathy status was improved, and plasma levels of ammonia and bilirubin decreased. Patients included in this study were not detected positive for PERV after extracorporeal liver support treatment.[87,143]

The system developed at the Charité in Berlin is based on a multi-compartment hollow-fibre structure.[144] It consists of three independent capillary systems, which form an interwoven capillary network for counter-current medium perfusion (via two bundles of the capillary systems), and direct oxygenation (via the third bundle). Thus, efficient mass transfer to the cells immobilized in the extra-capillary space (cell compartment) is provided. Thus, a micro-environment is created, which allows for 3D high-density culture of liver cells, mimicking the native environment of the liver with physiological cell-cell contacts and cell communication. The system can be combined with albumin dialysis to reduce the toxin load on cultured cells during extracorporeal liver support application.[35,88,89] The bioreactor system has been successfully tested in clinical extracorporeal liver support settings with primary porcine[145] or human hepatocytes.[26,146] Zeilinger *et al.* (2004) could show that primary liver cells re-organized to neo-tissue with formation of connective tissue by the cells in the bioreactor. Immunohistochemical staining revealed neo-biliary channels and neo-sinusoidal endothelial structures.[147,148] Improved cell regeneration and elevated growth factor expression was observed after perfusing the bioreactor system with acute liver failure plasma during extracorporeal liver support therapy,[148] suggesting that cells cultured in such a device respond to

alterations of the environment. Down-scaled variants of the technology developed for *in vitro* research showed stable maintenance of hepatocyte performances indicating that the technology can be scaled according to individual study designs and requirements.[149] In addition, their suitability for drug metabolism studies was shown.[77,150] *In vivo* like patterns of liver-specific transporter proteins involved in biliary excretion were demonstrated.[77,149,150] Furthermore, previous studies showed stable maintenance of human-relevant CYP enzyme activities when culturing the hepatoma cell line HepaRG in the four-compartment bioreactor system.[97,99]

1.4 Culture surveillance/monitoring of BAL devices

In order to ensure efficient and safe therapeutic application of cell-based extracorporeal liver support devices (BAL), methods and parameters have to be identified that allow evaluation of the quality of the bio-artificial liver system prior to clinical use and during therapeutic application. Parameters suitable to assess the BAL functionality have to provide information on cell integrity and metabolic performance of the culture. In the case of bio-artificial liver support, release rates of intracellular enzymes, e.g. aspartate aminotransferase (AST), alanine aminotransferase (ALT), lactate dehydrogenase (LDH), glutamate dehydrogenase (GLDH), alkaline phosphate, γ-glutamyltransferase and pseudocholinesterase, provide useful information on the cell integrity.[89,136,151–153] Monitoring of glucose production/consumption, lactate production and oxygen consumption give insight into energy metabolism of the cell culture housed in the device.[77,90,93,145,146,150,153] Ammonia elimination, urea production and bilirubin metabolism provide information on specific hepatic functions.[77,90,143,150,152–154] Additional parameters describing liver function are galactose and sorbitol clearance, CYP enzyme activities, albumin production or C-reactive protein release.[77,97,150,152,154]

Monitoring and control of environmental factors that could influence the culture quality are important to allow maintaining standardized and constant conditions for the cells in the bio-artificial liver. The temperature and pH value are crucial to cell viability and have to be maintained on a constant level.[135,138,147] Nutrient supply as well as removal of waste products of cell metabolism has to be controlled.[77,144] In addition, observation of system pressures is needed to prevent exceeding pressure fluctuations, which could influence the cell behaviour in the system.[93,135]

Furthermore, successful integration of non-invasive sensors for monitoring vital culture parameters would improve real-time surveillance of bioreactor cultures and allow for timely intervention. Oxygen measurement can give information about cell activity, energy metabolism and the occurrence of potential bacterial contamination. In addition, it can be used to estimate cell numbers in 3D constructs, provided that data on oxygen consumption of the used cell type are available.[155] Independently of using oxygen as an

evaluation parameter, the used oxygen flow rates have to be adjusted according to the need of cell culture.[135,138]

Impedance measurement describes a non-invasive label-free method for real-time monitoring of cell behaviour in 2D culture. The assay is based on measuring the resistance or capacitance of cells.[156,157] The cell membrane, which separates the cell cytoplasm from the extra-cellular space, is made of a phospholipid bilayer with cholesterol and proteins enclosed. Biological cells are poor electric conductors,[158] showing a resistance to an electrical field reflecting cell conditions. Thus, changes in the cell number and/or cell behaviour are reflected in an altered resistance. The method has been successfully established in the xCELLigence® system (Roche)[159] and was employed in various cell assays characterizing cell stress in response to drug or virus exposure.[157,159–165] Impedance measurement has also successfully used for characterization of cell culture conditions in a 3D environment.[156,166–168] Cell expansion as well as toxic reactions to anti-cancer drug application could be detected in a 3D culture system (perfusion microfluidic chip).[167] In addition, recent investigations using multiplexed 4-terminal impedance measurement revealed successful sensing of HepG2 cell aggregates in spatial location within large 3D gelatine scaffolds.[168]

Ammonia measurement can give information about the cells nitrogen metabolism describing the conversion of ammonia into glutamine and urea. Ammonia concentration can be used as a lead parameter characterising liver function since ammonia clearance represents one of the main aims of extracorporeal liver support application and is known to be closely related to hepatic encephalopathy.[39,68–70]

Several requirements have to be addressed to ensure safety and stability of sensor-based monitoring methods. In particular, biocompatibility of sensors getting in contact with cells and/or culture medium/plasma/blood has to be ensured. Therefore, sensor components have to be suitable for sterilisation with clinically approved sterilisation methods, e.g. ethylene oxide gas sterilisation and/or autoclaving/hot steam sterilisation at 121°C. In case of sensor integration in the BAL device, sensors should be adjustable to the pH-value set range (7.35-7.45) and to the temperature set range (37-39 °C) in the bioreactor circuit. Furthermore, alterations of the culture medium/plasma/blood components due to the sensors have to be excluded.

2 Aims of study

The work performed within this thesis was conducted within the d-LIVER project aiming to provide a bio-artificial liver support system with multi-parametric sensors enhancing the quality of medical treatment and management and to improve the quality of life for patients (see also http://www.D-LIVER.eu/).

Aims of this study were the investigation of experimental cell lines and the integration and evaluation of new non-invasive online sensor technologies in the used 3D bioreactor technology for potential clinical application.

The AR42J-B-13 (B-13) cell line shows potential to be a pioneer cell source for utilisation in extracorporeal liver support. Therefore, the first aim of this study was the evaluation of the trans-differentiation of rat pancreas progenitor cells (B-13 cells) and the maintenance of B-13/H cells in a 2 ml analytical bioreactor. Undifferentiated B-13 cells were trans-differentiated in bioreactors by dexamethasone addition for 8 or 15 days (group B-13T). In addition, to evaluate the maintenance of functional characteristics under 3D culture conditions, pre-differentiated B-13/H cells were cultured in parallel bioreactors over 15 days (group B-13/HP). The efficacy of trans-differentiation and the cell performance were assessed by determination of functional parameters in the bioreactor perfusate, including synthesis of glucose, lactate, urea and albumin. Cytochrome P450 (CYP) 1A1 activity and product conjugation by phase II enzymes were assessed by analysis of ethoxyresorufin metabolism. The reorganization grade of the cells in the bioreactor cell compartment and the distribution pattern of typical hepatocyte markers was analysed by immunofluorescence. In addition, PCR analysis was performed to determine the mRNA expression of liver-typical proteins.

The second aim described in this thesis focused on the investigation of non-invasive sensors integration for surveillance of cell quality and functionality in an extracorporeal liver support system. Therefore, impedance sensors were integrated and tested to give insight into the culture status. In addition, sensors detecting the ammonia level, which is a main clinical indicator for hepatic injury, and also pH and oxygen sensors were evaluated. Initial testing was performed in small-scale experimental bioreactors, using B-13/H cells as a model cell line. The multi-parametric sensor system was evaluated with respect to biocompatibility, comparing results from bioreactor systems containing named sensors with control bioreactors lacking those sensors. Furthermore, the sensitivity and reliability of non-invasive online sensors was compared to standard offline parameters measured daily in bioreactor culture perfusates (e.g. glucose, lactate, urea, albumin, ammonia, ALT, AST, LDH and GLDH). Methapyrilene, which has been

reported to exert a toxic effect on B-13/H cells, was used as a test substance to analyse the effect of toxin exposure and to evaluate potential recovery of cells from toxic stress in the bio-artificial liver (BAL) with incorporated multi-parametric sensors. To evaluate the BAL system in a clinical setting, primary porcine liver cells (ppL) were used due to their abundant availability. As a model for toxic patient plasma exposure to the cells, the effect of the hepatotoxic drug acetaminophen (APAP) was investigated in the bioreactor system.

The third aim of this thesis was to evaluate the use of the tested non-invasive online sensors in a large-scale bioreactor type for potential clinical use. Modifications on sensors were performed to facilitate incorporation into the clinical-scale bioreactor. In a pilot study a human-equivalent cell line to the B-13 cell line, namely the H-14 cell line derived by genetic modification of human pancreatic acinar cells (HPAC) was used in a clinical-scale BAL experiment.

According to the project aims, bioreactor experiments performed in this study are summarized in the schematic illustration shown in Figure 1. The figure shows the three main aims of the study: 1) Evaluation of trans-differentiation of B-13 cells and maintenance of B-13/H cells, 2) Evaluation of non-invasive multi-parametric sensors using B-13/H cells and ppL, and 3) Pilot study: System up-scaling using HPAC-derived H-14 cells. In the outlook, the application perspective for this sensor-based bioreactor technology is shown, using multi-parametric sensors as a decision tool for culture prediction and decision support in clinical extracorporeal liver support.

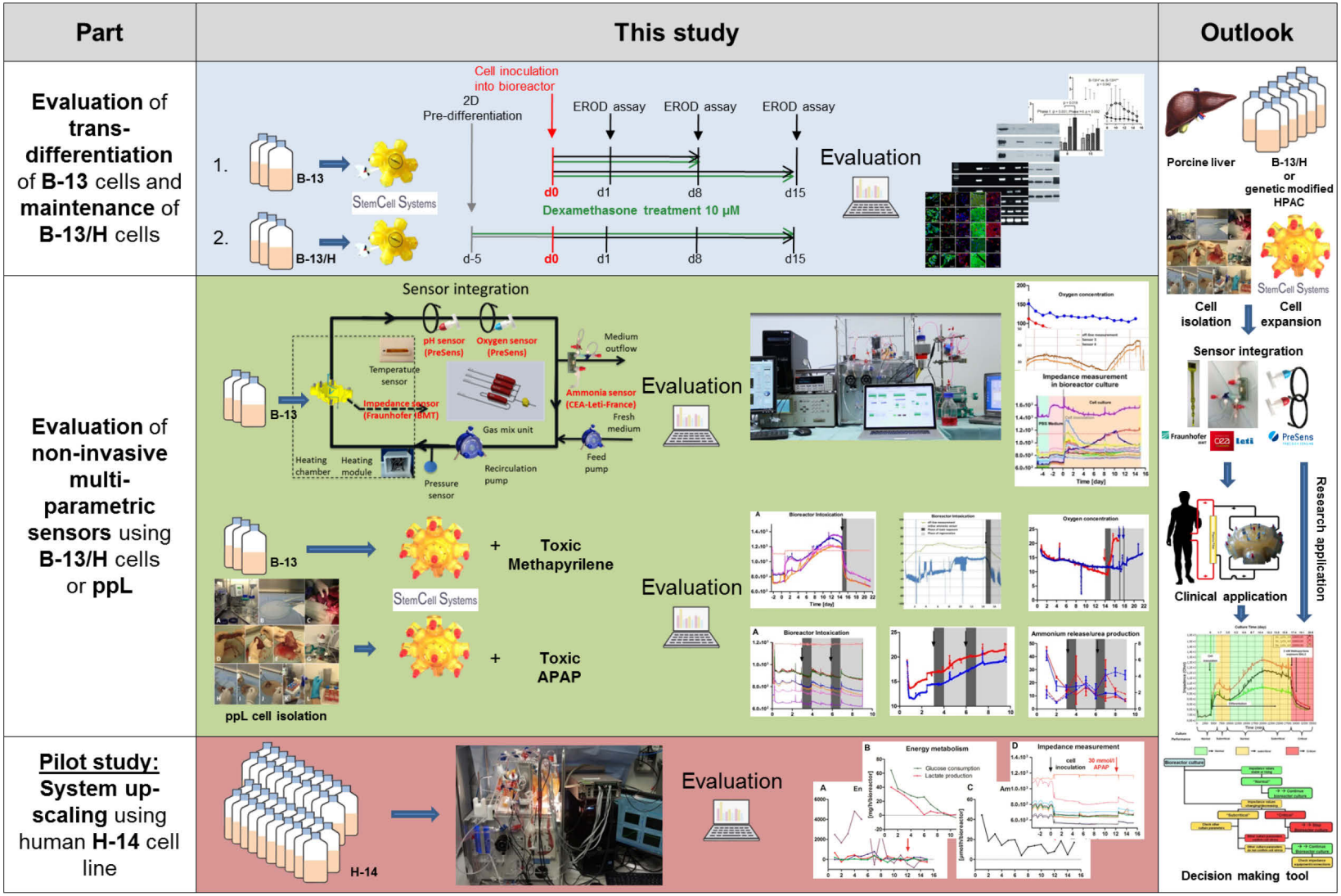

Figure 1: Structure of study.
The figure shows the three main aims of the study, the performed experiments in this study as well as an outlook for *in vitro* or clinical application.

3 Material and Methods

3.1 Materials

3.1.1 Chemicals and solutions

Phosphate buffered saline (PBS) w/o CaMg	Life Technologies, Carlsbad, CA, U.S.
4% paraformaldehyde solution	Herbeta Arzneimittel, Berlin
Aqua Polymount	Polysciences Inc., Warrington, PA, U.S.
Ethanol	Herbeta Arzneimittel
Ethanol absolute	Merck, Darmstadt
Hoechst 33342 Solution	Life Technologies
Hydrochloric acid	Carl Roth, Karlsruhe
Methanol	J.T. Baker, Deventer, Netherlands
ParaClear Intermedium; ProTaqs Clear	Quartett Immunodiagnostika Biotechnologie GmbH, Berlin
Paraffin (pastille)	Merck
Sodium hydroxide solution	Merck
TRIZOL® reagent	Life Technologies
Trypan blue, 0,5% w/v	Biochrom, Berlin

3.1.2 Material for kits and assays

Albumin ELISA

96-well plates, ELISA	Sarstedt, Nümbrecht-Rommelsdorf
Albumin fraction V	Carl Roth
Potassium bicarbonate	Merck
Rat albumin ELISA kit	Biomol GmbH, Hamburg
Sodium chloride	Merck

Sulphuric acid	Sigma-Aldrich, St. Louis, MO, U.S.
TMB substrate	Biomol
TRIZMA Base	Sigma-Aldrich
Tween 20	Merck

Ethoxyresorufin-O-deethylase (EROD) activity assay

96-well plate; Fluoronunc™	Nunc, Roskilde, Denmark
Resorufin	Sigma-Aldrich
Sodium acetate	Sigma-Aldrich
β-glucuronidase/arylsulfatase	Roche, Mannheim

Gene expression analysis

DNA ladder	New England Biolabs® Inc., Ipswich, MA, U.S.
ECL® kit	Life Technologies
Random primer	Promega Corporation, Madison, WI, U.S.

3.1.3 Primary liver cell isolation

The solutions listed in the following table were used for isolation of primary liver cells from resected porcine liver. They were stored at 4°C and used within four weeks after preparation.

Table 1: Compositions of solutions used for primary porcine liver cell isolation.

Compound	Company	Final concentration
Perfusion solution I (pH=7.4)		
Ethylene glycol-bis(2-amino-ethylether)-N,N,N',N'-tetraacetic acid (EGTA)	Sigma-Aldrich	2.4 mmol/l
Hepes	Sigma-Aldrich	10 mmol/l
N-Acetyl-L-cysteine	Carl Roth	1.26 mmol/l
Potassium chloride	Merck	6.7 mmol/l
Sodium chloride	Merck	142 mmol/l
Perfusion solution II (pH=7.6)		
Solution A (pH=7.6)		
Albumin fraction V	Carl Roth	0.5%
Hepes	Sigma-Aldrich	100 mmol/l
Potassium chloride	Merck	6.7 mmol/l
Sodium chloride	Merck	67 mmol/l
Solution B		
Calcium chloride	Sigma-Aldrich	6.3 mmol/l
Stop solution		
PBS w/o CaMg	Life Technologies	80% (v/v)
Foetal calf serum (FCS)	PAA, Dartmouth, MA, U.S.	20% (v/v)

Additional reagents

Collagenase P	Roche
Stainless steel cannula (1464 LL 1A)	Acufrim Ernst Kratz GmbH, Dreieich
Tissue glue (Histoacryl®)	B.Braun, Rubi, Spain
William's E medium, with Glutamax	Life Technologies

3.1.4 Culture media, additives and solutions for cell culture

The culture media listed in the following tables were used for culture of B-13 or B-13/H cells, ppL and H14 cells. They were stored at 4°C and used within two weeks after preparation.

Table 2: Composition of B-13 cell culture medium.

Compound	Company	Final concentration	
		2D culture	3D culture
DMEM high glucose	Biochrom	88% (v/v) Expansion 95.5% (v/v) Experiment	95.5% (v/v)
FCS	PAA	10% (v/v) Expansion 2.5% (v/v) Experiment	2.5% (v/v)
L-Glutamine, 200 mM	Life Technologies	2 mmol/l	
Penicillin/streptomycin, 10,000 U/ml/10,000 µg/ml	Life Technologies	100 U/ml/100 µg/ml	

Table 3: Composition of ppL culture medium.

Compound	Company	Final concentration	
		2D culture	3D culture
Heparmed Vito 143	Biochrom	88% (v/v)	98% (v/v)
FCS	PAA	10% (v/v)	-
Glucagon	Sigma-Aldrich	3µg/l	
Insulin-transferrin-selenium (ITS-G) (100x)	Life Technologies	1% (v/v)	
Penicillin/streptomycin, 10,000 U/ml/10,000 µg/ml	Life Technologies	100 U/ml/100 µg/ml	

Table 4: Composition of H14 cell culture medium.

Compound	Company	Final concentration	
		2D culture	3D culture
DMEM low glucose	Sigma-Aldrich	87.8% (v/v)	65.3% (v/v)
DMEM high glucose	Sigma-Aldrich	-	30% (v/v)
FCS	PAA	10% (v/v)	2.5% (v/v)
Genicitin (G418)	Life Technologies	100 mg/l	
L-Glutamine, 200 mM	Life Technologies	2 mmol/l	
Penicillin/streptomycin, 10,000 U/mL/10,000 µg/mL	Life Technologies	100 U/ml/100 µg/ml	

Table 5: Composition of freezing medium.

Compound	Company	Final concentration
DMSO	Sigma-Aldrich	10% (v/v)
FCS	PAA	90% (v/v)

Additional cell culture supplements and reagents:

Acetaminophen (APAP)	Sigma-Aldrich
Dexamethasone	Sigma-Aldrich
Diclofenac	Sigma-Aldrich
Geneticin G-418 Sulphate	Life Technologies
Methapyrilene HCl	Sigma-Aldrich
Resorufin ethyl ether	Biomol
Trypsin-EDTA (0.05%, 0.02%)	Biochrom
Trypsin-EDTA (0.5%, 10x)	Life Technologies

3.1.5 Cells

B-13 cell line	Kindly provided by Professor M.C. Wright, University of Newcastle, Newcastle upon Tyne, U.K., within the EU project “d-Liver” (Grant agreement no: 287596)
Primary porcine liver cells (ppL)	Isolated from resected liver of house swine. Organ harvesting from pigs for research was performed with approval (T 0130/15) from the Landesamt für Gesundheit und Soziales, Berlin (LAGESO).
H-14 cell line (human glucocorticoid-sensitive pancreatic ductal adenocarcinoma cell line [HPAC] capable of differentiation into hepatocyte-like cells, genetically modified to improve hepatic functionality)	Kindly provided by Professor M.C. Wright, University of Newcastle, Newcastle upon Tyne, U.K., within the EU project “d-Liver” (Grant agreement no: 287596)

3.1.6 Cell culture disposables

6-well plates	Falcon, BD Biosciences, San Jose, CA, U.S.
Cell culture flasks (25 cm^2 - 175 cm^2)	Falcon
Cover slides	Carl Roth
Falcon tubes (15mL/50mL)	BD Biosciences, San Jose, CA, USA
Glass slides; super frost plus	R. Langenbrinck, Emmendingen
Microcentrifuge tubes 1.5/2 ml	Sarstedt
Pipette tips 10-1000 µl	Sarsted
Serological pipettes 1- 50 ml	BD, Franklin Lakes, NJ, U.S.
Whatman™ paper	Schleicher & Schuell GmbH, Dassel

3.1.7 Bioreactors and supplies

Additional tubes, PharMed	Medorex, Nörten-Hardenberg
Bioreactors	Stem Cell Systems, Berlin
Combidyn® adapter	B.Braun, Melsungen
Combi-stopper luer-lock	Fresenius Kabi, Bad Homburg
Disposable cannula	B.Braun
Gas filter	Sartorius, Göttingen
Glass vessel (250mL/500mL)	Schott, Mainz
Liquid filter (0.45 µm)	Sartorius
Perfusion line	B.Braun
Syringes (1-50mL)	B.Braun
Three-way valves	B.Braun
Tubing system	Stem Cell Systems
Vessel lid with integrated luer-lock	Stem Cell Systems

3.1.8 External sensors

Oxygen sensor (Disp-FTC-PSt3-S)	PreSens-Precision Sensing GmbH, Regensburg
pH sensor (Disp-FTC-HP8-S)	PreSens-Precision Sensing GmbH
Ammonium flow-through cell and monitoring device	Kindly provided by CEA-Leti-France, Grenoble, France, within the EU project “d-Liver” (Grant agreement no: 287596)
Impedance sensor foil and measuring device with data analysis software	Kindly provided by Fraunhofer Institut (IBMT), St. Ingbert, within the EU project “d-Liver” (Grant agreement no: 287596)

3.1.9 Gene expression and Western blotting

Table 6: DNA oligonucleotide sequences employed in RT-PCR or PCR genotyping.

Oligo ID	5'-3' sequence	Annealing conditions (35 cycles)	Comments
rmCYP2E1US rmCYP2EDS	TCGACTACAATGACAAGAAGTGT CAAGATTGATGAATCTCTGGATCTC	42°C	Will amplify a rat CYP2E (NM_031543) cDNA sequence of 525bp
rmhGAPDHUS rmhGAPDHDS2	TGACATCAAGAAGGTGGTGAAG TCTTACTCCTTGGAGGCCATGT	50°	Will amplify rat (NM_017008), human (NM_002046) or mouse (NM_008084) glyceraldehyde 3 phosphate dehydrogenase cDNA sequence of 243bp
rCPS1US rCPS1DS	ATACAACGGCACGTGATGAA GCTTAACTAGCAGGCGGATG	55 °C	Will amplify rat CPS (NM_017072.1) cDNA sequence of 390bp
rmAMYLASEUS rmAMYLASEDS	CAAAATGGTTCTCCCAAGGA CAAAATGGTTCTCCCAAGGA	57°C	Will amplify rat pancreatic amylase 2 (NM_031502.1) cDNA sequence of 224bp
rCYP2C11 US rCYP2C11 DS	CTGCCATGGATCCAGTCCTAGTCC TTCCCTCTCCCAAAGCTCTGTCTCC	55°C	Will amplify rat (NM_019184.2) cDNA sequence of 88bp
rAlbumin US rAlbumin DS	CGTCAGAGGATGAAGTGCTC CTTAGCAAGTCTCAGCAGCAG	47°C	Will amplify rat albumin (NM_134326) cDNA sequence sequence of 471bp

3.1.10 Immunohistochemistry

Blocking buffer

PBS w/o CaMg	Life Technologies
+ 3% bovine serum albumin (BSA)	Sigma-Aldrich
+ 2% FCS	PAA

Citrate buffer (pH = 6.0)

Distilled water	
+ 1.8% 0.1 mmol/l citric acid	Merck
+ 8.2% 0.1 mmol/l sodium citrate	Sigma-Aldrich

Table 7: Primary and secondary antibodies used for immunohistochemical analysis of bioreactor tissue.

Antigen	Company	Isotype	Species	Immunogen	Dilution
Primary antibodies					
β-actin	Sigma-Aldrich	Monoclonal IgG	Mouse	Mouse, Rat, Human	WB 1:4000
Albumin	Abcam, Cambridge, U.K.	Polyclonal IgG	Chicken	Mouse, Rat, Human	WB 1:3000 IHC 1:400
Amylase	Abcam	Polyclonal IgG	Rabbit	Mouse, Human	WB 1:3000
	Santa Cruz, Dallas, TX, U.S.	Monoclonal IgG	Mouse	Mouse, Rat, Human	IHC 1:100
CEBP-β	Abcam	Polyclonal IgG	Rabbit	Mouse, Rat, Human	IHC 1:100
CK18	Abcam	Monoclonal IgG	Rabbit	Rat, Human	IHC 1:100
CPS-1	Abcam	Polyclonal IgG	Rabbit	Mouse, Rat	WB 1:2000
CYP2E1	Abcam	Polyclonal IgG	Rabbit	Mouse, Rat, Human	WB 1:5000 IHC 1:100
CYP3A4	Abcam	Polyclonal IgG	Rabbit	Human	WB 1:2000
MRP2	Sigma-Aldrich	Polyclonal IgG	Rabbit	Rat, Human	IHC 1:100

Antigen	Company	Fluorochrome	Species	Immunogen	Dilution
Secondary antibodies					
Anti-Goat HRP 2°	Sigma-Aldrich	-	Rabbit	Goat	1:3000
Anti-Mouse HRP 2°	Dako, Glostrup, Denmark	-	Goat	Mouse	1:3000
Anti-Rabbit HRP 2°	Dako	-	Goat	Rabbit	1:3000
Anti-Mouse	Life Technologies	Alexa Fluor 488	Goat	Mouse	1:1000
Anti-Rabbit	Life Technologies	Alexa Fluor 594	Goat	Rabbit	1:1000
Anti-Chicken	Life Technologies	Alexa Fluor 594	Goat	Chicken	1:1000

3.1.11 Equipment

Bench drill; OPTI B23 Pro	Optimum-Maschinen Germany GmbH, Hallstadt
Bioreactor perfusion device	Stem Cell Systems
Blood gas analyzer; ABL 700 Series	Radiometer, Brønshøj, Denmark
Centrifuge; Varifuge 3.OR	Heraeus Instruments, Hanau
Dako pen wax crayon	Dako, Hamburg
Device for gas valves	Vögtlin Instruments, Aesch, Switzerland
Fluorescence microscope camera; Retiga 2000R	QImaging, Surrey, BC, Canada
Fluorescence microscope lamp; AttoArc, HBO 100 W	Carl Zeiss, Göttingen
Fluorescence microscope; Axiovert 200M	Carl Zeiss
Heat exchange pump	Julabo GmbH, Seelbach
Incubators; Cytoperm CO_2 /O_2	Heraeus Instruments GmbH
Laminar air flow; HB2448	Heraeus Instruments GmbH
Light microscope camera; MicroPublisher 3.3 RTV	QImaging
Light microscope; Axiovert 40 CFL	Carl Zeiss, Jena
Microcentrifuge; 5417R	Eppendorf, Hamburg
Microtome; Microm HM355s	Microm-International, Walldorf
Paraffin embedding center AP 250	Microm-International
Perfusor; Secura FT	B.Braun
Plate-reading fluorometer; FumostarOptima	BMG Labtech, Ortenberg
Realtime cycler; Mastercycler ep Realplex 2	Eppendorf
Spectrophotometer; Nanodrop	Thermo Fisher Scientific, Waltham, MA, USA
Water bath	Julabo GmbH

3.1.12 Software

Get red-y 5	Vögtlin Instruments
Image Pro Plus	Media Cybernetics, Silver Spring, U.S.
LabView	National Instruments Germany GmbH, München
MATLAB	MathWorks, Natick, MA, U.S.
GraphPad Prism 5.0	GraphPad Software, San Diego, CA, U.S.
QCapture Pro 5.1	QImaging, Surrey, BC, Canada
SPSS Statistics 21	IBM Corporation, Armonk, NY, U.S.

3.2 Methods

3.2.1 2D culture of liver cell types used in the study

B-13, B-13/H, H14 and ppL cultures were maintained at 37°C in a humidified incubator in a mixture of 5% CO_2 and 95% air, unless otherwise indicated.

3.2.1.1 Expansion and trans-differentiation of B-13 cells in 2D culture

For cell expansion a number of 5×10^6 B-13 cells were seeded in 175 cm^2 cell culture flasks. Medium exchange was performed every second day using culture medium described in Table 2. Cells were passaged 1:5 to 1:10 when culture confluency reached 70-80%. For passaging, cells were trypsinized with 0.05% trypsin for 5-7 min at 37°C after rinsing once with PBS. Cells were frozen in appropriate aliquots using medium described in Table 5.

For experimental investigations a number of $0.75\text{-}1\times10^6$ B-13 cells were seeded in one well of a 6-well culture plate, respectively, and were maintained with "Experiment" medium Table 2, unless other indicated. Dexamethasone was added at a concentration of 10 µmol/l to trans-differentiate B-13 cells to liver-like B-13/H cells.

When using trans-differentiated B-13/H cells for bioreactor experiments 10×10^6 B-13 cells were seeded and cultured for 5 days in 175 cm^2 cell culture flasks using "Expansion" medium (Table 2) adjusted with 10 µM dexamethasone.

3.2.1.2 Expansion and trans-differentiation of H-14 cells in 2D culture

For cell expansion a number of $1.5\text{-}5\times10^6$ H-14 cells were seeded in 175 cm^2 cell culture flasks. Medium exchange was performed every second day using culture medium described in Table 4 and cells were passaged 1:10 when culture confluency reached 70-80%. For passaging, cells were trypsinized with 0.5% trypsin for 5-7 min at 37°C after rinsing twice with PBS. Cells were frozen in appropriate aliquots using medium described in Table 5. To trans-differentiate H-14 cells into liver-like cells 10 µmol/l dexamethasone were added to the culture medium.

3.2.1.3 Isolation of primary porcine liver cells via collagenase P perfusion

Cells were isolated from fresh porcine livers and used for characterization of the cell response to toxic stress using multi-parametric sensors.

The isolation procedure was performed according to primary human liver isolation protocols previously described.[169,170] Prior to cell isolation required materials and solutions were prepared. To start isolation the water bath with temperature control (set to 39°C), an empty glass vessel with funnel and a glass vessel with "Perfusion solution I" (Table 1) were placed under the sterile bench (Figure 2A). The working area was covered with a sterile drape sheet, and a glass petri dish, sterile compresses, a forceps, a scalpel and stainless steel cannulas for perfusion were placed on the drape sheet (Figure

2B). A piece of liver capsule was taken from the organ (Figure 2C) and stored in sterile 4°C cold Williams E medium for the transport from animal experimentation facilities to the laboratory. In the next step the resection area was examined to identify large vessels and bile ducts for cannulation (Figure 2D). Cannulas were fixed in large vessels using Histoacryl® tissue glue. To ensure optimal perfusion remaining vessels were closed with tissue glue (Figure 2E). Tissue perfusion was initiated using "Perfusion solution I" (Table 1) containing EGTA to remove blood and temperate the liver tissue. Perfusion with a volume of 400-500 ml "Perfusion solution I" over approx. 30 min was required to rinse out remaining blood. For collagen P digestion 100 mg of the enzyme were dissolved in 50 ml "Perfusion solution II" and 50 ml "Stop solution" and conducted through a sterile filter. The solution was kept on a temperature of 38°C to ensure sufficient enzyme activity. To reduce the enzyme amount required, the perfusion setup was changed to a recirculating mode. Emerged perfusate was captured in a glass vessel and re-perfused through the liver tissue (Figure 2F-G). Enzyme perfusion was terminated as soon as the liver deformed and did not regenerate when putting pressure to it, which was attained mostly after 10-11 min. Thereafter the liver piece was placed in a glass petri dish containing ice-cold "Stop solution" (Table 1) to inactivate collagenase P activity and prevent exceeding digestion. To open the liver capsule the liver tissue was cut in halves using scalpel and forceps, and liver cells were shaken out carefully in "Stop solution" (Figure 2H-J). The obtained cell solution was collected in 50 ml Falcon tubes using the funnel containing a compress to remove tissue debris. After a centrifugation step (5 min with 50 g at 4°C) performed to remove cell debris the cell pellet was carefully resuspended in "2D culture" medium (4°C) described in Table 3 (Figure 2K-L). The cell number and viability were assed using trypan blue (diluted 1:4 in PBS) and a Neubauer cell counter chamber. Thereafter the cells were prepared for 2D and/or bioreactor experiments.

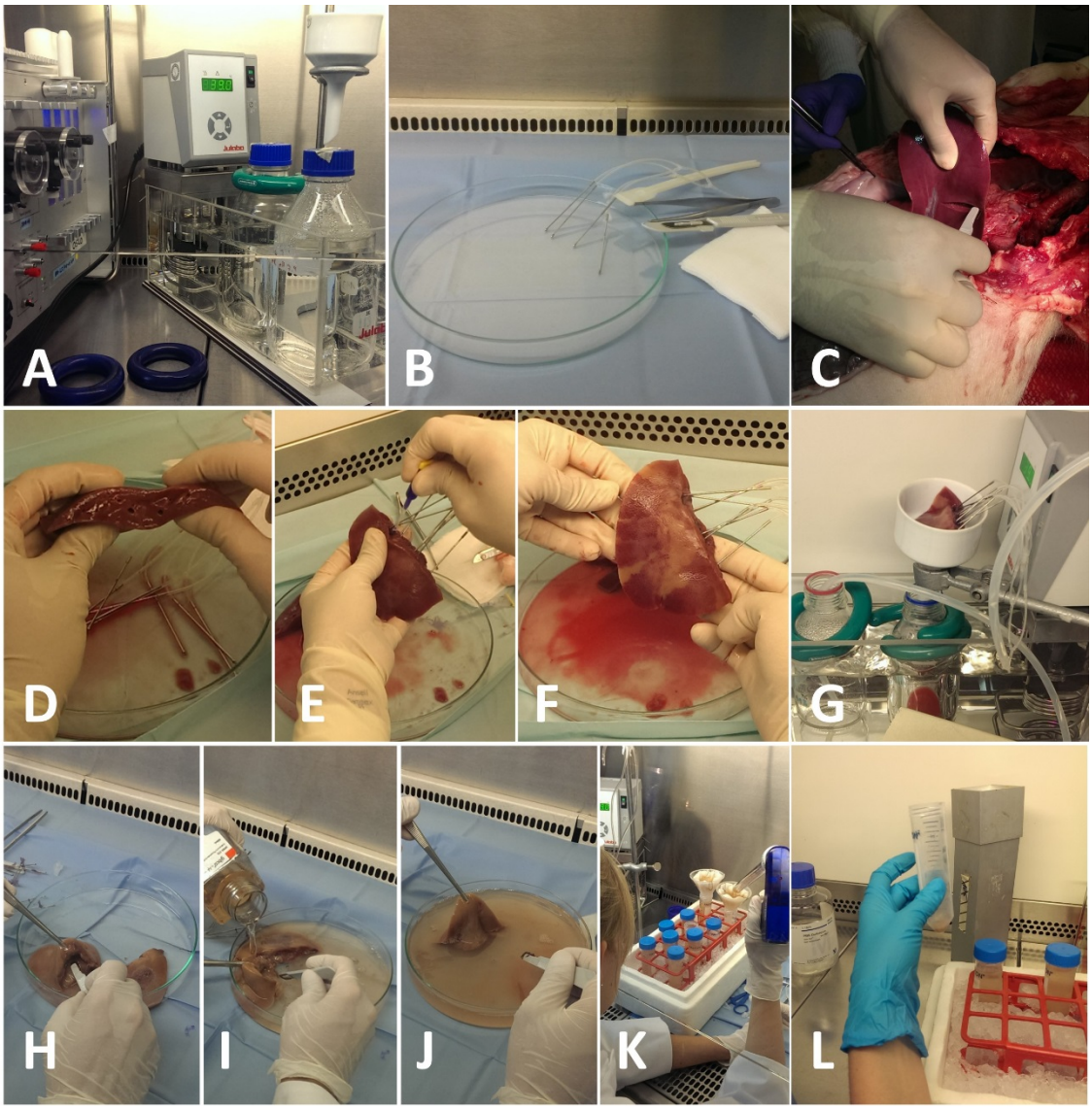

Figure 2: Procedure of primary porcine liver cell isolation using collagenase P perfusion. (A-B) Preparation of isolation equipment, (C) Liver capsule resection, (D-F) Fixation of cannula in vessels and bile ducts, (G) Perfusion of liver tissue with perfusion solutions, (H-J) Opening of liver capsule and cell harvesting, (K-L) Resuspension of obtained cell pellet.

3.2.1.4 Primary porcine liver cell 2D culture and toxicity testing

For experimental investigation freshly isolated ppL (see 3.2.1.3) were seeded into 6-well culture plates using culture medium (see Table 3). Prior to cell seeding, wells were coated with rat-tail collagen (1:100) for at least 30 min at room temperature. Thereafter the collagen solution was aspirated and a number of 2×10^6 cells were seeded in each well of a 6-well culture plate. After four hours the medium was exchanged by fresh medium to remove not attached or dead cells. A medium exchange was conducted every day and culture parameters (lactate and ammonia) were analysed in culture supernatants.

In order to induce different grades of stress, APAP or diclofenac were applied at three different concentrations to the cell culture. APAP was applied at 5, 10 or 30 mmol/l, and diclofenac at 100, 300 or 1000 µmol/l. Toxic stress was maintained for six days by daily medium exchange using fresh drug-containing culture medium. Each day culture parameters (lactate and ammonia) were analysed in supernatants.

3.2.2 3D cell culture model

For 3D liver culture a hollow fibre bioreactor technology developed in the group was used.[144]

3.2.2.1 Bioreactor technology and set up

The bioreactor is composed of four compartments to accomplish efficient mass exchange in cell culture. Two different types of hollow fibres are used, i) medium bearing hollow fibres made of polyether sulfone (MicroPRS® TF10, Membrana, Wuppertal, Germany) and ii) hydrophobic oxygenation hollow fibres (Mitsubishi MHF200TL, Mitsubishi Rayon, Tokyo, Japan). These are arranged in interwoven layers forming a 3D network enclosing the fourth compartment (cell compartment) as shown in Figure 3A. The capillary bundles are set in defined angles for efficient counter-cross medium perfusion with low mass gradients (Table 8). Additionally internal oxygenation through hydrophobic hollow fibres provides a large surface area for gas exchange and avoids oxygen gradients within the medium flow. Cells are located in the extra-capillary space enclosed by a polyurethane housing (Figure 3B). Cells are inoculated via silicone tubes into the cell compartment.

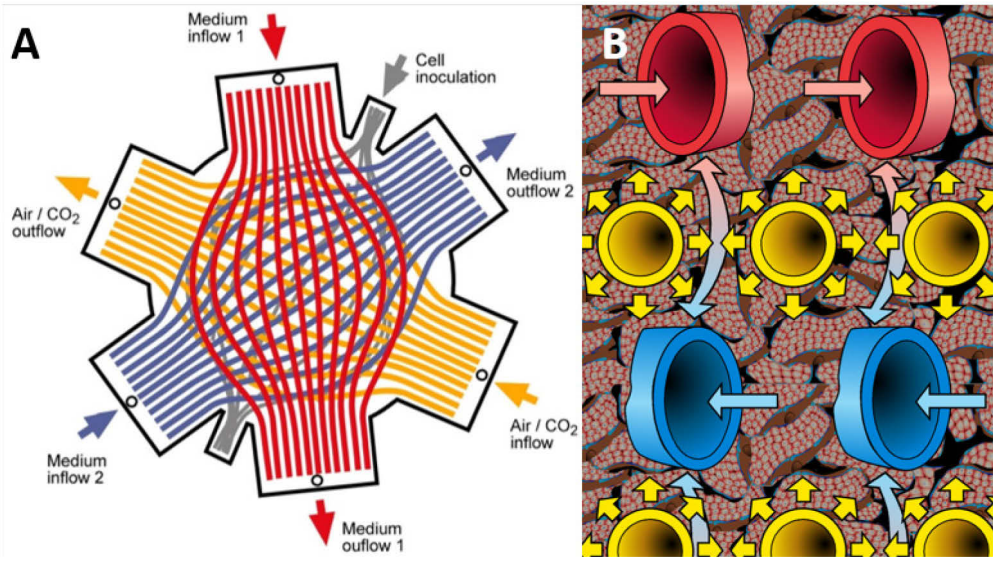

Figure 3: Architecture of 3D multi-compartment bioreactor.
(A) Illustration of the bioreactor showing the capillary structure in the bioreactor with two independent bundles of hollow fibre membranes serving for counter-current medium perfusion (blue and red) and an additional capillary system for integral oxygenation (yellow). (B) Illustration of cells located in the extra-capillary space.

In this study three different bioreactor types varying in cell compartment volume and surface area were used (Figure 4). Technical information for two analytical-scale bioreactors with 2 ml or 8 ml compartment volume and a clinical-scale bioreactor with 800 ml compartment volume are shown in Table 8.

Figure 4: Bioreactor used for 3D-cultivation.
Differently sized Bioreactors (from left to right: 800 ml clinical-scale, 8 ml analytical-scale and 2 ml analytical-scale) in front of the perfusion device for 3D-bioreactor operation (Stem Cell Systems). The device includes a heating chamber, a gas mixing unit and pumps for medium recirculation and fresh medium substitution. Additionally ports required for connection of optical-chemical oxygen and pH sensors (PreSens-Precision Sensing GmbH) are mounted. Perfusion parameters are regulated via labView software through an integrated PC.

Table 8: Technical properties of differently sized types of 3D multi-compartment bioreactors.

	Analytical-scale bioreactor (2 ml)	Analytical-scale bioreactor (8 ml)	Clinical-scale bioreactor (800 ml)
Technical properties			
Number of layers	40	56	166
Number of medium capillaries	500	1,020	8,430
Number of gas capillaries	600	1,380	16,530
Cell compartment volume (ml)	~2	~8	~800
Total system volume, including the tubing circuit (ml)	~20	~40	~1,300
Surface area (cm^2)	293	986	4.48×10^4
Angel between capillary bundles (Medium I-Medium II)	45°	45°	60°
Angel between capillary bundles (Medium I/II-Gas)	60°	45° and 90°	60°
Integrated impedance sensors	no	yes 3 sensor foils	yes 6 sensor foils
Integrated pH sensor	no	yes	yes
Integrated oxygen sensor	no	yes	yes
Integrated ammonia sensor	no	yes	yes

3.2.2.2 Bioreactor perfusion circuit

Hollow fibre bundles and inoculation tubes are connected via luer-lock connectors with the tubing system, which is operated in a special perfusion device. The tubing system is made out of tygon 2275. It consists of a recirculation circuit to ensure accumulation of substances produced and needed by cells and a feed-outflow system for provision of fresh medium and removal of used medium. The tubing system contains clamps for changing the perfusion modes, bubble traps to avoid gas import into the medium capillaries, pressure measurement lines and three-way-valves for sample collection. Bioreactors are placed in the heating chamber of the perfusion device (Figure 4) and maintained at a constant temperature of 37°C via sensor-based electronic temperature control. Medium flow rates are adjusted via roller pumps. Pressure sensors allow for monitoring of system pressures, and pump flow is automatically stopped if the system pressure increases above set system values. Gas influx is adjusted using electronically regulated gas valves for analytical-scale bioreactors (2 ml and 8 ml). For clinical

bioreactor operation gas supply is provided via manually controlled rotameters for air and CO_2.

3.2.2.3 Sensor integration

In some experiments, optical-chemical sensors for oxygen and pH (PreSens-Precision Sensing GmbH) were integrated into the recirculation tubing line, and ammonia sensors, provided by CEA-Leti-France, Grenoble France were mounted in the outlet line. Signals were detected via polymer optical fibres between sensors and the readout unit of the perfusion device for oxygen and pH monitoring or via electrical plugs for ammonia monitoring.

In case of oxygen or pH sensor integration (Figure 5A), sensors consist of a flow-through cell with an optical-chemical polymer layer placed inside allowing direct contact with the culture perfusate. This layer is excitable by the blue LED array and interacts with the components of the perfusate. The flow-through cells are connected to the transmitter via an optical fibre, which was carefully placed into the T-connector tube of the flow-through cell (Figure 5B). Afterwards sensors were connected to the perfusion device (Figure 5C). The pH or the oxygen concentration was monitored via dual lifetime referenced fluorometry,[171], which enables internally referenced measurements. Intensity changes were detected by a combination of different fluorescent dyes in the time domain. Calibration values for pH and oxygen sensors were set in the calibration mask of labView software prior use.

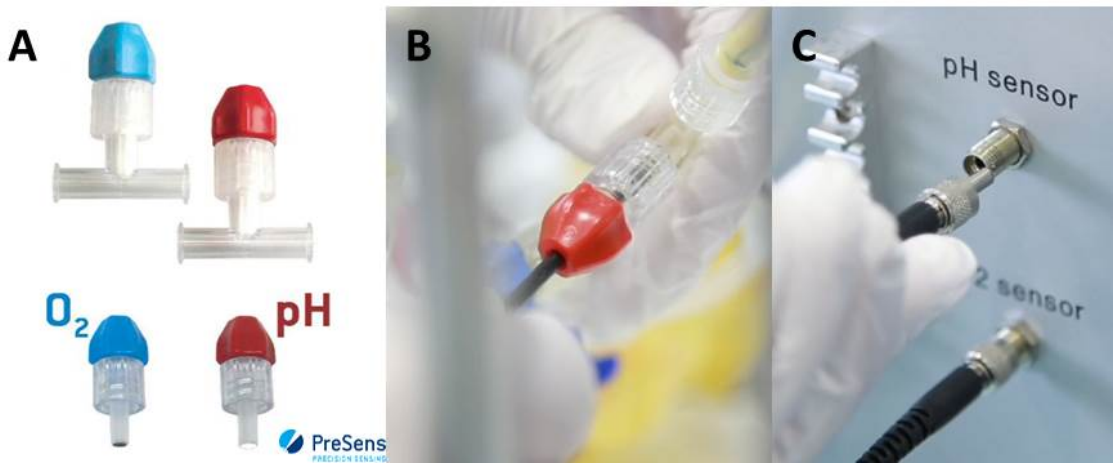

Figure 5: Online sensors for oxygen and pH measurement in the culture perfusate.
(A) Optical-chemical flow-through cell sensors (PreSens-Precision Sensing GmbH) for oxygen and pH. (B) Connecting the flow-through cell with optical fibres for signal detection. (C) Connecting optical-chemical sensors via optical fibres with readout units integrated in the perfusion device.

Online sensors to detect changes of ammonia concentrations in the culture perfusate were placed in the outlet line of the tubing system to minimize the risk of microbial contamination, since sterilization of sensors without harming them was only possible

with 70% EtOH. As shown in Figure 6 the sensor construct for ammonia consisted of two measurement chambers, with one chamber being flushed with medium leaving the bioreactor and the second camber being flushed with fresh medium serving as a reference for measured ammonia concentrations in the bioreactor perfusate. Both chambers housed cone sensors for ammonia measurement. The sensor consisted of a polyvinyl chloride (PVC) cavity containing an internal electrolyte solution and a working electrode made of chlorinated silver wire. The cavity was sealed with an ammonium sensitive membrane, which stays in contact with the culture medium in the chamber for measurement of the electric potential. To avoid air entry into the chambers, which could disturb detection of ammonia, bubble traps were placed in front of measurement chambers. Both chambers were connected via tubes for measurement and join the waste line. Sensors were connected with the read-out device via electrical plugs.

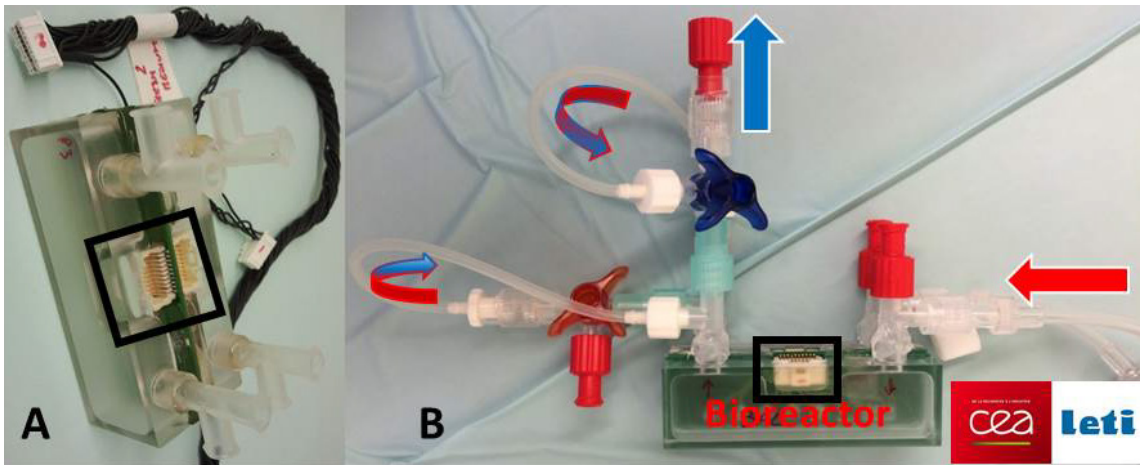

Figure 6: Online sensor for ammonia measurement in the culture perfusate (CEA-Leti-France).
(A) The ammonia sensor consists of two medium chambers. One of these is flushed with bioreactor perfusate and the second one with fresh medium serving as a reference. (B) Bioreactor perfusate and fresh medium is flushed through the chambers after passing bubble traps to avoid air bubbles on ammonium sensitive membranes (red arrow). Both chambers are connected via tubes for measurement of the reference potential (red-blue arrows). Both outlets of measurement chambers join the waste line (blue arrow). Electrical plugs are introduced into corresponding electrical sockets (black square).

Further, in some experiments foil-based impedance sensors, provided by the Fraunhofer IBMT were integrated into the cell compartment of the 8 ml analytical-scale or 800 ml clinical-scale bioreactors by the manufacturer (Stem Cell Systems). Sensor foils are made of polyimide covered by a platinum electrode array where impedance is measured between two electrodes each (channel). The impedance describes the electric resistance to the set voltage, which depends on the frequency. Cells inoculated into the bioreactor show natural poor conductor ability due to their composition and force changes in impedance measurement when attaching to sensor electrodes and therefore offer a resistance. Three sensor foils containing eight sensor points each were integrated in one

8 ml analytical-scale bioreactor as shown in Figure 7A-B, and six sensor foils containing eight sensor points each were placed vertically in an angle of 60° to each other in the cell compartment of the 800 ml clinical-scale bioreactor (Figure 7C). Impedance sensors were carefully connected with the adapter board. Therefore the sensor foils were inserted into the connector and fixed. By fastening the adapter board to metal angles the sensor construct was hold in place to avoid tensile stress to the sensor foil. The flat ribbon cable, which connects the adapter board with the Multiplexer/Switch, was stabilized with a cable relief to avoid broken solder joints on the adapter board Figure 7D.

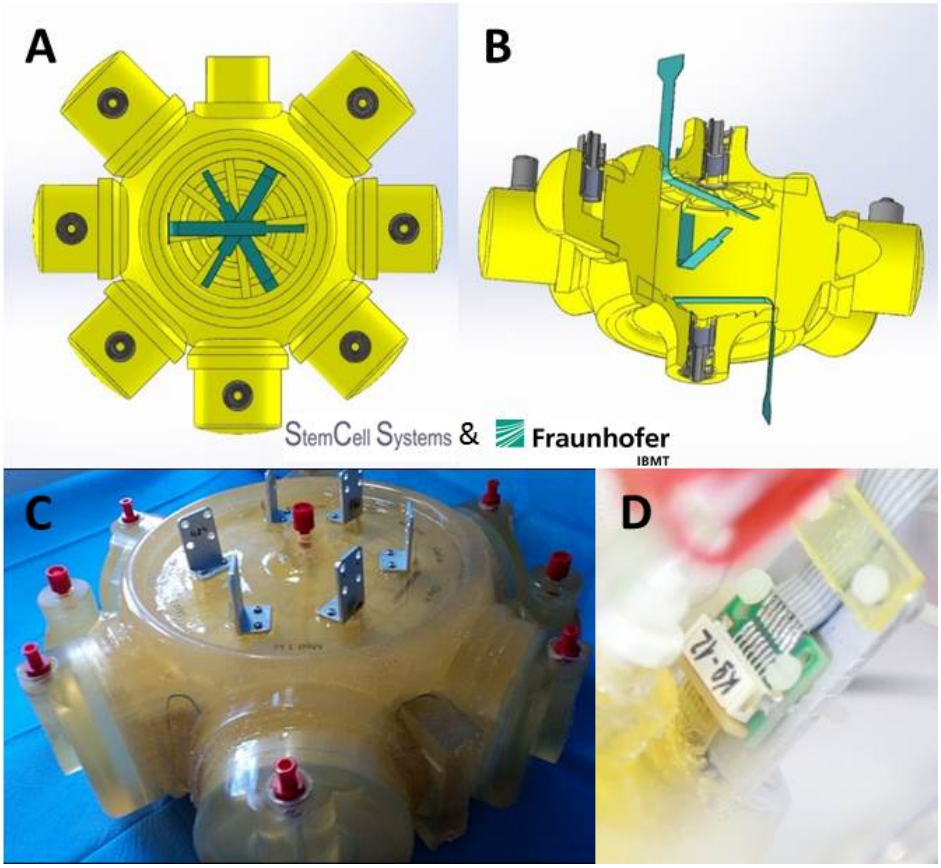

Figure 7: Foil-based impedance sensors located in the cell compartment of bioreactors.
(A-B) Localisation and arrangement of sensor foils in the cell compartment of the 8 ml analytical-scale bioreactor. (C) Localisation and arrangement of sensor foils in the cell compartment of the 800 ml clinical-scale bioreactor. (D) Fixation of sensor foil-adapter board construct to metal angle on bioreactor shell.

Readout units for oxygen and pH measurement were integrated in the perfusion device. For ammonia and impedance measurement external detection devices in combination with data analysis software provided by the cooperation partners CEA-Leti-France and Fraunhofer IBMT were used. The set-up and assembly of the bioreactor culture system with flexible variation in bioreactor-scale and online sensor integration is shown in Figure 8.

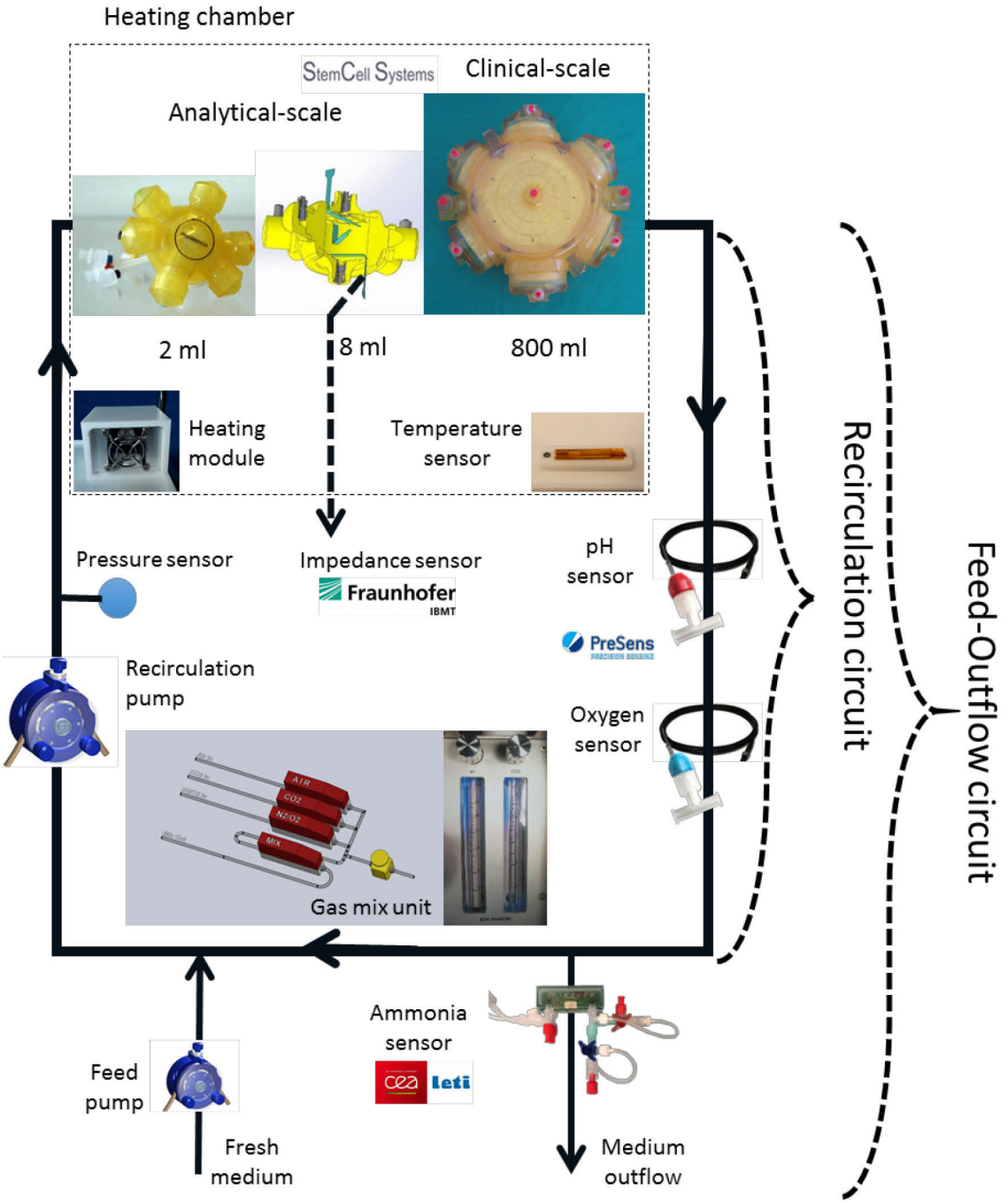

Figure 8: Set up and architecture of bioreactor culture system.
Tubing system consists of a recirculation and a feed-outflow circuit where medium flow rates are controlled via roller pumps. Different variance of bioreactor-scale can be placed in heating chamber, where heating module is controlled via temperature sensor. An electronic gas mixing unit is used for fumigation. Bioreactor culture system can be equipped with i) impedance sensor foils (Fraunhofer IBMT) mounted in the cell compartment, ii) optical-chemical sensors for oxygen or pH (PreSens-Precision Sensing GmbH) mounted in the recirculation circuit or iii) ammonia sensor (CEA-Leti-France) mounted in the outlet line of the feed-outflow circuit.

3.2.3 3D bioreactor culture of liver cell types used in the study

B-13, B-13/H, H14 cells or ppL were maintained in bioreactors at 37°C and using a gas mixture of 5% CO_2 and 95% air, unless otherwise indicated. In some experiments, online sensors were integrated into bioreactors as previously described. Bioreactors and tubing systems were exposed to formaldehyde gas (60°C) for sterilisation. Before starting bioreactor experiments the assembled bioreactor system was flushed with PBS for at least two days at room temperature to eliminate possible residues from manufacturing and sterilisation. Prior to cell inoculation PBS was exchanged with the required culture medium and the heating chamber was heated up to 37°C. Values of pH were measured in daily samples (3.2.4.2) or via online pH sensors (3.2.4.3). The concentration of CO_2 in the supplied gas mixture was adjusted, if required, to maintain the pH between 7.2 and 7.4. Table 9 shows medium and gas flow rates required for different types of bioreactors used in this study. Bioreactors can be operated in different perfusion modes according to study requirements: i) standard perfusion mode (medium recirculation with continuous feed and medium removal), ii) closed perfusion mode (medium recirculation without feed and medium removal) and iii) single-pass perfusion (feed and medium removal without medium recirculation).

Table 9: Perfusion parameters used for 3D-bioreactor culture

	Analytical-scale bioreactor (2 ml)	Analytical-scale bioreactor (8 ml)	Clinical-scale bioreactor (800 ml)
Perfusion parameters			
Recirculation rate (ml/min)	10	20	250
Medium feed rate (ml/h)	2	6 (B-13/H, ppL during the first 24 h of culture) 2 (ppL after the first 24h of culture)	20-50 (in dependence of glucose consumption rates)
Gas flow rate (ml/min)	20	40	500

3.2.3.1 Trans-differentiation of B-13 cells and maintenance of B-13/H cells in 2 ml and 8 ml analytical-scale bioreactors

In this study, the trans-differentiation of B-13 cells into hepatocyte-like cells (B-13/H) and their functional performance in the bioreactor culture system was investigated. In the first approach (B-13/HT) a number of 4×10^7 undifferentiated B-13 cells were inoculated into the 2 ml analytical bioreactor. Bioreactors were perfused with culture medium (see Table 2). After 24 hours of culture an EROD assay was performed (3.2.4.4), followed by treatment with 10 µmol/l dexamethasone to initiate trans-differentiation to B-13/H cells. The culture was continued over 15 days in the presence

of dexamethasone. The EROD assay was repeated on day 8 and 15 of culture. To evaluate the maintenance of functional characteristics under 3D culture conditions, trans-differentiated B-13/H cells were inoculated and cultured in parallel bioreactors over 15 days (second approach: B-13/HP). Therefore 1×10^8 differentiated B-13/H cells were inoculated into the bioreactor system. The cells were then treated with 10 µmol/l dexamethasone and maintained for 15 days. On day 1, 8 and 15 of culture, an EROD assay was performed (3.2.4.4). Culture parameters were analysed daily in samples from the bioreactor perfusate (3.2.4.2). Upon termination of the bioreactor cultures, cell material for protein and RNA analysis was withdrawn from the cell compartment by drilling it open. For RNA analysis, cells were re-suspended in TRIZOL, while cells for Western blotting were used without further processing (3.2.4.5). For immunohistochemistry (3.2.4.6), cell material (including capillary layers) was fixed in 4% formaldehyde buffer, dehydrated and embedded in paraffin.

To investigate the efficacy of multi-parametric online sensors 8 ml analytical-scale bioreactors were used. A number of 2×10^8 undifferentiated B-13 cells were inoculated into the cell compartment of 8 ml bioreactors. On day 1, 8 and 15 of culture, and EROD assay was performed (3.2.4.4). After the first EROD assay the culture medium was supplemented with 10 µmol/l dexamethasone to initiate trans-differentiation to B-13/H cells. Sample taking and processing for analysis of culture parameters and immunohistochemistry analysis was performed as described above.

3.2.3.2 Methapyrilene application to trans-differentiated B-13 cells in 8 ml analytical-scale bioreactors

To investigate the effect of methapyrilene exposure in trans-differentiated B-13 cell (B-13/H) cultures, two 8 ml analytical-scale bioreactors were inoculated with B-13 cells as previously described in 3.2.3.1. Methapyrilene is metabolised in a toxic product by CYP2C11, which is present in B-13/H cells but not in undifferentiated B-13 cells. The culture medium was supplemented with 10 µmol/l dexamethasone and cells were trans-differentiated for 11-14 days to ensure efficient trans-differentiation of B-13/H cells in the bioreactor. For the purpose of dose finding in the bioreactor culture, methapyrilene was applied consecutively in four different concentrations (0.2, 0.4, 0.8 and 1.6 mmol/l / standard perfusion mode) for six hours, respectively, to the same bioreactor. After each methapyrilene session the bioreactor system was flushed (single-pass perfusion mode) with fresh culture medium to wash out residual toxic products. After 1.5 days of culture regeneration the next methapyrilene concentration was applied. An untreated further bioreactor was run in parallel as a control. Culture parameters were analysed in daily samples as described above (3.2.4.2).

To investigate the response of oxygen, pH and impedance to methapyrilene exposure in B-13/H bioreactor cultures two 8 ml analytical-scale bioreactors were identically

prepared with respective online sensors. A concentration of 2 mmol/l methapyrilene was chosen based on dose finding experiments to ensure detectable toxic stress upon drug exposure. After 14 days of trans-differentiation one bioreactor was exposed to methapyrilene for 24 hours, whereas the second bioreactor was used as an untreated control. Intoxication was followed by flushing the bioreactors to wash out residual toxic products. Thereafter, bioreactors were set in standard perfusion mode with continuous medium feed. On day 17 and 18 control bioreactor was exposed to 2 mmol/l methapyrilene for 2.5 h to validate the response of sensor signals to drug-induced cell stress.

3.2.3.3 APAP exposure in primary porcine liver cells cultured in 8 ml analytical-scale bioreactors

For each experiment two bioreactors were run in parallel. Primary porcine liver cells (ppL) were isolated as previously described (3.2.1.3). A number of 2.5-4×10^8 ppL were inoculated in each bioreactor. Cells were cultured in the medium described in Table 3. After an adaption phase of three days, APAP was applied at a final concentration of 5 mmol/l to one of the bioreactors for 24 hours (standard perfusion mode). Thereafter the bioreactor was flushed (single-pass perfusion mode) with fresh culture medium to wash out residual toxic products followed by a regeneration phase of two days. On day 6 the procedure of APAP application was repeated. The second bioreactor was used as untreated control. Culture parameters were analysed in daily taken samples (3.2.4.2). Online monitoring of oxygen concentrations, pH value and impedance signals was performed as described in 3.2.4.3.

3.2.3.4 Culture of H-14 cells in an 800 ml clinical-scale bioreactor

The human H-14 cell line derived from HPAC was provided by the group of Professor Wright (University Newcastle, U.K.). The cell line showed successful culture performance in previous experiments using small-scale 2 ml bioreactors (data not shown). For the pilot study using an up-scaled 800 ml clinical-scale bioreactor H-14 cells were expanded in 2D culture before inoculation in the bioreactor. The composition of the culture medium used is provided in Table 4. The bioreactor system was prepared as followed: i) oxygen and pH sensors were integrated in volume adapted flow-through cells, ii) an ammonia sensor was mounted at the outlet line and iii) six impedance sensor foils were vertically integrated into the cell compartment of the clinical-scale bioreactor. Readout devices were prepared and tested: i) provided calibration values (PreSens-Precision Sensing GmbH) were registered in sensor software, ii) ammonia sensors were calibrated via different ammonia concentrations by CEA-Leti-France and iii) impedance measurement was tested when bioreactor was flushed with PBS showing values of approx. 10^3 Ω when the sensor was functional.

A number of 5.8×10^8 H-14 cells were inoculated into the cell compartment and cultured over 15 days. From day 12 of culture, 30 mmol/l APAP were continuously applied to the bioreactor culture over three days. Culture parameters were analysed in daily taken samples (3.2.4.2). Online monitoring of oxygen concentrations, pH value and impedance signals was performed as described in 3.2.4.3.

3.2.4 Evaluation of cell quantity and quality in 2D- and 3D cultures

3.2.4.1 Morphological characterization

The morphology of B-13, B-13/H, ppL or H-14 cells in 2D cultures was daily evaluated using a phase contrast light microscope. Pictures were acquired using the digital imaging software QCapture Pro 5.1. Cells were characterized analysing the cell shape, size, nucleus-cytoplasm ratio, cell density, cytoplasmic granulation and in case of proliferating cell lines the expansion capacity.

3.2.4.2 Metabolic offline parameters

Daily medium samples were taken from bioreactor perfusates or 2D supernatants and analysed for ALT, AST, GLDH, LDH, amylase (only in B-13, B-13/H and H-14 cultures), urea and ammonia concentrations using an automated clinical chemistry analyser. Glucose, lactate and oxygen concentrations as well as pH values were analysed using a clinical blood gas analyser. Albumin concentrations were determined by means of an ELISA (according to manufacturer instruction). Metabolic rates were calculated using the following equation according to Hoffmann *et al*. (2012).[77]

Equation 1: Calculation of metabolic rates in bioreactor cultures

$$P.rate = \frac{\rho_R(t_2)\times V_R - \rho_R(t_1)\times (V_R - V_S) - V_s\times\rho_B + \left(\frac{\rho_R(t_2)+\rho_R(t_1)}{2} - \rho_B\right)\times V_{Waste}(t_2)}{\Delta t}$$

P.Rate: production rate

$\rho_R(t)$: concentration in recirculation at time t

ρ_B: medium blank concentration

V_R: volume in recirculation

V_S: sampling volume

V_{Waste}: waste volume

Δt: time between sampling at t_1 and t_2

3.2.4.3 Online parameter monitoring using non-invasive online sensors

Online signals for oxygen concentration and pH were determined every 100 seconds. Signals for ammonia concentrations were determined every 30 seconds and the electrical potential between the sensor and the reference electrode was measured and plotted as a function of time. Signals for impedance measurement (in total 40 independent measuring channels) were determined every 15 minutes at a frequency of 10 kHz.

3.2.4.4 Ethoxyresorufin-O-deethylase (EROD) assay

The CYP1A1 activity of the cultures was tested by measuring the conversion of 7-ethoxy-resorufin to its product resorufin, which is detected fluorometrically using an extinction wavelength of 544 nm and an emission wavelength of 590 nm. The substrate was applied at a final concentration of 20 µmol/l to the recirculation circuit. The bioreactor culture was switched to closed perfusion mode (recirculation without feed and medium removal). After substrate application samples were taken from the perfusate after 0.5, 1, 1.5 and 2 hours. At the end of the assay the bioreactor was flushed and set to standard perfusion mode (recirculation with feed and medium removal). Samples were analysed fluorometrically with an ELISA reader using authentic resorufin in a concentration range of 5-320 nmol/l as a standard for the free product concentration. In order to detect the absolute amount of product, including conjugated metabolites, conjugates were cleaved by addition of β-glucuronidase/arylsulfatase. Therefore 150 µl of sample and 150 µl of 1 mol/l sodium acetate solution (pH=5.5) were mixed with 20 µl of the enzyme solution and incubated at 37°C overnight. Resorufin formation rates were calculated from the slope of the regression line of the concentration-time curve.

3.2.4.5 Gene expression and Western blot analysis

Gene expression and Western blot analysis were performed by Dr. Emma Fairhall (University of Newcastle) as previously described.[172] Details of DNA oligonucleotide sequences employed in RT-PCR or PCR genotyping and primary antibodies used can be found in Table 6 and Table 7 respectively. In addition to bioreactor samples, RNA from freshly isolated primary rat hepatocytes and rat pancreas (kindly provided by Pharmacelsus, Saarbrücken, Germany) and B-13 and B-13/H cells cultured in 2D flasks as described before in 3.2.1.1 was investigated for comparison.

3.2.4.6 Immunohistochemical analysis of tissue from 3D bioreactors

Upon termination of bioreactor cultures, cell material was retrieved from the cell compartment for immunohistochemical staining. The cell material (including capillaries) was fixated using 4% formaldehyde buffer, stepwisely dehydrated (50%, 70%, 80%, 96%, 100% EtOH and 100% Paraclear) and embedded in paraffin.

Thereafter slides of 3-4 µm of thickness were prepared. Afterwards, slides were deparaffinised (100% Paraclear) and re-hydrated (100%, 96%, 80%, 70% EtOH). For antigen retrieval slides were covered with citrate buffer (3.1.10) and heated in a pressure cooker for 15 minutes. Afterwards blocking buffer (3.1.10) was applied for one hour to reduce unspecific binding. Double staining was performed using monoclonal mouse in combination with polyclonal rabbit or chicken antibodies, which were diluted in blocking buffer. The corresponding secondary antibodies contained Alexa fluorochromes for fluorescence detection at 488 nm or 594 nm wavelength (excitation). Each incubation step was performed for one hour at room temperature. Between each incubation step the slides were rinsed three times with PBS. Primary and secondary antibodies were employed as described in Table 7. Counterstaining of nuclei was performed using bisBenzimide H 33342 trihydrochloride (Hoechst) according to the manufacturer´s instructions. After completion of the staining procedure slides were mounted with Aqua Polymount solution and analysed with a fluorescence microscope. Unspecific staining was excluded by performance of negative controls omitting the primary antibody (no primary antibody control).

3.2.5 Statistical evaluation

Each experiment was performed three times with cultures from different cell passages (B-13 or H14 cells) or donors (ppL) if not indicated otherwise. Values are shown as means ± SEM, if not otherwise indicated. Changes over time in bioreactor experiments with B-13 cells were compared using multivariate analysis of variance (MANOVA) with the two approaches (B-13/HT and B-13/HP) as inter-subject variables. Two-sided p values ≤ 0.05 are considered significant. No Bonferroni correction was performed. SPSS 21 was used for statistical calculation.

4 Results and discussion

4.1 Evaluation of trans-differentiation of B-13 cells and maintenance of B-13/H cells in 2 ml analytical-scale bioreactors

In the first part of the study, the trans-differentiation of B-13 cells into hepatocyte-like cells (B-13/H) and their functional performance in the bioreactor culture system were investigated using 2 ml analytical bioreactors. In the first approach, undifferentiated B-13 cells were trans-differentiated in bioreactors by dexamethasone addition over 8 or 15 days (group B-13/HT). To evaluate the maintenance of functional characteristics under 3D culture conditions, pre-differentiated B-13/H cells were cultured in parallel bioreactors over 15 days (group B-13/HP). The efficacy of trans-differentiation and the cell performance were assessed by determination of functional parameters in the bioreactor perfusate, including synthesis of glucose, lactate, urea and albumin. CYP1A1 activity and product conjugation by phase II enzymes were assessed by analysis of 7-ethoxy-resorufin metabolism. The reorganization grade of the cells in the bioreactor cell compartment and the distribution pattern of typical hepatocyte markers were analysed by immunofluorescence. In addition, PCR analysis was performed to determine the mRNA expression of liver-typical proteins.

4.1.1 Assessment of metabolic activity and liver specific-functions in bioreactor cultures

Bioreactor cultures of B-13 cells subjected to trans-differentiation (B-13/HT) showed a significant increase in glucose consumption ($p = 0.029$) during first three days. Those, inoculated with cells pre-differentiated prior to seeding into the bioreactor (B-13/HP) showed an increase in glucose ($p = 0.005$) and lactate ($p = 0.009$) metabolism until day 6 followed by stable rates. Both groups showed significant differences in energy metabolism considering the overall culture period (glucose consumption: $p = 0.001$; lactate production: $p < 0.001$), but no significant difference between both groups was observed at the end of culture time (glucose consumption: $p = 0.609$; lactate production: $p = 0.691$) (Figure 9).

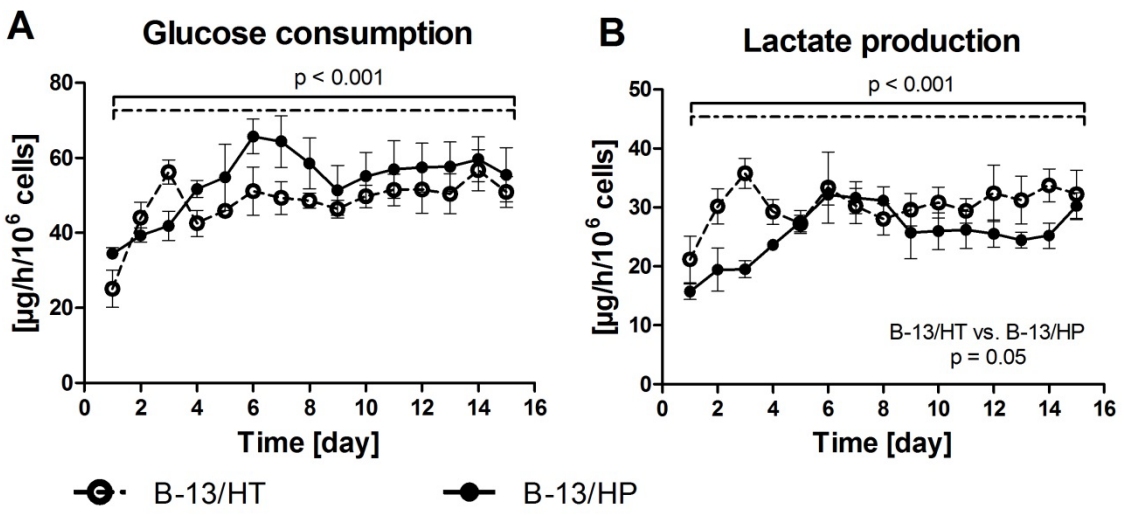

Figure 9: Energy metabolism in B-13/H bioreactor cultures.
Glucose consumption (A) and lactate production (B) in 3D multi-compartment bioreactors with B-13 cells subjected to trans-differentiation in the bioreactor (B-13/HT / dotted line) or with pre-differentiated B-13/H cells (B-13/HP / solid line) over a time period of 15 days. Values were calculated as rates per 10^6 cells. Comparisons concerning changes over time were performed using multivariate analysis of variance (MANOVA) with the two approaches as inter-subject variables. Two-sided p values ≤ 0.05 are considered significant. Significant changes over time are marked as bars enclosing respective time intervals. (n=3, means ± SEM)

The release of intracellular enzymes (ALT, AST, GLDH and LDH) was analysed in bioreactor perfusates to detect potential cell damage in the cultures (Figure 10). ALT and AST levels showed in both approaches a slight, yet significant increase during the culture period ($p = 0.028$ and $p < 0.001$), while GLDH only significantly increased in the B-13/HP group from day 9 to 15 ($p = 0.045$). Release rates of ALT were significantly different in both groups ($p = 0.026$). The levels of LDH activity were constant with no significant increase ($p = 0.635$) over the culture period, with slightly higher enzyme release rates in B-13/HP in comparison to B-13/HT.

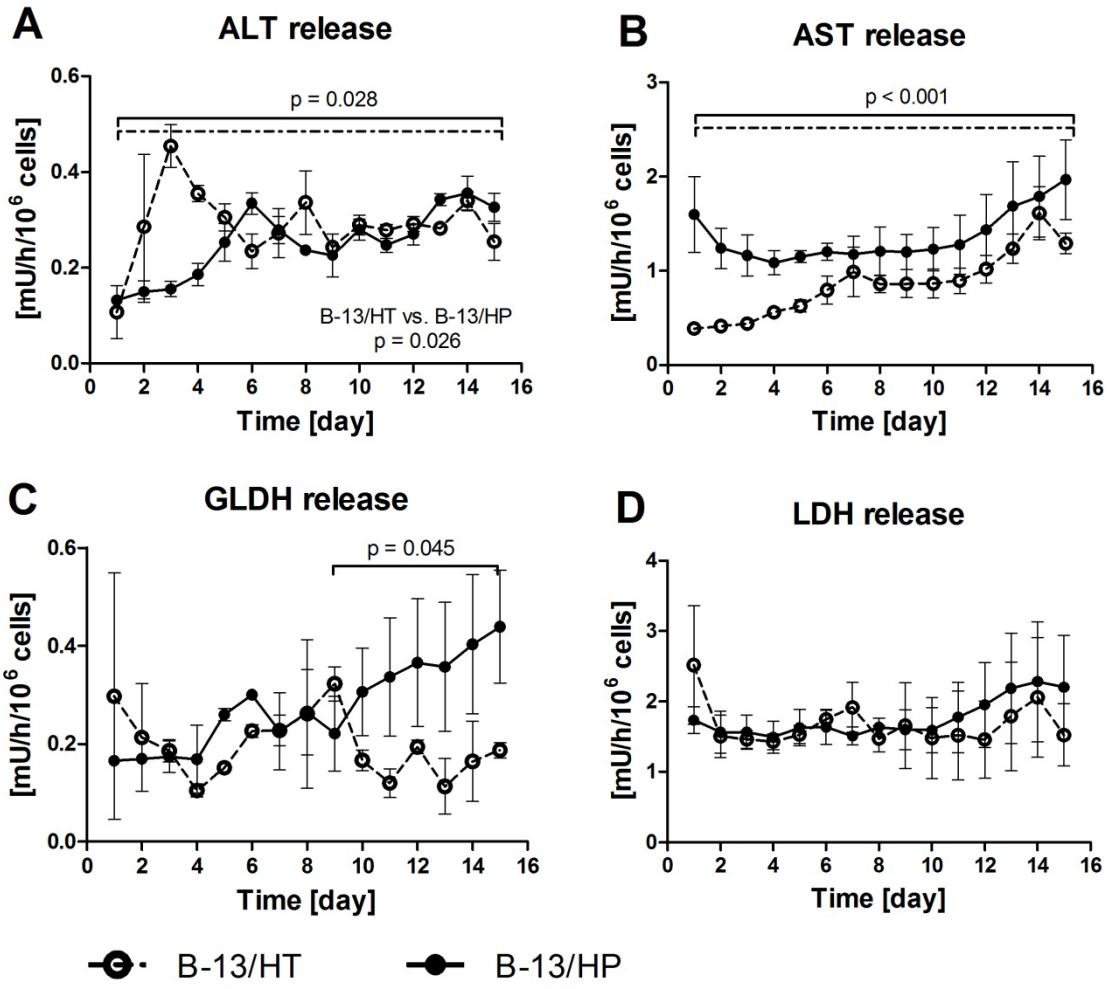

Figure 10: Cell integrity in B-13/H bioreactor cultures.
Enzyme release of ALT (A), AST (B), GLDH (C) and LDH (D) in 3D multi-compartment bioreactors with B-13 cells subjected to trans-differentiation in the bioreactor (B-13/HT / dotted line) or with pre-differentiated B-13/H cells (B-13/HP / solid line) over a time period of 15 days. Values were calculated as rates per 10^6 cells. Comparisons concerning changes over time were performed using multivariate analysis of variance (MANOVA) with the two approaches as inter-subject variables. Two-sided p values ≤ 0.05 are considered significant. Significant changes over time are marked as bars enclosing respective time intervals. (n=3, means ± SEM)

Figure 11A-B shows the course of urea and albumin concentrations in bioreactor culture supernatants. Urea production in B-13/HT bioreactors showed an increase, though not significant, until day 3 after dexamethasone induction and declined afterwards. In B-13/HP bioreactors urea production increased significantly until day 6 ($p = 0.043$) followed by a slight decrease to a stable level for the remaining culture time with no significant changes in production rates. In total B-13/HP showed significantly higher production rates than B-13/HT ($p = 0.012$). Albumin synthesis showed a tendency, though not significant ($p = 0.365$), towards increase from day 7 in B-13/HT bioreactors with a peak on day 10, while B-13/HP showed a maximum in albumin synthesis on day 3 followed by a slight, yet not significant ($p = 0.175$) decline. Both groups showed different albumin production rates considering the overall culture time, although the difference was not significant ($p = 0.081$). Ammonia release showed a similar course as urea production in both groups, with a significant increase until day 6 in B-13/HP cultures ($p = 0.042$) and rather stable values thereafter with no significant changes. Similarly, ammonia levels in B-13/HT increased during the first days, although not significant ($p = 0.106$), and slowly declined to ammonia levels comparable to B-13/HP cultures until the end of culture (Figure 11C). B-14/HT showed significantly higher ammonia release rates as compared with B-13/HP ($p = 0.001$). Amylase release characteristic for pancreas exocrine cells also significantly increased over the first week of culture ($p < 0.047$) in the B-13/HT group and stayed stable thereafter with no significant changes. Initial values for amylase release were lower for B-13/HP compared to B-13/HT and did not significantly change over the culture period ($p = 0.11$) (Figure 11D). Amylase release rates were significantly different between both groups during bioreactor culture ($p = 0.022$).

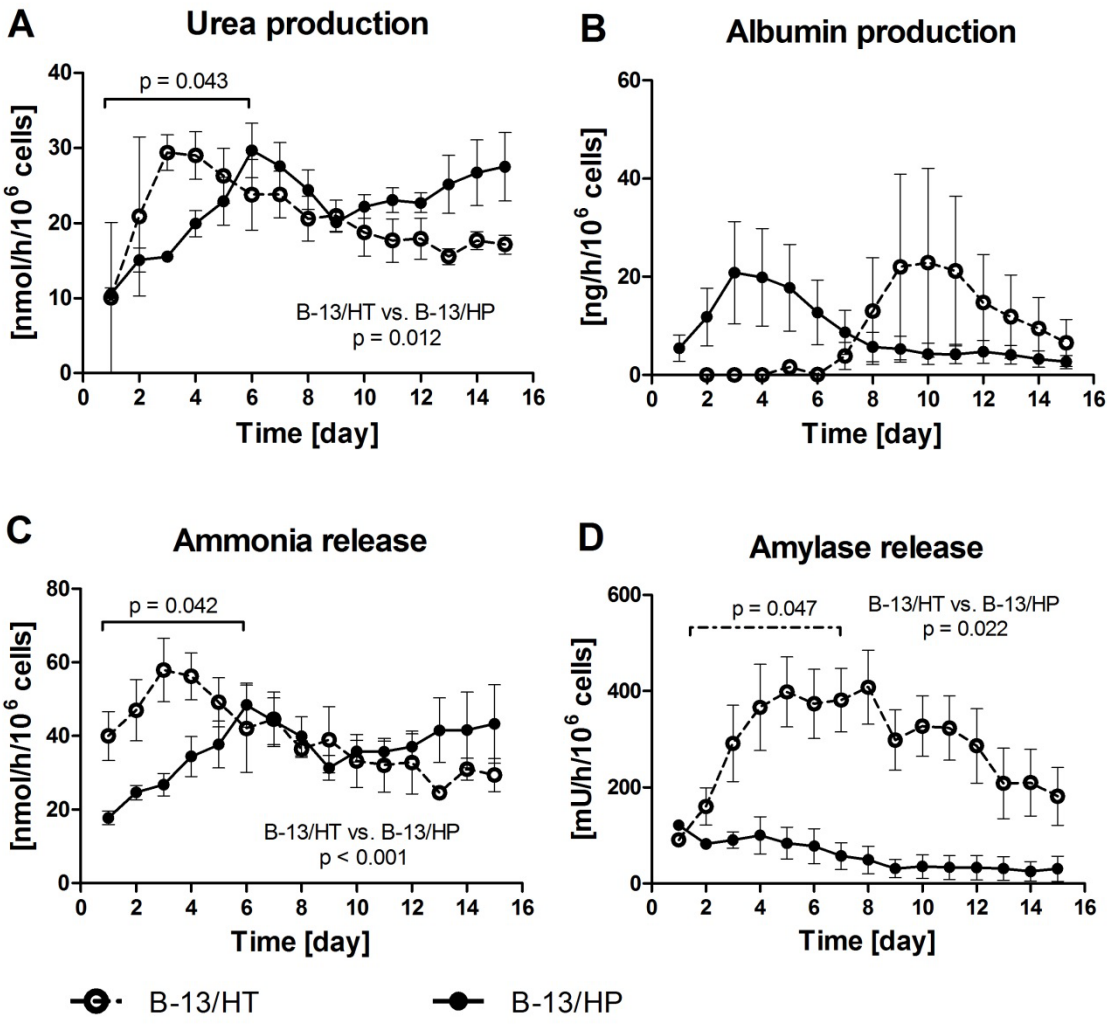

Figure 11: Liver- and pancreas-specific marker expression in B-13/H bioreactor cultures. Production rates of urea (A), albumin (B) and release rates of ammonia (C) and amylase (D) in 3D multi-compartment bioreactors with B-13 cells subjected to trans-differentiation in the bioreactor (B-13/HT / dotted line) or with pre-differentiated B-13/H cells (B-13/HP / solid line) over a time period of 15 days. Values were calculated as rates per 10^6 cells. Comparisons concerning changes over time were performed using multivariate analysis of variance (MANOVA) with the two approaches as inter-subject variables. Two-sided p values ≤ 0.05 are considered significant. Significant changes over time are marked as bars enclosing respective time intervals. (n=3, means ± SEM)

4.1.2 Ethoxyresorufin-O-deethylase (EROD) activity of trans-differentiated B-13 cells in the bioreactor system

CYP1A1 dependent deethylation of ethoxyresorufin was analysed on day 1, day 8 and day 15 by detection of the fluorescent product 7-hydroxyresorufin. In both bioreactor groups (B-13/HT and B-13/HP), formation rates of non-conjugated (phase I) and conjugated (phase II) 7-hydroxyresorufin could be measured from day 1 to day 15, with phase I+II showing a significant increase (phase I: $p = 0.128$; phase I+II: $p = 0.014$). Values were significantly different between groups for phase I+II ($p = 0.033$) (Figure 12). B-13/HP cultures showed higher formation rates of 7-hydroxyresorufin on day 8

when compared to B-13/HT ($p = 0.033$), although not at a significant level for phase I ($p = 0.114$), while on day 15 of culture similar formation rates were observed. Cleavage of conjugated 7-hydroxyresorufin (phase II) resulted in the detection of higher amounts of the free product in the B-13/HP group, although not at a significant level.

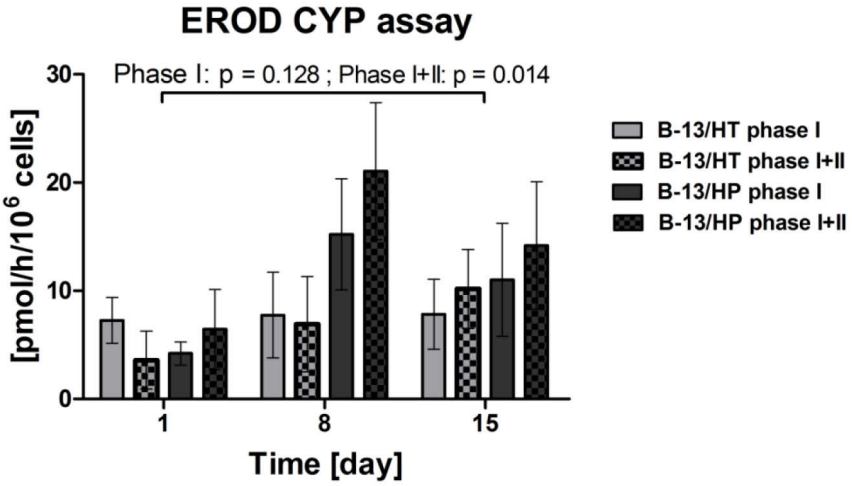

Figure 12: Ethoxyresorufin-O-deethylase activity in B-13/H bioreactor cultures.
Biotransformation of 7-ethoxyresorufin in 3D multi-compartment bioreactors with B-13 cells subjected to trans-differentiation in the bioreactor (B-13/HT / grey) or with pre-differentiated B-13/H cells (B-13/HP / black-grey) on day 1, 8 and 15 of culture. Phase I: Formation rate of the free product, phase I+II: Sum of formation rates of free and conjugated products. Values were calculated as rates per 10^6 cells. Comparisons concerning changes over time were performed using multivariate analysis of variance (MANOVA) with the two approaches as inter-subject variables. Two-sided p values ≤ 0.05 are considered significant. Significant changes over time are marked as bars enclosing respective time intervals. (n=3, means ± SEM)

4.1.3 Gene expression and protein analysis of hepatocyte-specific genes in trans-differentiated B-13 cells

The expression of hepatic and pancreatic markers at the mRNA and protein levels was investigated in B-13/HT on day 8 and 15 and in B-13/HP on day 15 in comparison with B-13 cells and B-13/H cells cultured in 2D flasks, as well as rat pancreatic tissue and primary rat hepatocytes (Figure 13).

The expression of genes encoding liver-specific CPS-1 and albumin was similar in the experimental groups B-13/HT and B-13/HP as in 2D cultured B-13/H cells, but lower as compared to primary hepatocytes (Figure 13A). The expression of CYP2E1 and also of CYP2C11 specific for male rats could be demonstrated for B-13/HT, while B-13/HP cultures showed expression of CYP2E1, but not of CYP2C11, similar to B-13/H cells cultured under 2D conditions. The expression of liver-specific markers increased from day 8 to day 15 in B-13/HT bioreactors. Amylase mRNA transcripts characteristic for exocrine pancreas cells were expressed in B-13/HT and B-13/HP cultures at a similar

level as in B-13/H cells maintained in 2D cultures, but its expression was lower than in native rat pancreas or undifferentiated B-13 cells.

Western blot analysis (Figure 13B) showed a weaker expression of CPS-1, albumin and CYP2E1 in B-13/HT or B-13/HP bioreactors than in primary rat hepatocytes, while CYP3A expression was comparable to that of primary cells. The expression of liver-specific markers (albumin, CPS-1, CYP2E1 and CYP3A) was similar to that of B-13/H cells generated in 2D culture. Amylase expression was comparable to B-13 and B-13/H cells, with a lower intensity than in pancreatic tissue in all approaches. In accordance with results from PCR analysis, an increase of liver-specific markers and a decline of pancreatic amylase between day 8 and day 15 of culture were observed.

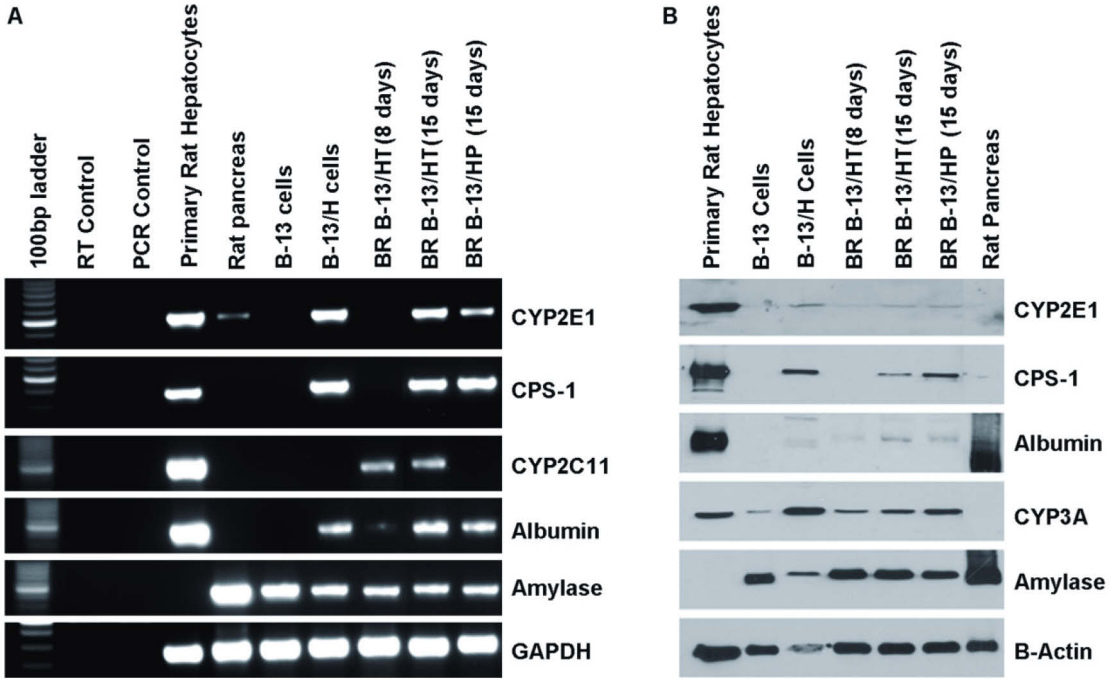

Figure 13: Gene and protein expression of B-13/H bioreactor cultures.
Analysis of hepatocyte-specific markers via RT-PCR and Western blot in 3D multi-compartment bioreactors with B-13 cells subjected to trans-differentiation in the bioreactor (B-13/HT, day 8 and 15) or with pre-differentiated B-13/H cells (B-13/HP, day 15) compared to B-13 or B-13/H cells cultured in 2D, primary rat hepatocytes and rat pancreas tissue. (A) RT-PCR for the indicated transcripts and RT control amplification in the absence of input RNA. (B) Western blot of the indicated proteins.

4.1.4 Immunohistochemical characterization of B-13 cells in the bioreactor

Immunofluorescence staining of liver- and pancreas-specific markers was performed in B-13/HT bioreactors on day 8 and 15 and in B-13/HP cultures on day 15 and compared to tissue of rat pancreas and liver (Figure 14). Double-staining was performed using antibodies against pancreas-specific amylase in combination with antibodies against various liver-specific marker antigens (Table 7).

Amylase was observed only in a few cells in B-13/HT and B-13/HP cultures on day 15. In B-13/HT bioreactors a decrease was detected from day 8 to day 15.

The liver-specific markers albumin, CK18 and CCAAT/enhancer-binding protein (CEBP-β), a marker of early liver development, showed a similar distribution in B-13/HT (day 15) and B-13/HP bioreactors. An increase in expression of these markers between day 8 and day 15 was observed in B-13/HT, indicating progression of trans-differentiation. CYP2E1 showed a higher expression in B-13/HT cultures than in B-13/HP cultures, while positive staining for multidrug resistance-associated protein 2 (MRP2), an apical membrane transporter found in primary hepatocytes, was only observed in B-13/HP bioreactors.

Native rat and liver tissue investigated for comparison showed the typical expression of specific markers. Rat liver tissue showed albumin, CK18, CYP2E1 and MRP2 positive cells but no amylase, whereas rat pancreas tissue strongly expressed amylase, but no CYP2E1, albumin or CEBP-β. Cytokeratin 18 showed immunoreactivity in some cells of pancreatic tissue, probably associated with pancreatic duct epithelia. Negative controls (no primary antibody control) showed no unspecific staining by secondary antibodies (Figure 14/row 6).

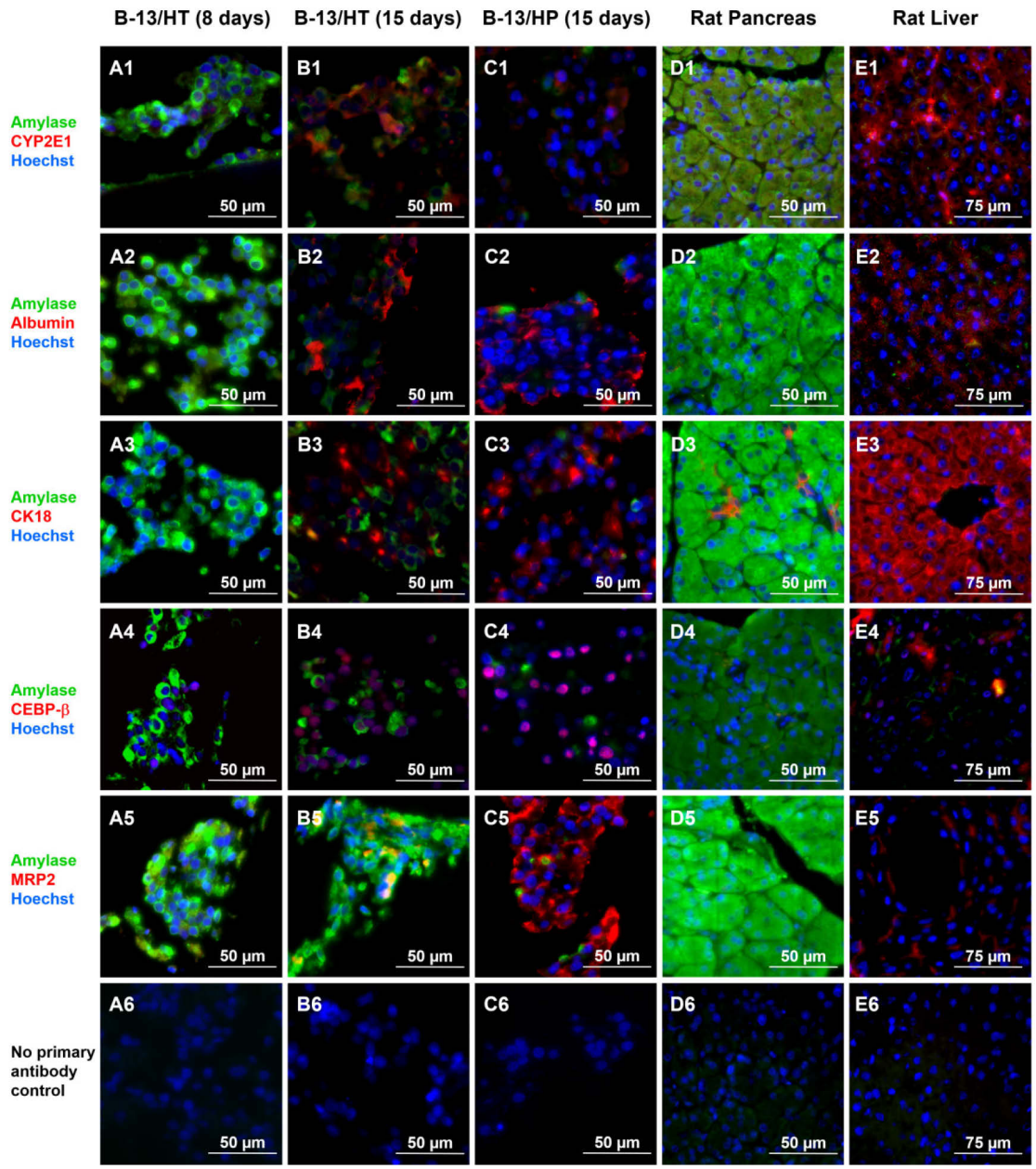

Figure 14: Immunohistochemical analysis of tissue retrieved from bioreactor cultures. Immunohistochemical analysis of hepatic and pancreatic markers in B-13 cells trans-differentiated in the bioreactor system (B-13/HT) over 8 (A) or 15 (B) days, B-13/H cells cultured in the bioreactor system for 15 days (B-13/HP, C), native pancreas (D), and native liver (E) in 400x magnification. Amylase positive cells are shown in green and markers characteristic for the liver are shown in red. Row (1) shows amylase and CYP2E1, row (2) amylase and albumin, row (3) amylase and CK18, row (4) amylase and CEBP-β, and row (5) amylase and MRP2 immunoreactivity. Row (6) shows negative controls (no primary antibody control). Counterstaining of nuclei was performed with Hoechst staining (blue).

4.1.5 Chapter discussion

The B-13 cell line has shown to be a potential candidate capable of providing a donor-free supply of functional hepatocyte-like cells in an up-scaled manner without the requirement of intensive culture requirements using simple cost effective culture medium supplemented with glucocorticoids and short proliferation time (doubling time of 30±7.3 hours).[76,118–120] The majority of B-13 cells convert to liver-like B-13/H in response to glucocorticoid exposure providing yields of up to 95%. Therefore this cell source shows an advantage in producing large cell numbers in a quite pure population of functional hepatocytes with relative low effort and expense. Additionally, the B-13/H phenotype gained can be maintained for several weeks in culture, in contrast to primary hepatocytes which rapidly de-differentiate in 2D cultures requiring more complex culture conditions.[76,77,173] Since the 3D multi-compartment bioreactor culture system used in this study showed successful liver cell cultivation for application in extracorporeal liver support[89,145,146] or analysis of drug metabolism in small-scale systems[77,97,149,150] the suitability of the technology to support hepatic trans-differentiation of B-13 cells was investigated in the present study. Previous experiments with other cell types (e.g. primary human hepatocytes or human embryonic stem cells) seeded into the bioreactors had demonstrated that the cells do not only adhere to the artificial capillaries, but also to each other.[149,174] In another experiment B-13 cells were cultured in suspension by seeding them in plastic dishes coated with poly-2hydroxyethylmethacrylate (P2HEMA), which prevents attachment of the cells to the surface.[175,176]

In this study, cells were treated with or without dexamethasone to investigate trans-differentiation behaviour in designed state. Experiments resulted in aggregation of undifferentiated B-13 as well as trans-differentiated B-13 cells (B-13/H) showing liver-specific marker expression (e.g. albumin, CPS1, CYP2E1). Furthermore, clusters without evolving necrotic centres were formed. Suspension cultures showed suppressed proliferation upon glucocorticoid exposure similar to 2D cultures.[176] Conducted experiments encouraged culturing these cells in the 3D high density bioreactor system to investigate if it is suitable to support trans-differentiation of B-13 cells (B-13/HT) and to maintain the hepatocyte-like phenotype of pre-differentiated B-13/H cells (B-13/HP). Since proliferation is suppressed but not stopped when dexamethasone is applied to the B-13 culture medium different cell densities used for bioreactor inoculation of the two different approaches had to be used.[172] Due to analysis of proliferation in B-13 suspension culture experiments a 2.5 fold gain in cell mass during 14 days of bioreactor culture was estimated.[176]

Monitoring of metabolic parameters in bioreactor perfusate showed successful culture of B-13 or B-13/H cells in the system. B-13/HT and B-13/HP showed similar glucose

consumption and lactate production rates with an increase in lactate production during the first days and stable metabolism afterwards. The lower initial production of lactate could be due to adaptation of the cells to the culture environment. Increasing lactate values at the beginning could be a sign of cell proliferation to fill out the space due to lower inoculation cell density in B-13/HT. Interestingly, glucose/lactate metabolism of B-13/HT approximated that in B-13/HP at the end of the culture period. This indicates that a comparable cell number and metabolic status was attained in both groups after 15 days supporting the estimated proliferation rate of 2.5 over the culture duration in B-13/HT used as a basis of data calculation.

The analysis of enzyme release (ALT, AST, GLDH and LDH) in bioreactor perfusates as indicators for possible cell damage,[77,149,153] showed a continuous increase, although at low levels, in parallel with increasing metabolic activity, which can be interpreted as necrosis of a small proportion of cultured cells during cell growth (B-13/HT) and trans-differentiation. No drastic peaks in enzyme release were observed over the entire culture period indicating no harmful stress to the cells.

Production of albumin, the most abundant protein produced by hepatocytes, was detected in both approaches with a maximum in the first week in the pre-differentiated cultures (B-13/HP) and in the second week in cultures trans-differentiated in the 3D bioreactor (B-13/HT), demonstrating successful induction of hepatic protein synthesis upon dexamethasone exposure. Furthermore, stable production of urea, generated by hepatocytes for nitrogen elimination via the urea cycle, was monitored over the culture period in bioreactor perfusates. The finding of lower urea concentrations in B-13/HT than in B-13/HP cultures suggests lower activity in cultures subjected to trans-differentiation within the 3D bioreactor. This is supported by the results from ammonia measurements, which show a correlation of ammonia release with urea secretion, indicating insufficient ammonia detoxification via the urea cycle. To enhance urea formation, stimulation of the urea cycle, e.g. by addition of N-carbamoyl-glutamate could be tested, which has been successfully used for improving the differentiation state of HepaRG cells.[175,177]

Amylase, characteristic for exocrine pancreas cells, is typically expressed by undifferentiated B-13 cells.[76] Increasing rates of amylase as reported for B-13/H cells during trans-differentiation of B-13 cells[119] could be observed in B-13/HT bioreactor cultures after addition of 10 µmol/l dexamethasone to the culture medium. The decrease of amylase release observed in bioreactor cultures of B-13/HP and B-13/HT in the second week of culture indicates a decrease of pancreas-specific characteristics in the cultures.

As a further functional parameter, the expression and activity of CYP isoenzymes, which are responsible for hepatic xenobiotic metabolism (phase I reaction), were

assessed. Formation of 7-hydroxyresorufin from 7-ethoxyresorufin, a known CYP1A1 substrate,[178] was detected in both bioreactor groups, with B-13/HP bioreactors showing higher formation rates than B-13/HT cultures on day 8, but comparable values on day 15. Furthermore, the ongoing rise of phase I + II metabolism between day 1 and day 15 in B-13/HT cultures indicated ongoing progression of trans-differentiation in these cultures. Thus, further prolongation of the trans-differentiation period could be useful to increase CYP activities even further.

The analysis of mRNA expression (RT-PCR) and protein expression (Western blot) confirmed successful differentiation of B-13 cells to hepatic B-13/H cells in the bioreactor culture system. The expression of hepatocyte-specific markers previously described for B-13/H 2D cultures[111,118] was maintained at both the mRNA and protein expression level. The CYP isoenzymes CYP2E1, CYP3A1, and CYP2C11, typical for rat liver[179] could be detected. Furthermore, mRNA transcript levels of albumin and of CPS-1 were comparable in B-13/HT and B-13/ HP to primary hepatocytes. Expression of albumin and CPS-1 proteins was also detected, though in low levels. CPS-1 is an important enzyme involved in the urea cycle and its expression in B-13/HT and B-13/HP on gene and protein levels further confirms urea production via the urea cycle. However it cannot be excluded that part of the observed urea release is produced via hydrolysis of arginine by arginase as described for human liver cell line C3A.[35,94]

Immunohistochemical staining showed the formation of 3D cell clusters in bioreactor cultures and confirmed the hepatic differentiation of B-13 cells in the 3D bioreactor culture system in that there was a loss in expression of amylase and an increase in hepatocyte-specific markers. CYP2E1 and albumin expression confirmed the results of gene expression and Western blot analysis. In addition, cells positive for CK18, a marker for liver epithelial cells,[77] as well as expression of MRP2, a major canalicular transporter responsible for biliary elimination of drugs in hepatocytes[180] indicate a liver-like phenotype of B-13/H cells in the bioreactor cultures. Further, activation of CEBP-β shows the involvement of this transcription factor in generating liver-like tissue, according to results from other studies.[119]

In conclusion, the studies show successful hepatic trans-differentiation of B-13 cells as well as stable maintenance of B-13/H cells over two weeks in the bioreactor. Significant improvement of hepatic differentiation in 3D as compared with 2D cultures could not be demonstrated in our study. However some liver markers, e.g. CPS-1 and albumin, while showing lower expression in suspension cultures than in 2D cultures, showed at least equal expression in bioreactor cultures of pre-differentiated (B-13/HP) or trans-differentiated (B-13/HT) cells. In both 2D and 3D culture systems B-13/H cells do not attain the functionality of native hepatocytes. These results suggest that trans-differentiation takes more time in 3D configuration but liver functions may be preserved

much longer. Additionally improvement of this cell line may need further genetic modification. For example expression of metabolically functional human CYP1A2 was achieved by introducing the corresponding gene into the cells.[121] If approaches for improvement are successful, B-13 cells could provide a cost-effective, plenty available cell source for larger scale *in vitro* studies, if improved hepatic maturation and human is achieved. Moreover, the use of B-13/H cells in the described 3D bioreactor system would be an option for clinical liver support therapy, since these cells do not show engraftment in soft tissue reducing the risk of tumour formation in the body, if cells are transferred into the patient´s blood circulation.[118]

4.2 Sensor integration and evaluation for clinical application

In this part of the study multi-parametric sensors integrated in the 8 ml analytical-scale bioreactor system were established and evaluated. At first the biocompatibility of the integrated online sensors was investigated followed by evaluation of the sensor performance during bioreactor culture. B-13/H cells or ppL were used as model cell types to investigate points of interest. For monitoring the cell response to toxic stress occurring during exposure to toxic plasma from acute liver failure patients, B-13/H bioreactor cultures were treated with the reference substance methapyrilene, which has been shown to exert rat hepatocytes and trans-differentiated B-13 cells. Primary porcine liver cells (ppL) cultured in 8 ml bioreactors were treated with APAP as a drug with known hepatotoxicity for humans for validation of the sensor-based monitoring system.

4.2.1 Investigation of the efficiency of multi-parametric sensors for quality assessment of bioreactor cultures

To evaluate multi-parametric sensors integrated in the bioreactor system, the biocompatibility, functionality and sensitivity of the used sensors were investigated. For these purposes two 8 ml analytical-scale bioreactors equipped with oxygen, pH, ammonia and impedance sensors were inoculated with B-13 cells. The cultures were subjected to trans-differentiation by applying dexamethasone after an adaption phase of 24 hours. In order to detect possible effects of sensors on the cell viability and function, data from sensor-equipped bioreactors were compared with those from a bioreactor run in parallel without sensors. In addition to sensor-based online parameters, a number of offline parameters were measured daily (release of ALT, AST, GLDH, LDH, ammonia and amylase, glucose consumption, production of lactate, urea and albumin, pH value, oxygen concentration). Cultures were conducted over 15 days. An EROD activity assay was performed on day 1, 8 and 15. Upon termination bioreactor tissue material for immunohistochemical investigation was retrieved. Figure 15 shows the experimental set-up of the bioreactor system with integrated sensors and corresponding measuring devices.

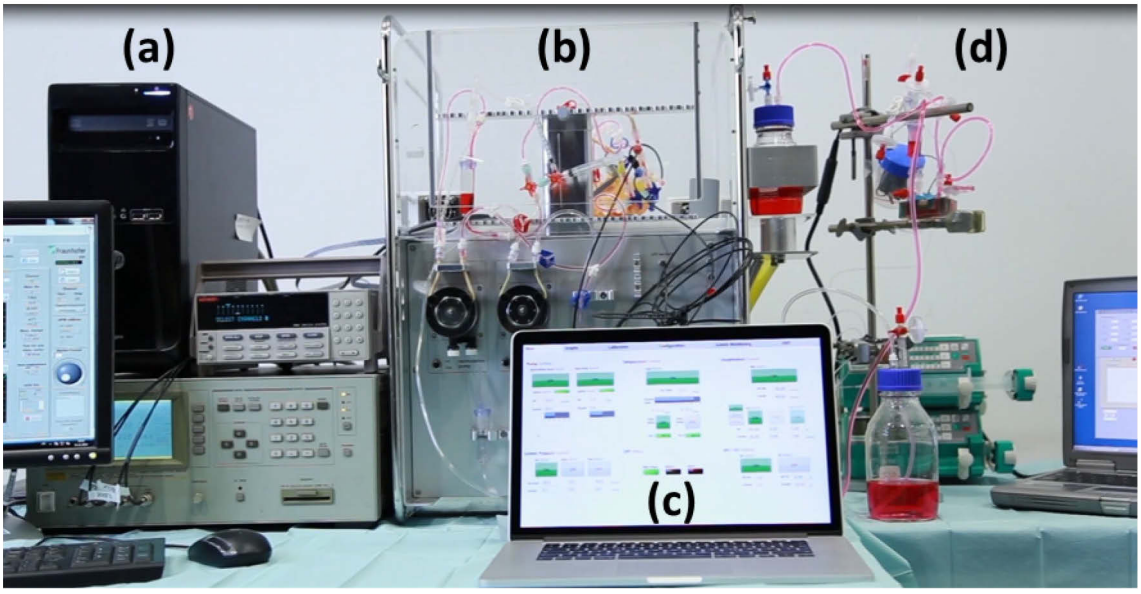

Figure 15: Experimental set-up of the bioreactor system for non-invasive, sensor-based monitoring of system functions and culture parameters.
Impedance measuring device with data analysis software (Fraunhofer IBMT) **(a)**. Perfusion device holding an 8 ml analytical-scale bioreactor (Stem Cell Systems) with integrated impedance sensors (Fraunhofer IBMT) and pH and oxygen sensors (PreSens-Precision Sensing GmbH) integrated into the tubing system of the recirculation circuit **(b)**. Perfusion parameters are set via an external computer unit **(c)**. Online ammonia sensor and ammonia readout device (CEA-Leti-France) **(d)**.

4.2.1.1 Comparison of metabolic offline parameters in bioreactor cultures with or without multi-parametric sensors

Measured offline parameters including glucose, lactate, enzyme leakage (ALT, AST, GLDH and LDH), urea, albumin, ammonia, amylase and CYP1A1 dependent conversion of ethoxyresorufin in bioreactor cultures with or without integrated sensors showed a similar performance as previously evaluated in B-13/HT and B-13/HP bioreactor cultures (4.1.1 and 4.1.2). No difference in marker detection could be found between groups when immunofluorescence staining of liver- and pancreas-specific markers was performed. Bioreactor tissue in both groups expressed cells positive for amylase, characteristic for pancreas or B-13 cells, and also cells showing liver-specific marker expression (albumin, C/EBP β, CK18, CYP2E1 and MRP2) as previously described (4.1.4).

4.2.1.2 Evaluation of sensor-based oxygen and pH measurement in the bioreactor system

Online sensor-based monitoring of oxygen and pH was compared with offline analysis of these parameters to assess the comparability and sensitivity of the methods. Oxygen concentrations in the circulating medium of bioreactors with B-13 cells showed a continuous decrease over 15 days of culture. Offline measurement by means of a blood gas analyser (ABL) was comparable between bioreactors with or without integrated

sensors. Absolute values measured online via flow-through sensors (PreSens-Precision Sensing GmbH) were lower than offline values, but the course of oxygen levels was similar to offline measurement (Figure 16A).

Comparison of online and offline pH measurement also revealed generally lower absolute values for online measurements, while both measurement methods showed a similar time-course of pH values (Figure 16B). After an initial fluctuation during the adaption phase, stable pH was maintained until the end of culture. An outlier for pH online sensor was detected on day 11 showing temporary lower values which recovered on the next day.

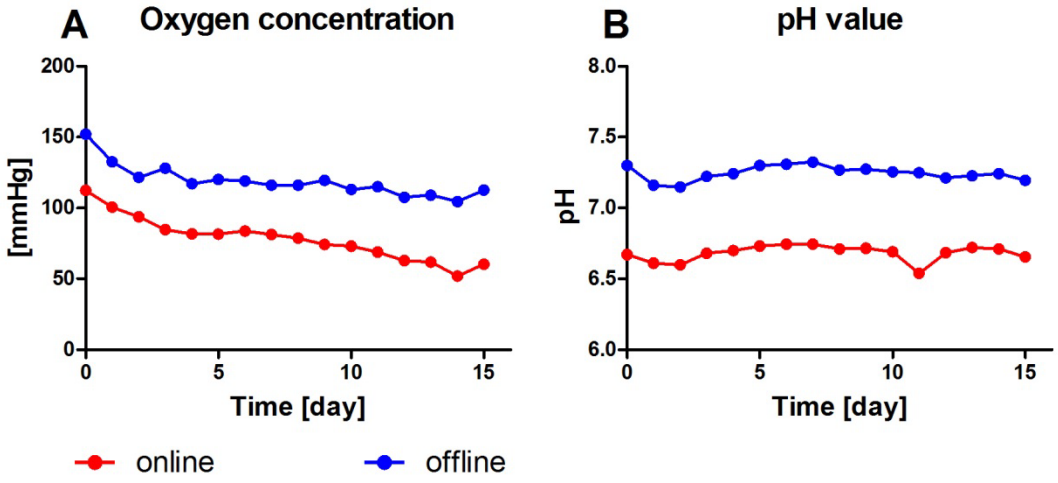

Figure 16: Offline versus online measurement of oxygen (A) and pH values (B) in an 8 ml analytical-scale bioreactor.
B-13 cells were trans-differentiated in 8 ml analytical-scale bioreactors over 15 days. Sensors for online measurement for oxygen and pH (PreSens-Precision Sensing GmbH) were integrated in two bioreactors (red) and data were compared to values obtained from offline measurement via blood gas analyser (blue) of daily samples. Graphs show mean values of two experiments.

4.2.1.3 Evaluation of ammonia sensors in the bioreactor system

Two ammonia sensors for online measurement were integrated each into outlet lines of two 8 ml analytical-scale bioreactors. Bioreactors were run with B-13 cells subjected to trans-differentiation and ammonia was continuous measured from day 10 (completion of trans-differentiation) until the end of culture on day 15. Every sensor was integrated in a flow-through cell (Figure 17) and mounted at the medium outlet line of the tubing system. Sensors were calibrated using different concentrations of NH_4Cl before and after sensor integration to check their functionality, and they were flushed with fresh culture medium prior to use. Additionally, one bioreactor (Bioreactor 01) received a true reference electrode, whereas for the second bioreactor (Bioreactor 02) a pseudo-reference electrode was used. Electrical potential curves were generated for each bioreactor using the readout device and compared with offline measured ammonia

concentrations. Analysis and plotting of received data was accomplished by the cooperation partner CEA-Leti-France.

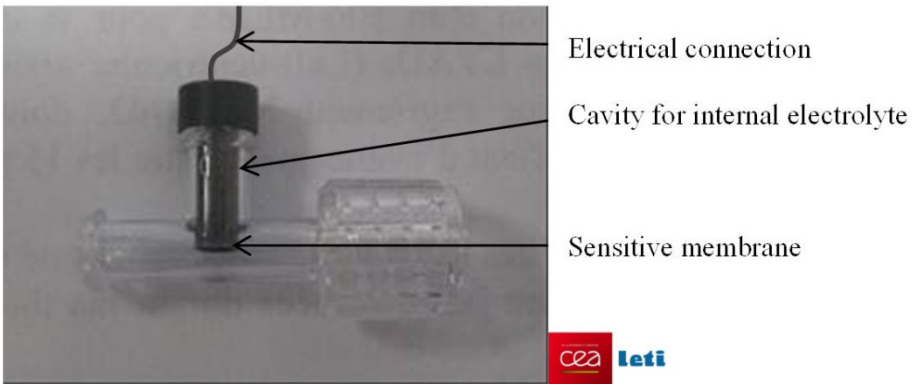

Figure 17: Individual ammonia sensor integrated in a Luer-Lock T-connector (CEA-Leti-France).
The sensor is composed of a PVC cavity containing an internal electrolyte solution, a working electrode, which is connected to the readout device. The cavity is sealed with an ammonium sensitive membrane, which stays in contact with the culture medium. The ammonia sensor is integrated in a three-way valve.

At the beginning of ammonia measurement sensors detected an increase of potential when sensors got in contact with culture medium flowing out from the bioreactor circuit. In the following, stable values were maintained until culture termination (Figure 18).

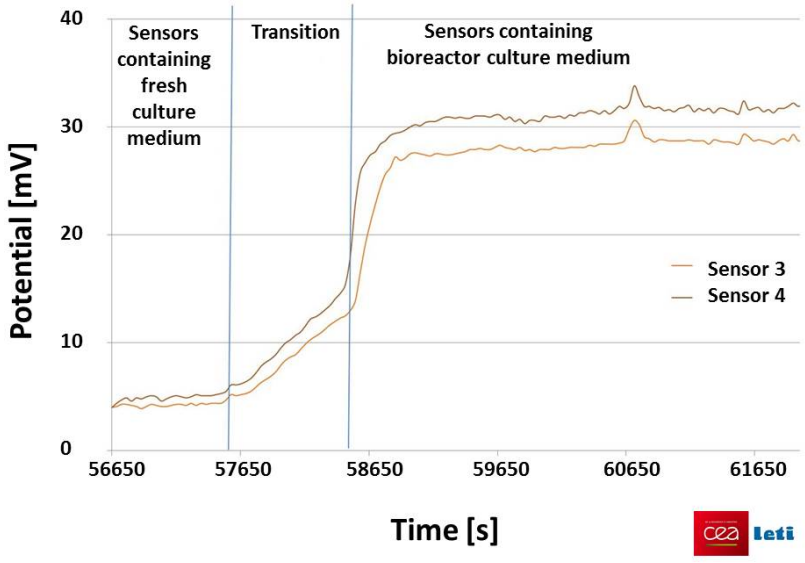

Figure 18: Ammonia sensor potential performance at the beginning of online measurement.
Electrical potential development is shown at the beginning of ammonia measurement for sensor 3 and 4 of bioreactor 02 on culture day 10 for 83 min. Initially sensors were flushed with fresh culture medium and needed a transition time of approx. 1000 s to adapt to bioreactor culture medium. Analysis and plotting of received data was accomplished by the cooperation partner CEA-Leti-France.

Monitoring of ammonia concentration in culture perfusates measured online or offline is shown in Figure 19. After filtering interferences, which regularly occurred, monitoring of ammonia concentrations in bioreactor 01 (Figure 19A) showed no potential variation for Sensor 1. In contrast Sensor 2 showed comparable performance in potential detection when compared to the performance of offline ammonia concentrations measured in daily samples in the clinical laboratory. Sensor 2 recorded some oscillations on culture day 11. Sensors 3 and 4 used in the bioreactor 02 showed a similar performance of electric potentials (Figure 19B). After a short increase at the beginning of ammonia measurement values slowly declined until day 13. Thereafter a strong increase in potentials could be observed while offline measured ammonia concentrations remained relatively stable.

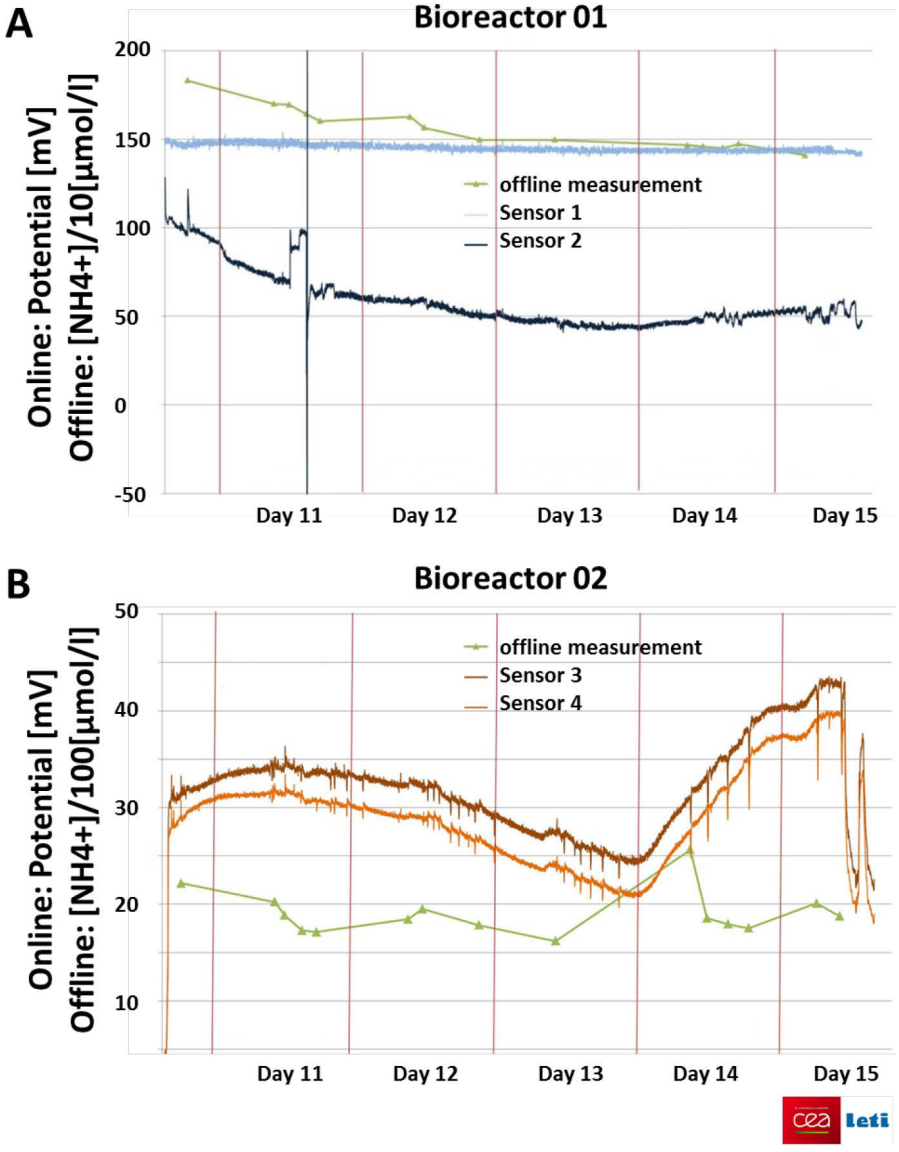

Figure 19: Comparison of online and offline measurement of ammonia in bioreactors with B-13 cells.

B-13 cells were trans-differentiated in two 8 ml analytical-scale bioreactors over 15 days. From day 10 on (completion of trans-differentiation) ammonia concentrations were measured either online via sensors in outlet lines of bioreactor tubing system or offline in daily samples from the bioreactor perfusates. Sensor performances for online measurement (blue and brown lines) of ammonia were compared to offline measurement (green lines). Analysis and plotting of received data was accomplished by the cooperation partner CEA-Leti-France.

4.2.1.4 Evaluation of impedance sensors in the bioreactor system

The time-course of impedance signals was investigated in two 8 ml analytical-scale bioreactors cultured with B-13 cells subjected to trans-differentiation. Figure 20 exemplarily shows the time course of impedance values in one of these bioreactors. The individual sensors located at different sites within the bioreactor cell compartment showed a comparable time course, although absolute values partly differed between the sensors. Channels 1-12 describe the measurement of two electrodes directly on impedance sensor foils comparable to the situation in 2D cultures whereas channels 13-19 describe impedance measurements between sensor foils exhibiting rather characteristics of a 3D environment. Channel 20 monitored the temperature development during the experiment. During initial perfusion of the bioreactor with PBS (day -5 to day -3) basal signals were detected, followed by a slightly increase in impedance signal after changing to culture medium perfusion (day -3 to day 0). Cell inoculation on day 0 caused a marked peak in impedance signals. In the majority of measurement channels an increase of approx. 100 Ω could be observed when cells were cultured in the bioreactor system, resulting in approximately 1000 Ω. Values decreased to stable levels during the first five days of culture until culture termination. Channel 12 of the shown bioreactor showed higher impedance values during the whole measurement period than the other channels, but no increase was observed after cell inoculation. Furthermore, channel 2 and 16 showed a continuous increase in impedance signals subsequent to cell inoculation, which persisted until day 10 (channel 16) or day 15 (channel 2). Aberrant signals observed for some of the channels indicate defect sensors or disturbed impedance measurement (not shown).

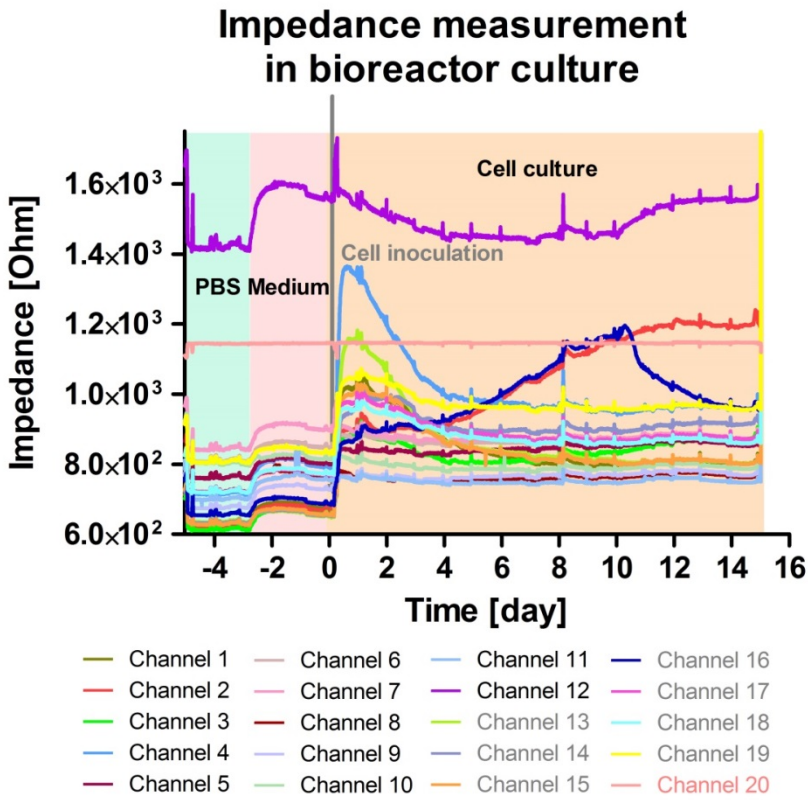

Figure 20: Impedance signal detection in an 8 ml analytical-scale bioreactor with B-13 cells.
The graph shows the time-course of impedance values in bioreactor cultures with B-13 cells subjected to trans-differentiation. Three impedance sensor foils were integrated in the cell compartment of the bioreactor. During the first two days (day -5 to day -3) PBS perfusion was performed followed by three days of culture medium perfusion (day -3 to day 0). Thereafter undifferentiated B-13 cells were inoculated and trans-differentiated over 15 days. The graph shows 20 channels of impedance measurement in one exemplary bioreactor over the culture time. Channels 1-12 show measurements on impedance sensor foils, channels 13-19 show impedance measurements between impedance sensor foils and channel 20 shows temperature measurement over time.

4.2.2 Identification of toxic drug induced cell damage in bioreactor cultures

The culture behaviour of B-13/H cells during toxic stress was investigated in 8 ml analytical-scale bioreactors (Figure 21). Methapyrilene was used to induce toxic stress to B-13/H cell cultures, since trans-differentiated B-13 cells possess the CYP isoform CYP2C11 responsible for toxic product formation from methapyrilene. Previous studies in 2D cultures have shown that a concentration of 0.2 mmol/l of methapyilene resulted in cell death when applied to B-13/H cells.[121]

Methapyrilene was successively applied in increasing concentrations to identify toxic concentrations in 3D bioreactor cultures. Two 8 ml analytical-scale bioreactors were inoculated with undifferentiated B-13 cells followed by 11 days of trans-differentiation

using 10 µmol/l dexamethasone. On day 11, 13, 15 and 17 methapyrilene was applied at a final concentration of 0.2, 0.4, 0.8 and 1.6 mmol/l to one of the bioreactors for six hours, respectively. The second bioreactor was used as untreated control during this time. Bioreactors were flushed with fresh culture medium and allowed to regenerate for 1.5 days after each toxic stress induction. The bioreactor exposed to methapyrilene treatment was terminated on day 22, whereas the control bioreactor was treated with 0.8 µmol/l methapyrilene for validation of the toxic effect of the drug at that concentration.

During the trans-differentiation period of 11 days both bioreactors showed similar performance in enzyme release (AST, LDH) and energy metabolism (glucose consumption and lactate production), as shown in Figure 21. Release rates of AST remained on basal levels over time. LDH started with increased values but declined to basal values during the first six days and stayed stable thereafter. Glucose and lactate decreased until day 5 followed by a continuous increase until day 11. Methapyrilene exposure resulted in a moderate increase in AST and LDH release at a concentration of 0.8 mmol/l, and in a drastic increase of enzyme release at 1.6 mmol/l. The untreated control bioreactor maintained stable values during toxic stress induction. Glucose consumption and lactate production showed a similar performance in the bioreactor treated with methapyrilene and in the untreated control bioreactor up to 0.8 mmol/l, with the exception of slight oscillations immediately after methapyrilene exposure. A drastic decrease in glucose consumption and lactate production was observed when the bioreactor (Bioreactor Intoxication) was exposed to 1.6 mmol/l methapyrilene and thereafter no regeneration could be observed. In accordance with the findings from the drug-treated bioreactor, AST and LDH release rates also increased dramatically in the control bioreactor when induced to 0.8 mmol/l methapyrilene on day 23, while glucose consumption and lactate production showed a prompt decrease.

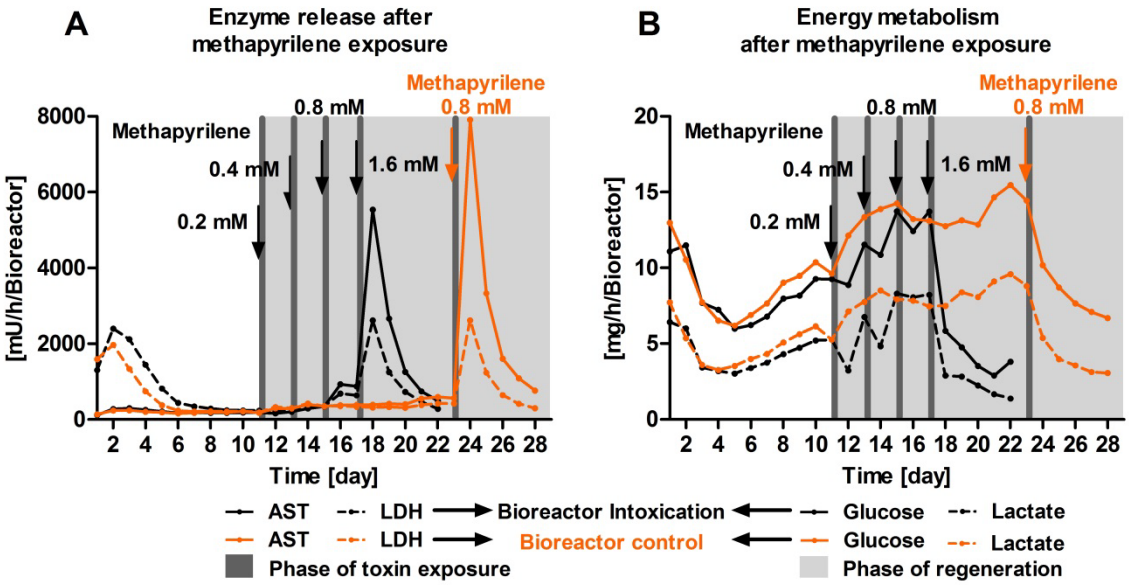

Figure 21: Identification of toxic methapyrilene concentrations in B-13/H bioreactor cultures.
Enzyme leakage of AST and LDH (A) as well as glucose consumption and lactate production (B) are shown over 22 days (black) or 28 days (orange) in B-13/H bioreactor cultures. Different concentrations of methapyrilene (0.2, 0.4, 0.8 and 1.6 mmol/l) with an incubation time of 6 hours were successively applied on days 11, 13, 15 and 17 (dark grey) in one bioreactor (black, Bioreactor Intoxication) with a parallel bioreactor used as a control (orange, Bioreactor Control). After each methapyrilene treatment a regeneration phase of approx. 36 hours (light grey) was performed. For further evaluation of methapyrilene toxicity the control bioreactor was exposed to 0.8 mmol/l methapyrilene on day 23.

To investigate the suitability and sensitivity of multi-parametric sensors (oxygen, ammonia and impedance) to detect toxicity in response to methapyrilene exposure in B-13/H bioreactor cultures two analytical-scale bioreactors were identically prepared. A concentration of 2 mmol/l methapyrilene was chosen based on dose-finding experiments to ensure detectable stress by integrated non-invasive online sensors. After 14 days of trans-differentiation one of the bioreactors was exposed to methapyrilene for 24 hours whereas the second bioreactor was used as an untreated control. Intoxication was followed by flushing the bioreactors to wash out residual toxic products. Afterwards bioreactors were set in standard perfusion mode with medium recirculation and continuous feed. To validate the results from the drug-treated bioreactor, the control bioreactor was also exposed to 2 mmol/l methapyrilene after termination of the first bioreactor, i.e. on day 17 and 18. Drug incubation was performed for 2.5 h each to detect potential cell regeneration between the drug applications.

The time-courses of offline parameters during the experiment are described in Figure 22. Enzyme release rates and rates of glucose and lactate metabolism showed a similar course as previously described until day 14. Methapyrilene exposure resulted in a temporary increase in AST and LDH release, which declined afterwards to almost zero.

Glucose and lactate metabolism decreased to zero after 2 mmol/l methapyrilene was introduced to the bioreactor culture, whereas the control bioreactor was unaffected. During intoxication of the control bioreactor on day 17 and 18, a similar reaction to methapyrilene in enzyme release and energy metabolism was observed, confirming the results from the first bioreactor. No indications for cell regeneration could be detected between methapyrilene applications. Intoxication on day 18 did not intensify the effect on enzyme release and energy metabolism.

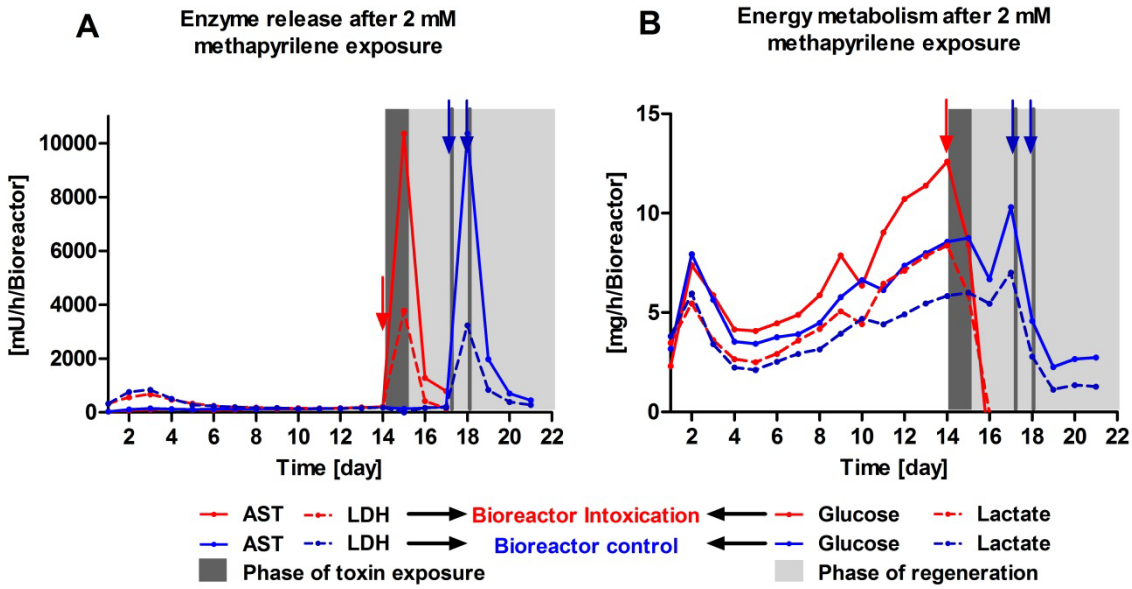

Figure 22: Enzyme release and energy metabolism in B-13/H bioreactor cultures treated with toxic doses of methapyrilene.
AST and LDH leakage (A) as well as glucose consumption and lactate production (B) are shown over 17 days (red) or 21 days (blue) of B-13/H bioreactor cultures. The bioreactor treated with 2 mmol/l methapyrilene on day 14 (red, Bioreactor Intoxication) was observed over 17 days and the control bioreactor over 21 days (blue, Bioreactor Control). For validation of the toxic stress response the control bioreactor was exposed to 2 mmol/l methapyrilene on day 17 and 18 each.

Monitoring of B-13/H bioreactor cultures using multi-parametric sensors resulted in recording signals in response to toxic methapyrilene induction for integrated sensors respectively.

Oxygen concentration in the circulating medium (Figure 23) continuously decreased during trans-differentiation of B-13 cells over 14 days in both bioreactors. Some short-time increases or decreases could be detected during this phase, which are probably due to temporary air bubbles disturbing optical-chemical sensor measurement. Application of 2 mmol/l methapyrilene for 24 h on day 14 resulted in a rapid increase in oxygen concentration until day 17 indicating a decrease in oxygen consumption by the cells, in consistence with the observed decrease in glucose metabolism. In contrast, the control bioreactor was not affected. However, an increase in oxygen concentration was shown

in the control bioreactor after exposure to 2 mmol/l methapyrilene on day 17 and 18 supporting the findings from the first bioreactor.

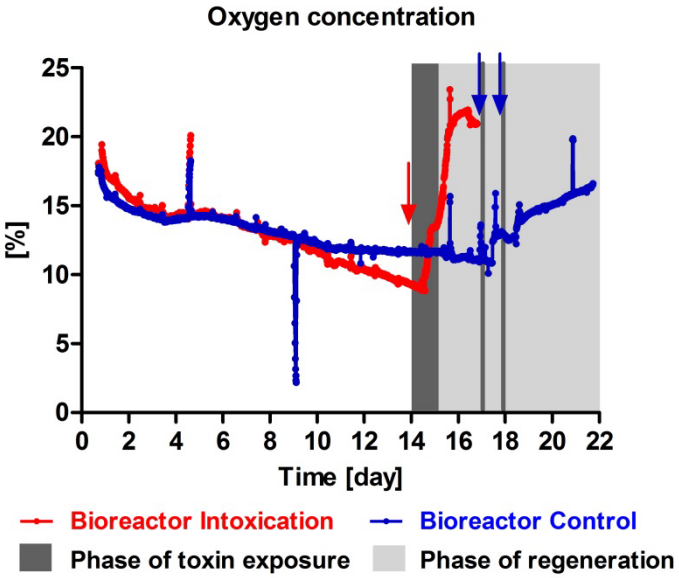

Figure 23: Online monitoring of oxygen concentrations in B-13/H bioreactor cultures exposed to 2 mmol/l methapyrilene.
One bioreactor (red, Bioreactor Intoxication) was treated with 2 mmol/l methapyrilene on day 14 (arrow) and observed over 17 days, whereas the control bioreactor (blue, Bioreactor Control) was continued until day 21. For validation of the toxic stress response the control bioreactor was applied to 2 mmol/l methapyrilene on day 17 and 18 (arrows).

Concentrations of ammonia in bioreactor culture perfusate (Figure 24) were measured offline as well as online, using an improved ammonia sensor (see 3.2.2.3). Both bioreactors showed a slight but continuous increase for online sensor measurement during 14 days of trans-differentiation whereas the electrical potential increase was more pronounced in the intoxication bioreactor as compared to the control bioreactor. Offline values of ammonia increased until day 5 and remained stable until day 15. Application of 2 mmol/l methapyrilene on day 15 resulted in a decline in ammonia release, which was detected with both, offline and online measurements. Regeneration from toxic injury was not observed thereafter. In the control bioreactor, the performance of online sensors integrated in the tubing system was comparable with values measured in daily samples (offline) out of bioreactor culture perfusate. Similar to the first bioreactor, a decline during 24 h of intoxication on day 17 and 18 was observed. Measurements of daily samples mostly showed values matching online values, except for some fluctuations in online signals due to medium or gas leakage in the sensor connections. In addition, data obtained by online sensors showed considerable background noises in signal retrieval. Analysis and plotting of received data was accomplished by the cooperation partner CEA-Leti-France.

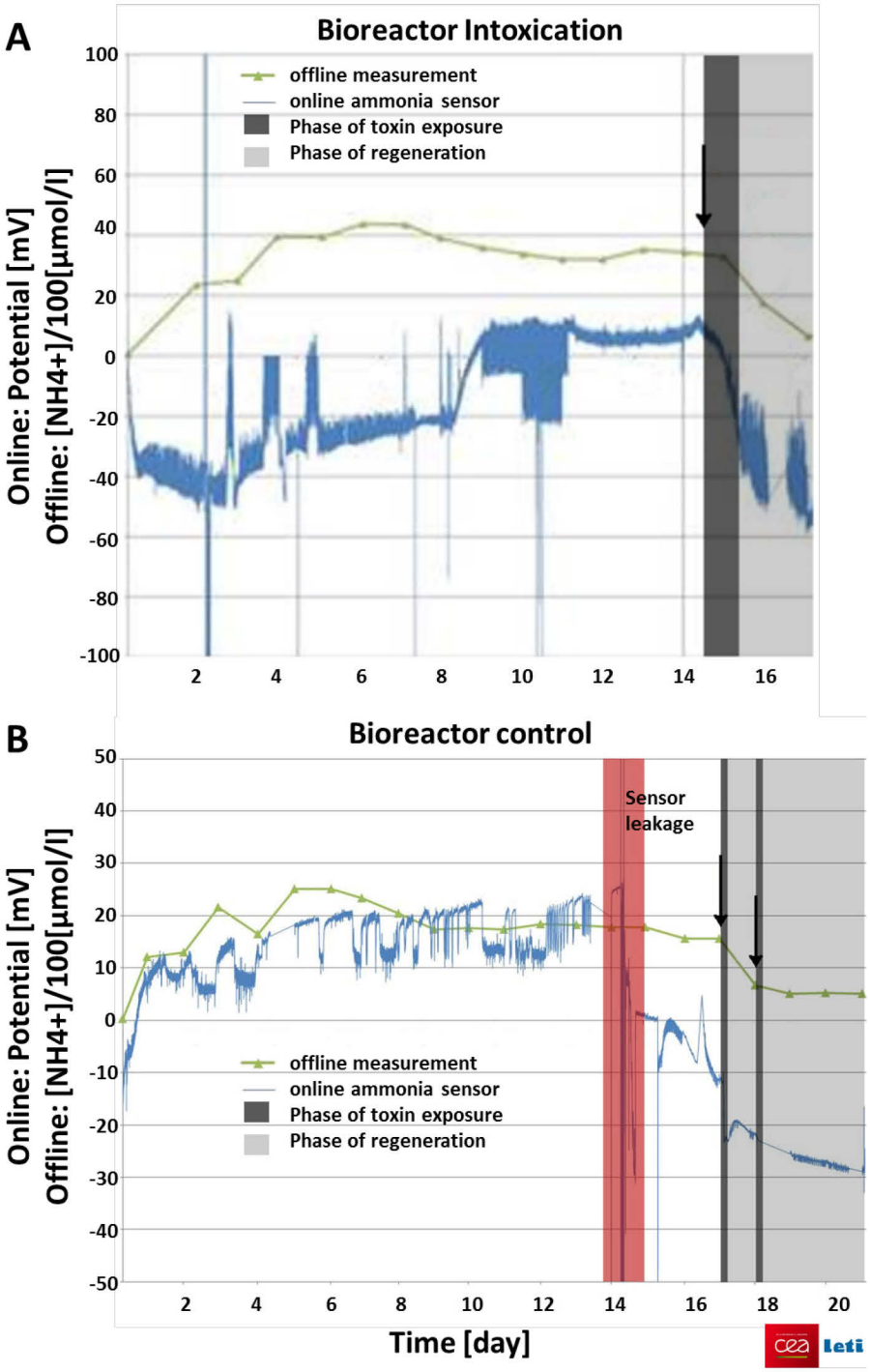

Figure 24: Online and Offline monitoring of ammonia concentrations in B-13/H bioreactor cultures exposed to 2 mmol/l methapyrilene.
The potential obtained from online ammonia sensors (blue) and ammonia concentrations measured offline (green) was analysed in B-13/H bioreactor cultures subjected to intoxication on day 15 (A, Bioreactor Intoxication) or used as a control during day 15 and intoxicated on days 17 and 18 (B, Bioreactor Control). Arrows and areas marked in dark grey indicate the application of 2 mmol/l methapyrilene for 24 h (A) or 2.5 h (B). Thereafter, a regeneration period was applied (shown in light grey). The red zone illustrates leakage occurring in ammonia sensors of the control bioreactor culture on day 14. Analysis and plotting of received data was accomplished by the cooperation partner CEA-Leti-France.

Impedance signals showed an initial increase after cell inoculation (Figure 25) in both bioreactors followed by rising values of impedance during the first 14 days of culture. Impedance signals rapidly declined to values similar to those measured prior to cell inoculation after application of 2 mmol/l methapyrilene to the first bioreactor on day 14 (Bioreactor Intoxication, Figure 25A / channel 1-4), while the untreated bioreactor (Bioreactor control) showed stable impedance signals on day 14 (Figure 25B / 6-9). This bioreactor showed a drastic decline in impedance signals when exposed to 2 mmol/l methapyrilene on day 17 and 18 for 2.5 h. Thus, a comparable response to toxin exposure was observed in both bioreactor cultures. Repeated small signal peaks of impedance signals correlating with daily sample taking management were detected during the whole culture period. Further peaks were observed during flushing of bioreactors after toxin exposure on day 14 (Bioreactor Intoxication) resp. day 17 and 18 (Bioreactor control).

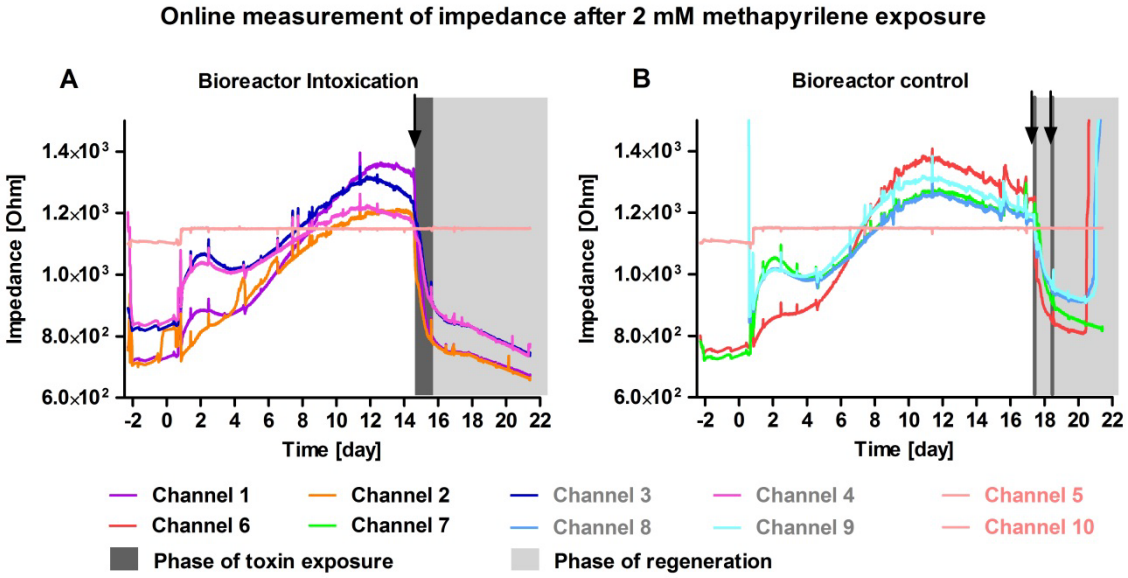

Figure 25: Online monitoring of impedance in B-13/H bioreactor cultures exposed to 2 mmol/l methapyrilene.
Impedance signals were monitored during PBS perfusion prior to cell inoculation (day -2 to day 0) and during B-13 cell culture, including 14 days of trans-differentiation followed by toxic drug application. The first bioreactor (A, Bioreactor Intoxication) was subjected to intoxication with 2 mmol/l methapyrilene on day 14 for 24 h (black arrow). In addition, methapyrilene was applied to the untreated control (B, Bioreactor Control) on day 17 and 18 for 2.5 h each (black arrow) for validation. Channels 1, 2, 6 and 7 show measurements on impedance sensor foils, channels 3, 4, 8 and 9 show impedance measurement between different impedance sensor foils and channels 5 and 10 show temperature measurements over time.

4.2.3 Evaluation of primary porcine liver cell culture in the bioreactor system equipped with multi-parametric sensors

To evaluate the multi-parametric sensor system in a clinical setting, ppL were investigated in the system as an optional cell source for the establishment of a clinical-grade bio-artificial liver. As a surrogate for toxic patient plasma, the effect of exposure to the hepatotoxic drugs APAP and diclofenac was investigated.

4.2.3.1 Assessment of acetaminophen and diclofenac toxicity in 2D cultures

In order to identify suitable doses of APAP and diclofenac to induce a toxic stress response in ppL, initial tests were performed in 2D cultures treated with different drug concentrations (APAP: 5 mmol/l, 10 mmol/l, 30 mmol/l, diclofenac: 100 µmol/l, 300 µmol/l, 1000 µmol/l). Figure 26 shows morphological changes in 2D cultures of ppL after three days of toxin exposure. The application of 5 mmol/l APAP had no apparent effect on the cells, while 10 or 30 mmol/l APAP resulted in cell injury with loosening of cell-cell contacts, detachment from culture plate surface and cell disintegration. Similar effects were observed for diclofenac at a concentration of 1000 µmol/l. Analysis of metabolic parameters (Figure 27) revealed a decline in lactate production, which increased with increasing concentrations of APAP or diclofenac over six days of drug exposure. In accordance with findings from lactate production, increasing ammonia release rates were observed with increasing substance concentrations indicating increasing cell injury. In contrast to the findings from microscopic observation, metabolic data indicate an effect of drug exposure already at the lowest concentrations investigated, i.e. 5 mmol/l for APAP and 100 µmol/l for diclofenac.

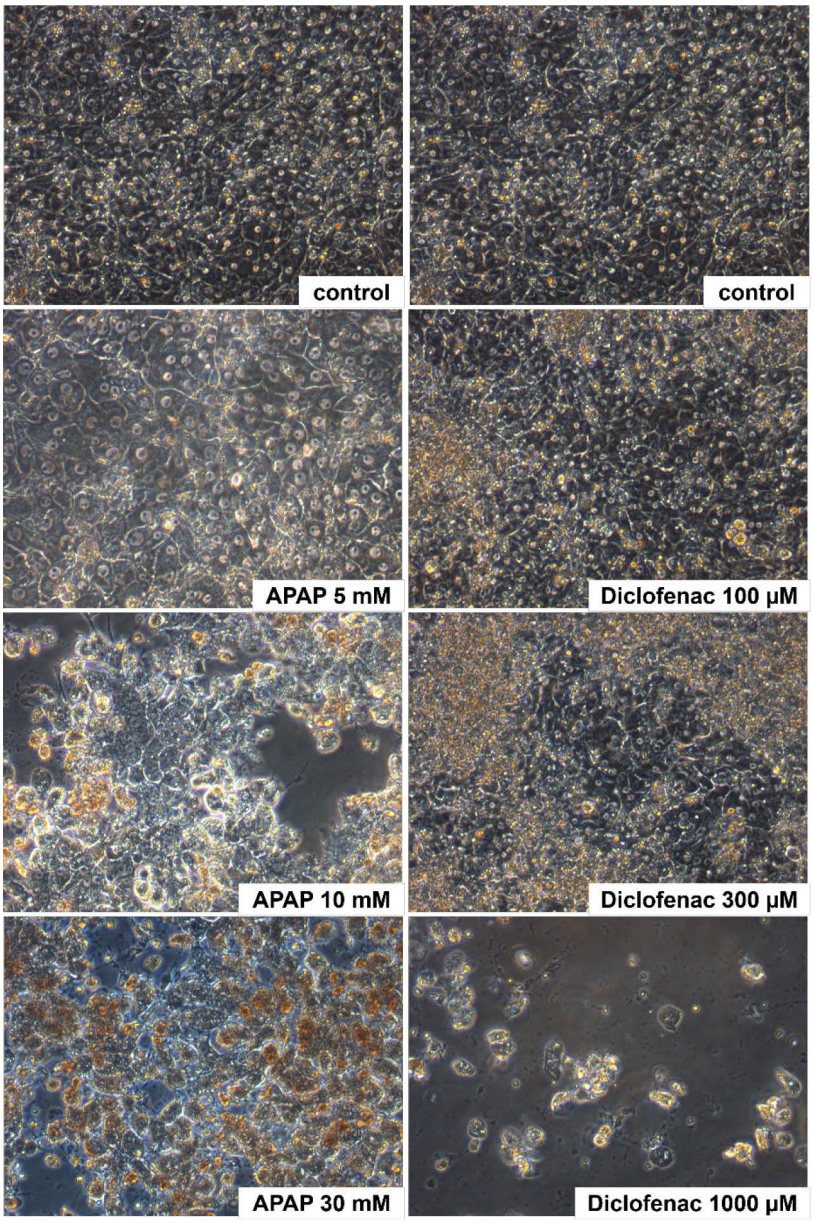

Figure 26: Morphological alterations in ppL treated with APAP or diclofenac in 2D culture systems.
Light microscopic pictures (Magnification 100x) of ppL exposed to APAP (left) or diclofenac (right) at different concentrations, as compared with untreated control cultures. Cultures were examined after three days of drug application.

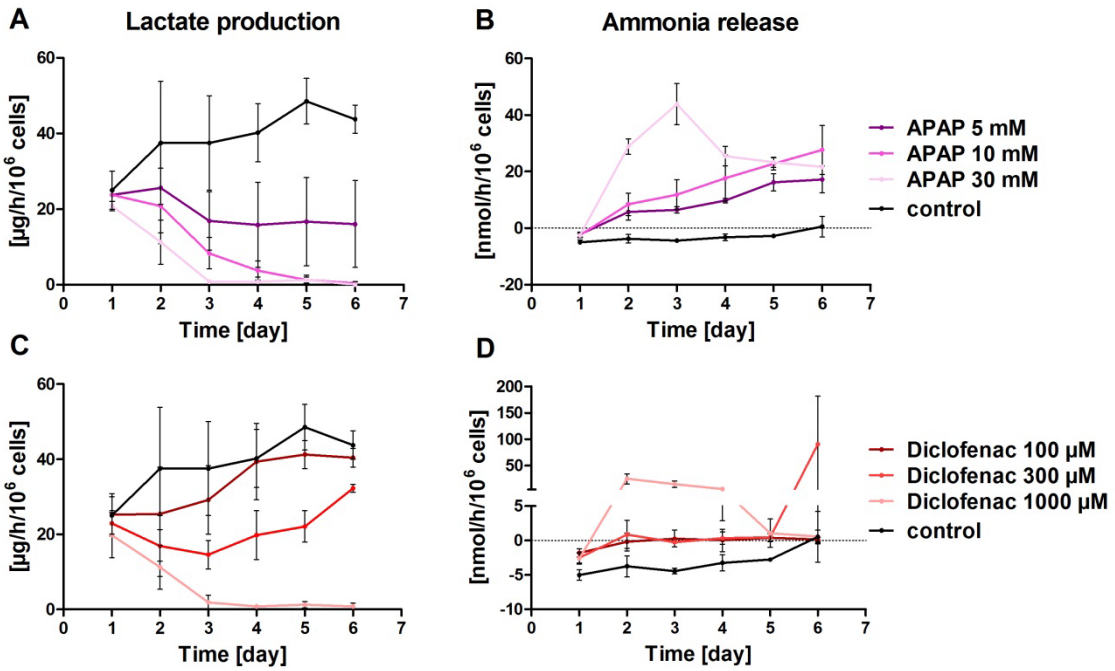

Figure 27: Lactate production and ammonia release in ppL treated with APAP or diclofenac in 2D culture systems.
The metabolic performance (lactate and ammonia production) of ppL exposed to different concentrations of APAP or diclofenac is shown over a time period of six days. Values were calculated as rates per 10^6 cells.

4.2.3.2 APAP intoxication in bioreactor cultures with primary porcine liver cells

Based on the results from 2D cultures, APAP was used to assess the effect of toxin exposure in bioreactor cultures with integrated multi-parametric sensors. Experiments were performed in 8 ml analytical bioreactors equipped with online sensors for impedance, ammonia, pH and oxygen measurement. In each experiment, one bioreactor was chosen as intoxication model whereas the second one was used as untreated control. A concentration of 5 mmol/l APAP was chosen to enable cell regeneration after 24 h of APAP exposure. Experiments were conducted three times with cells from different preparations.

Evaluation of primary porcine liver cell cultures in the bioreactor system (Figure 28) showed an increase in ammonia release during 5 mmol/l APAP exposure (24 h), which declined to levels prior to APAP application after flushing the system with fresh culture medium. Production of urea started with increased values, which strongly declined until day 3, followed by relatively stable values during the further culture. Control bioreactors showed no significant increase in ammonia release during first APAP intoxication, but during the second APAP exposure on day 6 ammonia release increased and maintained levels until end of culture. Urea production was not influenced during intoxication period but declined to similar levels of bioreactors subjected to 5 mmol/l

APAP intoxication. Upon application of 5 mmol/l APAP, values declined further but regenerated to values prior to APAP exposure after flushing with fresh culture medium. Glucose and lactate production showed a stable performance during 9 days of culture with a slow decrease for glucose until day 4. Production rates of both parameters were reduced during intoxication and slowly regenerated thereafter. Glucose production showed higher values in the control bioreactor than in the bioreactor treated with 5 mmol/l APAP and levels remained stable during the culture period. Lactate production was not markedly affected by APAP exposure.

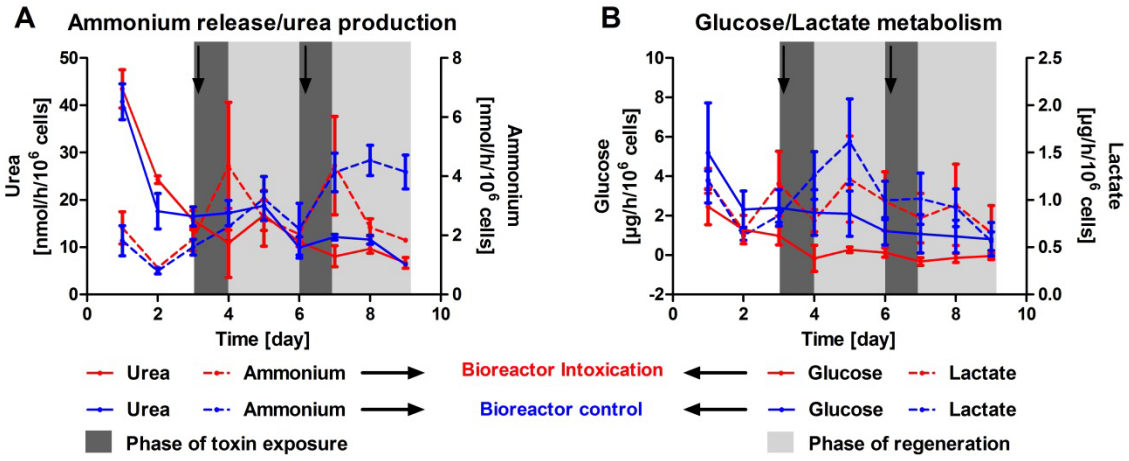

Figure 28: Performance of offline parameters during APAP application in ppL bioreactor cultures.
Bioreactor cultures were maintained over 9 days with daily measurement of ammonia release, urea, glucose and lactate production. One group of bioreactors (red, Bioreactor Intoxication) were exposed to APAP at a concentration of 5 mmol/l for 24 h on day 3 and day 6 (dark grey) followed by a regeneration phase (light grey) of two days. Untreated bioreactor cultures (blue, Bioreactor Control) were used as a control. Graphs show means ± SEM of three independent experiments (n=3).

Time-courses of oxygen concentrations measured online in culture perfusates are shown in Figure 29. After cell inoculation the concentration of oxygen drastically declined until day 1 describing values between 12-15%. Thereafter a continuously increase could be observed until the end of culture reaching values of 19-21%. Absolute oxygen concentrations in culture perfusates were lower in control bioreactors than in bioreactor cultures subjected to intoxication, while the course of the oxygen curve was comparable. No effect could be detected during exposure of 5 mmol/l APAP on day 3 and day 6.

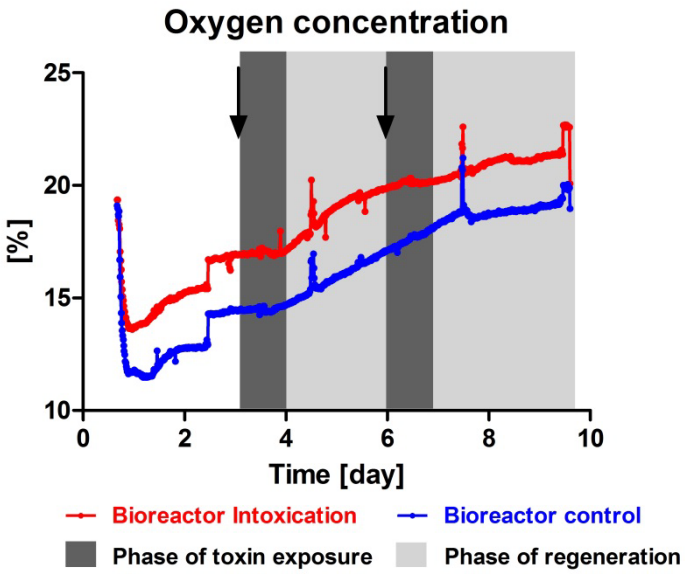

Figure 29: Online monitoring of oxygen concentrations during APAP application in ppL bioreactor cultures.
Bioreactor cultures were maintained over 9 days with continuous measurement of oxygen concentration in the culture perfusate. One group of bioreactors (red, Bioreactor Intoxication) were exposed to APAP at a concentration of 5 mmol/l for 24 h on day 3 and day 6 (dark grey) followed by a regeneration phase (light grey) of two days. Untreated bioreactor cultures (blue, Bioreactor Control) were used as a control. Graphs show means ± SEM of three independent experiments (n=3).

Unfortunately data of online ammonia measurement using upgraded ammonia sensors (Figure 6) could not be used for these experiments due to occurrence of electrical noises, which disturbed signals throughout the experiments (data not shown). The usage of an inverter did not reduce the source of noise.

Impedance measurement showed a temporary peak during cell inoculation. Thereafter impedance values remained rather stable until the first intoxication session. During exposure of 5 mmol/l APAP for 24 h impedance values declined in bioreactor cultures subjected to intoxication whereas control bioreactor cultures were unaffected. Flushing the bioreactors with fresh culture medium at the end of APAP application resulted in a strong increase in impedance to values similar to those detected prior to intoxication. Toxic effects were less marked during second APAP application session on day 6. In total a slight decrease could be observed during nine days of culture in bioreactors subjected to intoxication, whereas impedance values of control bioreactors were stable. Signal courses of representative impedance channels are shown in Figure 30.

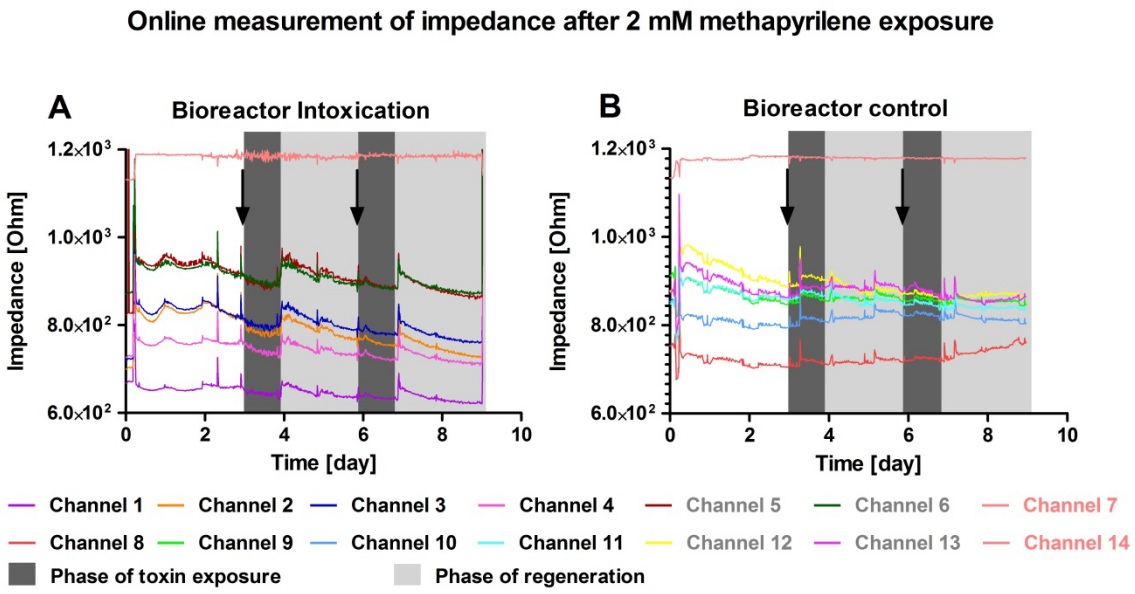

Figure 30: Online monitoring of impedance during APAP application in primary ppL bioreactor cultures.
Bioreactor cultures were maintained over 9 days with continuous measurement of impedance. One group of bioreactors (A) was exposed to APAP at a concentration of 5 mmol/l for 24 h on day 3 and day 6 (dark grey, arrows) followed by a regeneration phase (light grey) of two days. Untreated bioreactor cultures (B) were used as a control. Graphs show representative signal curves of impedance channels. Channels 1-4 and 8-11 show measurements on impedance sensor foils, channels 5, 6, 12 and 13 show impedance measurements between different impedance sensor foils and channels 7 and 14 show temperature measurement over time.

4.2.4 Chapter discussion

In order to ensure efficient and safe therapeutic application of a bio-artificial liver device in extracorporeal liver support sessions the cell source housed in such a device has to be closely observed before and during clinical application. To ensure patient safety in clinical applications, system functions and culture quality parameters need to be monitored on a regular basis to control culture conditions and ensure sufficient metabolic activity of the cells during therapeutic use. In addition, an early prediction of the culture quality could improve the decision about potential clinical use of the culture. Therefore, integration of online sensors for monitoring of the cell behaviour and perfusion conditions, would contribute to the successful and safe clinical application of the bio-artificial liver device. In particular, non-invasive real-time monitoring methods are of interest for culture evaluation in clinical liver support sessions.

In this part of the thesis potential online sensors for oxygen, pH, ammonia and impedance when integrated in the bio-artificial liver device were investigated. Oxygen sensors can give information about cell activity and can also be used to estimate cell numbers in 3D constructs, if data on oxygen consumption of the used cell type are available.[155] Further, the determination of ammonia concentration in the culture perfusate would be of interest since ammonia clearance represents one of the main aims of extracorporeal liver support application.[39,69] Impedance measurement describes an option to assess the cell behaviour during culture due to the non-invasive label-free methodology.[156,157] The cell viability and proliferation activity in 2D cultures are usually assessed by means of microscopic observation or destructive analytical methods (e.g. cell counting in a counting chamber, quantification of DNA or live/dead fluorescent dye staining). Such end-point analyses would require opening of the bioreactor and are therefore not feasible during clinical application. [156,168]

To ensure safe usage, possible effects of sensors intended for use in the bio-artificial liver device were tested comparing the metabolic activity and functionality of B-13 cells in bioreactors with or without integrated sensors (oxygen, pH, ammonia, impedance). Results from experiments culturing B-13 cells in 8 ml analytical-scale bioreactors confirmed previously obtained results when evaluating B-13 cell trans-differentiation in the 2 ml analytical-scale bioreactor system (B-13/HT)(4.1). The comparison of offline parameters (glucose and lactate metabolism, enzyme release [ALT, AST, GLDH, LDH, amylase], production of urea and albumin or transformation of CYP1A1 substrate) in bioreactors with or without integrated sensors showed no negative effects on cell performance when online sensors were integrated into the bioreactor or the tubing system. Immunohistochemical staining confirmed these observations. Thus, integration of non-invasive online sensors for oxygen, pH, ammonia and impedance measurement did not impair the outcome of B-13 cell trans-differentiation in 3D bioreactor system.

Flow-through optical-chemical sensors integrated in the recirculation tubing were used for oxygen and pH monitoring in bioreactor cultures due to their easy accessibility, smooth integration into the system and stable performance. Oxygen sensors detected a continuous decrease in oxygen concentration in the culture perfusate during B-13 cell trans-differentiation over 15 days, which was confirmed by daily offline measurement using a clinical blood gas analyser. Overall lower values measured via online sensors compared to offline measurement can be attributed to sensor calibration using PBS solution conducted by the supplier. Different compositions of culture medium used corresponded to variances in signal manifestation. Similar, lower online pH values were revealed compared to offline measurement during evaluation of pH online sensors due to PBS calibration conducted by the supplier. Temporary occurrence of signal oscillations can be ascribed to air bubble formation blocking the contact of the optical-chemical polymer layer to the culture perfusate. As a precaution it is advisable to set medium bubble traps in front of the optical-chemical flow-through cells to minimize the described disturbing interference.

Since ammonia is a critical marker in ALF or ACLF, it is regularly measured during extracorporeal liver support, e.g. via micro-diffusion apparatus or via enzymatic methods using the reaction of GLDH or ammonium electrodes.[35,60,88–90,139] The ammonia sensor construct used in this study was made of a three-way flow-through cell containing in one outlet the cone sized ammonia sensor. Ammonia sensors were placed in the outlet line of the bioreactor tubing system, which represents the inlet line conducting plasma to the patient after passing the bioreactor. Thus, measurement at this site allows for assessment of the ammonia concentration supplied to the patient during liver support treatment. The ammonium sensitive membrane was in direct contact with the culture perfusate. To allow for accurate determination of actual ammonia concentrations in the perfusate, ammonia was measured in culture perfusate from the bioreactor and fresh culture medium, and the ammonia production was calculated based on the difference between both values. For evaluation of online ammonia sensors, these had to be sterilized to avoid microbial contamination. Studies performed at the cooperation partner CEA-Leti-France showed that gamma or beta irradiation of ammonium sensitive membranes caused uninterpretable and noisy signal detection. Hot steam sterilization at 121°C would have harmed the ammonium sensitive membrane. Thus, sensors were assembled under sterile conditions and flushed with 70% ethanol for sterilization, which showed no influence on sensor performance. Since sensors were integrated into the outlet line of the bioreactor tubing system equipped with a recoil valve to prevent retrograde flow of the perfusate, the risk for contamination was low in the *in vitro* experiments performed in this study. However, the sterilization process has to be optimized before potential clinical use of the system.

First measurements using ammonia sensors resulted in positive ammonia detection in the bioreactor culture perfusate. In the B-13 bioreactor experiments analysed by CEA-Leti-France the time-course of ammonia recorded with the online sensors was similar to that of offline values analysed in samples from the culture perfusate. Critical issues of ammonia sensors can be seen in the regular occurrence of interference in signal detection and also in the limited detection range of approx. 1800 µmol/l. The disturbances observed in the electric potential could be due to air bubbles on ammonium sensitive membrane, as it was also shown for optical-chemical flow-through cells of oxygen or pH measurement. As a solution bubble traps were integrated prior to ammonia sensors to prevent those signal interferences. Another problem was in frequent sensor leakages increasing the risk of microbial contamination. The sensor construct was quite instable in its current structure suggesting an update of the design. The use of a pseudo-reference electrode (Bioreactor 02) strongly affected the lifetime of the ammonia sensor (approx. 3.5 days) due to induction of a drift of the electric potential, suggesting the usage of true reference electrodes for further experiments. Therefore, CEA-Leti-France changed the design of the ammonia sensor construct as described in 3.2.2.3, and the modified version of the sensor was investigated in the following experiments (4.3).

For measurement of impedance to monitor changes in the cell behaviour sensor electrodes were placed inside the cell compartment of the bioreactor. The foil-based impedance sensors were selected due to their flexibility making the integration procedure more practicable. First cell culture tests at the cooperation partner Fraunhofer IBMT showed the suitability of designed foil-based impedance sensors for cell adherence and culture (data not shown). For online measurement of impedance, sensor electrodes were placed between the capillaries inside the cell compartment of the 8 ml analytical bioreactor by the cooperation partner Stem Cell Systems, Berlin. Three sensor foils were used in the 8 ml analytical bioreactor carrying 8 electrodes each, which creates a network of 24 independent electrodes in the cell compartment. Thus measurement of impedance variances between each sensor point was possible, with single sensor failure being compensated by parallel measurement. Furthermore, measurements between single sensor electrodes on different sensor foils integrated at different locations in the cell compartment were performed to enable a better overall evaluation of cells housed in different areas within the bioreactor. Formaldehyde gas sterilisation was used and did not influence impedance measurement. Pilot bioreactor experiments using B-13 cells subjected to trans-differentiation revealed that impedance measurement can be used as a sensitive non-invasive method to observe the culture performance in the bioreactor. Impedance measurement was capable of detecting changes of the culture medium. Furthermore, cell inoculation was detected by strong

impedance increase, probably caused by cell attachment on single sensor electrodes. The following decline of impedance signals can be attributed to partial loss of cells due to initial cell stress, in consistence with the observed peak in LDH release during the first days of culture. Stable values were observed after 3 days of culture, showing approx. 100 Ω higher impedance values compared to values prior to cell inoculation, which indicates successful and stable adherence of a number of cells to the foils. Cell attachment can be found in an area of around 1000 Ω whereas decreasing values indicate cell detachment or cell damage resulting in decreased electric potentials. Impedance sensor performance showing a constant increase could be ascribed to cell proliferation.

Values above 10^6 Ω or steadily increasing can indicate sensor failure. One possibility causing sensor failure could be defaults in the manufacturing process, e.g. encapsulation of sensor electrodes in the polyurethane housing resulting in a strong interference of the impedance measurement. Another critical point is the sensor connection to the measuring device. The sensor foil has a thickness of only 20 µm to minimize possible disturbing effects to the internal medium flow in the cell compartment. Thus, the foils are quite fragile and bear the risk of sensor snapping. This was improved by making the sensor ends thicker for safe connection to the adapter board. A continuous increase in impedance signals gaining values above $1.5x10^3$ Ω as observed in part of the bioreactors can be due to air bubble accumulation on sensor electrodes in the cell compartment, which can disturb impedance measurement. To avoid this effect, regular degassing of the cell compartment should be performed.

Methapyrilene was selected as a model drug for investigating toxicity in B-13/H bioreactor cell cultures, since it is bioactivated by CYP2C11,[181] which is found to be expressed in B-13/H cells.[121] Toxicity experiments showed methapyrilene induced stress in B-13 bioreactor cultures subjected to trans-differentiation, as previously described for 2D cultures by Probert *et al*.[121] Investigation of different methapyrilene concentrations revealed toxic effects in a concentration range of 0.8-1.6 mM. Cell damage was indicated by a strong increase in release of liver enzymes (AST, LDH) and a decline in glucose consumption and lactate production. Enzyme levels decreased rapidly until day 17 of culture, which can be explained by exhaustion of cytosolic enzyme stores. Compared to 2D experiments conducted by Probert *et al*.[121] an 8-fold higher methapyrilene concentration was required to induce toxic stress in bioreactor cultures. One explanation could be incomplete trans-differentiation of B-13 cells in the bioreactor, for example due to adsorption of dexamethasone, used to induce B-13 cell differentiation, to the bioreactor material. However, such binding processes were excluded by comparing absolute levels of dexamethasone in bioreactor perfusates and 2D cultures.[172] The trans-differentiation success of B-13 cells in the bioreactor system

was shown to depend on the cell density favouring the use of lower densities.[172] Furthermore, bioreactor cultures maintained for prolonged time periods revealed higher numbers of differentiated B-13/H cells in association with higher liver-specific marker expression, suggesting that the trans-differentiation process in the 3D environment requires more time compared to B-13 2D cultures. This hypothesis is supported by the finding that exposure to 0.8 mmol/l methapyrilene showed only slight effects in the bioreactor when applied on day 15, but induced strong toxic stress upon exposure on day 23, which indicates an increased sensitivity of the cells on day 23 due to advanced cell maturation with higher CYP2C11 activity. Methapyrilene exposure at increased concentrations from day 11 to day 17 showed distinct toxic stress from a concentration of 1.6 mmol/l, as indicated by increased enzyme release and decline in glucose metabolism.

Based on these results a concentration of 2 mmol/l methayprilene applied for 24 h in B-13/H bioreactor cultures was chosen for the investigation of non-invasive sensor performance during toxic stress application. Toxic stress was successfully monitored via non-invasive sensors integrated in the bioreactor system. The application of 2 mmol/l methapyrilene for 24 h resulted in a rapid increase in oxygen concentration indicating decreasing oxygen uptake of the cells, which can be ascribed to cell damage leading to impaired energy metabolism of the cells. As expected, the untreated bioreactor showed no changes in oxygen concentration in the culture medium, as recorded by the online sensors. The toxic effect of 2 mmol/l methapyrilene also resulted in a decrease in ammonia production by the cells measured via online sensors, which was confirmed by offline measurement of daily samples. During the second week the ammonia sensor in the control bioreactor showed leakage causing drying out of the ammonia sensor, which resulted in a drastic signal decline to a lower level. Despite of this disturbance, intoxication on day 17 resulted in a decrease in ammonia concentration as well, which was confirmed by offline measurement of ammonia in culture samples. Another problem was the occurrence of background signals during potential measurement of the ammonia sensors. Analysis of the frequency spectrum via Fast Fourier Transformation would be an option to identify the source of electric noises. As a compromise CEA-Leti-France added an inverter to their measurement device to avoid electrical noise for further experiments.

Foil-based impedance measurement allowed for continuous real-time detection of changes in the bioreactor culture after toxic methapyrilene exposure. A rapid decline in impedance signals to values similar to those measured prior to cell inoculation was observed upon 2 mmol/l methapyrilene application. The observed decrease could be the result of cell detachment from the sensor electrodes and/or morphologic changes due to apoptosis or necrosis of the B-13 cells induced by toxin exposure. No recovery in

impedance signals was observed after flushing the bioreactor, indicating that cells were irreversibly damaged by toxic methapyrilene exposure. Comparable responses to toxin exposure were observed in the bioreactor treated on day 14 (Bioreactor Intoxication) and in the bioreactor treated on day 17 (Bioreactor Control). The second treatment on day 18 of the control bioreactor did not result in a further decrease confirming irreversible cell damage after the first treatment, in consistence with offline parameters showing an exhaustion of intracellular enzyme stores and a breakdown in energy metabolism.

To evaluate the bio-artificial bioreactor system including multi-parametric sensors in a clinical setting, ppL were isolated and cultured in the bioreactor system. Primary porcine liver cells (ppL) had proven to be a competent candidate in the realization of extracorporeal liver support therapies.[35,88,135–137,139,141] As a model for toxic patient plasma perfusion of bioreactor cultures, the effect of toxic drug exposition was investigated. Studies in 2D primary porcine liver cell cultures revealed distinct morphological and metabolic changes when using APAP in a concentration range of 10-30 mmol/l or diclofenac at a concentration of 300 µmol/l to 1000 µmol/l. As a model drug in bioreactor experiments APAP was chosen, since it is a widely used analgetic and antipyretic agent and is known to cause severe liver damage when applied in high doses.[182] Investigations focused on the identification of drug-induced cell stress by non-invasive sensors. To enable cell recovery after toxic drug exposure APAP was applied at a concentration of 5 mmol/l for 24 h followed by a regeneration phase of 48 h.

Measurement of offline parameters (urea, ammonia, glucose and lactate) in primary porcine liver cell bioreactors showed an increased glucose production during the first days of culture, which can be ascribed to glycogen breakdown in the initial culture phase, when cells are stressed by the preceding cell isolation procedure.[77,169] After an adaption time of approx. three days stable metabolic performance of cell cultures was observed. Measurement of offline parameters revealed a direct influence of APAP exposure on cell metabolism. APAP induced stress was manifested by increasing ammonia levels in the intoxicated bioreactor, in addition to a temporal decrease in urea and lactate production indicating impaired cell metabolism. Cells regenerated afterwards during the recovery phase as indicated by stabilization of metabolic activities. The untreated control bioreactor cultures showed no direct affection by APAP exposure on day 3, but ammonia levels increased after day 6 and urea and lactate production declined after day 5. A possible reason for these changes in metabolic behaviour of the cells can be seen in air intake into the cell compartment of the control bioreactor. Air intake into the bioreactor cell compartment can result from overpressure produced by the gas supply device resulting in the bursting of the gas capillaries. Blocking of the degassing tube during daily bioreactor management could have

produced a similar effect. During the experiments it was not possible to clearly identify the cause of undesired air intake

APAP induced cell stress could not be recognized via online oxygen measurements. The continuous increase in oxygen concentrations over the culture period indicates a decrease in metabolic activity of the cells, which was not further affected by drug exposure. Direct measurement of oxygen uptake by the cells in the cell compartment could be more suitable to detect induced stress, but this would require temporary stopping of perfusion and gas supply and therefore may negatively impact medium flow and pressure conditions in the system. Integration of micro-sensors, e.g. needle-type oxygen micro-sensor (PreSens-Precision Sensing GmbH), into the cell compartment would be another option but bears an additional risk of microbial contamination during integration of sensor channels. In addition, using such micro-sensors in the bioreactor device is difficult due to their fragility.

Investigation of ammonia measurement unfortunately still showed deficiencies due to the offspring of unidentified noises in signal detection. The integration of an inverter into the ammonia measurement device did not reveal the source of noises. Thus, evaluation of results from ammonia measurement was not possible.

The results of online impedance measurements showed a decline of signals after drug exposure. Cell regeneration during the recovery phase was detected by increasing impedance signals, indicating reversible changes in cell morphology and/or cell composition upon drug exposure. Impedance measurements in the control bioreactors showed less pronounced changes in impedance signal performance after intoxication on day 6, probably due to the undesired intake of air into the cell compartment, indicated by an increase in impedance values up to greater than 2000 Ω resulting in several measured channels (data not shown).

In conclusion, optical-chemical flow-through cell sensors for oxygen or pH showed good correlation with offline values of those parameters, easy feasibility and provide options for closed-loop culture management keeping culture conditions constant, e.g. pH or gas supply. The online ammonia sensors used showed acceptable correlation to ammonia concentrations measured in offline samples. Still further effort has to be taken into sensor development to avoid noise evolvement and liquid leakage during signal detection. In addition, a suitable method for sensor sterilisation according to clinical requirements has to be established. The chemical material for ammonium sensitive membrane showed low sensitivity and cross-reaction with other ions, e.g. Na+, K+ and Cl-, which limits the sensor sensitivity. Thus, alternative options could be considered, e.g. use of fibre optic ammonia sensors[183] but need to be adapted for clinical application. Furthermore, based on the experimental results a concept for culture prediction and decision-making was established based on impedance measurement. The

development of impedance signals in a 3D high-density liver cell bioreactor culture can be classified into three culture states namely “Normal”, “Sub-critical” and “Critical”. The “Normal” state describes constant or rising impedance values representing stable cell culture performance. In case of B-13 cell culture it additional describes cell proliferation and successful trans-differentiation in the bio-artificial liver. The “Sub-critical” state describes a moderate decrease in impedance values indicating possible cell stress or cell damage with the possibility of recovery, or changes in the cell morphology, composition or adhesion to impedance sensor foils. If this scenario occurs, the bio-artificial liver cell culture has to be kept under careful surveillance. In particular, any further changes in impedance values and additional parameters (e.g. oxygen, ammonia) should be taken into account to make a decision about measures to be taken, e.g. additional application of albumin dialysis for detoxification of the plasma to protect the cells from toxic injury. The “Critical” state in impedance signal interpretation indicates a sudden and drastic decrease in impedance values describing significant stress resulting in irreversible damage to the bio-artificial bioreactor culture. If this scenario occurs, recovery of the bioreactor culture will be unlikely and the bioreactor culture should be terminated. Figure 31 describes the concept for culture prediction and decision-making based on B-13 bioreactor cultures subjected to trans-differentiation and intoxication using 2 mmol/l methapyrilene.

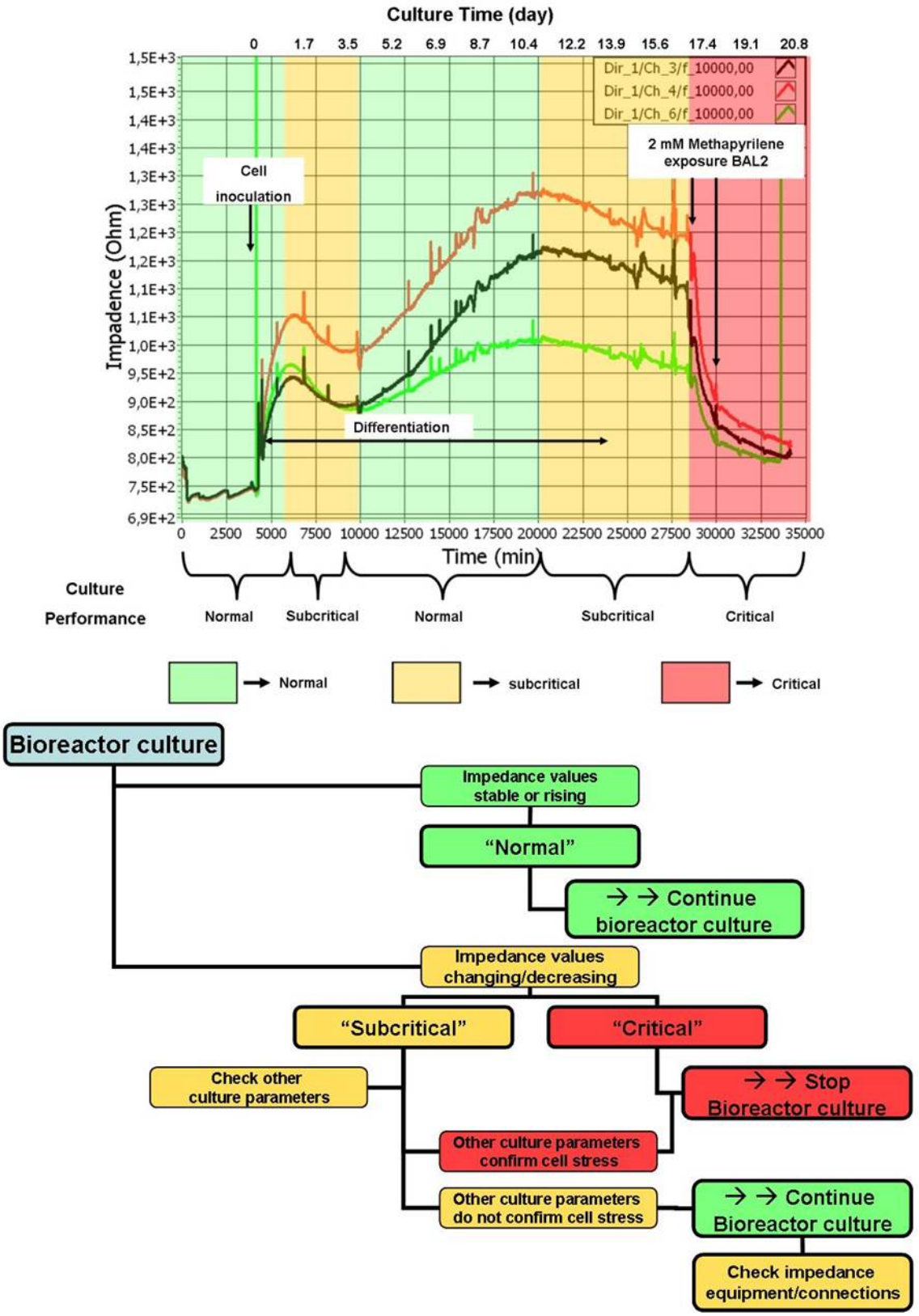

Figure 31: Classification of bio-artificial liver culture behaviour
Classification of the status of the cell culture by impedance measurement and procedures for culture surveillance and decision making, based on the three different scenarios for bio-artificial liver support: "Normal", "Sub-critical" and "Critical" exemplarily using B-13 bioreactor culture subjected to trans-differentiation and intoxication to 2 mmol/l methapyrilene.

4.3 Investigation of an up-scaled bioreactor system for potential clinical application using HPAC-derived H-14 cells

For the pilot experiment performed in this study H-14 cells expanded in 2D culture were inoculated in an up-scaled 800 ml bioreactor. Sensor constructs and tubing systems were modified and adapted with respect to the larger volume of the bioreactor system.

4.3.1 Pilot study with H-14 cells cultured in an 800 ml clinical-scale bioreactor

Impedance, oxygen and pH sensors were successfully initiated after assembling the 800 ml bioreactor system. The ammonia sensor had to be removed from the system due to strong leakage, which could not be prevented during the experiment. A number of 5.8×10^8 H-14 cells were inoculated into the bioreactor cell compartment and cultured over 15 days. From day 12 of culture, 30 mmol/l APAP were continuously applied to the bioreactor culture over three days to record the response to toxic stress of cultured cells.

Technical system parameters, including temperature, gas perfusion, pump circulation and online monitoring showed stable functionality during the whole culture period.

Results of metabolic parameters and impedance measurement data are shown in Figure 32. Enzyme leakage of the H-14 cells maintained in the up-scaled 800 ml bioreactor was at basal levels for ALT, AST and GLDH while LDH release showed an increase over the first four days and declined to basal values afterwards. Glucose consumption and lactate production continuously decreased. The time course of ammonia showed a decreasing performance during the first day followed by relatively stable values until the end of culture. Online measurement of oxygen concentration in the culture perfusate revealed no significant changes over the whole culture period (data not shown). Impedance measurement showed a signal decrease during cell inoculation and no increase thereafter. The application of 30 mmol/l APAP induced a temporary increase in ammonia, urea and glucose production followed by a sharp decrease. A slight increase was also detected via impedance monitoring.

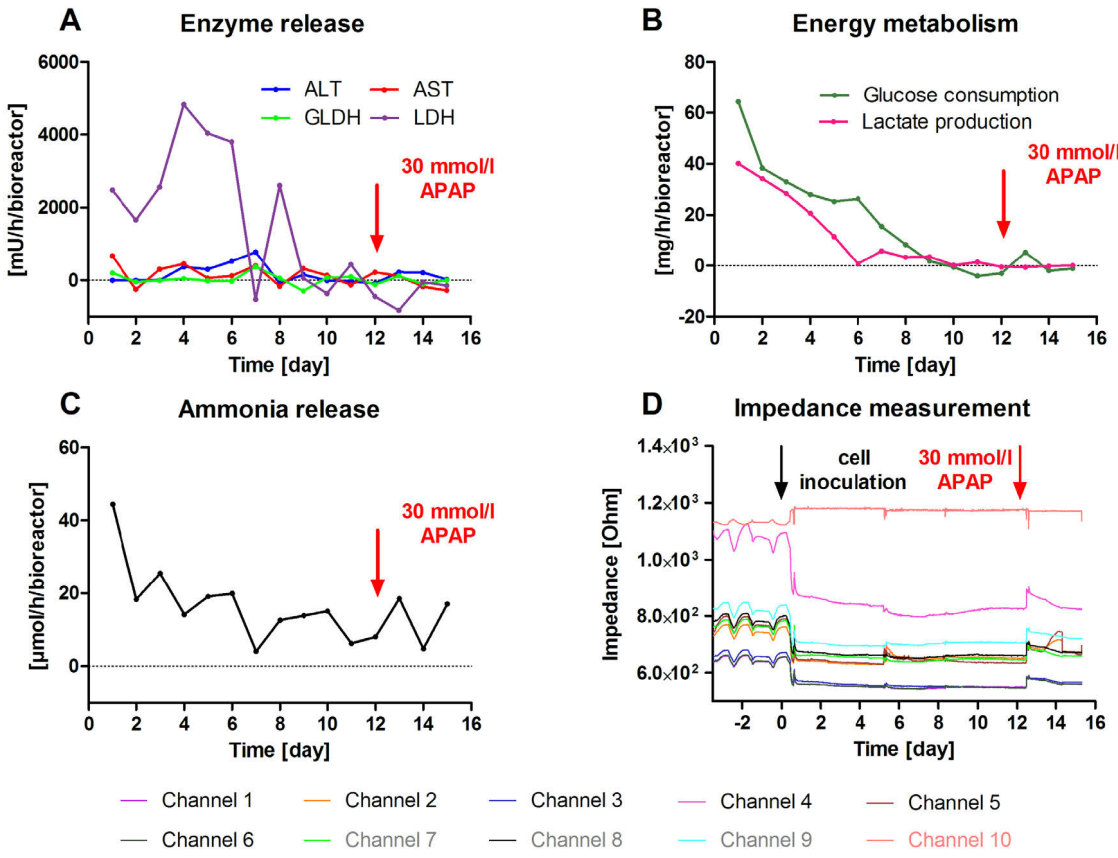

Figure 32: Metabolic performance and impedance measurement of humanized H-14 cells in an up-scaled 800 ml bioreactor.
The bioreactor was inoculated with H-14 cells and run over 15 days. On day 12 APAP was applied at a concentration of 30 mmol/l. Daily samples from the culture perfusate were analysed for enzyme leakage (A), energy metabolism (B) and ammonia release (C). In addition, the culture behaviour was observed using online impedance measurement (D). Six sensor foils were integrated into the bioreactor cell compartment providing 40 independent measurement points. Graph (D) shows a selection. Channels 1-6 show measurements on impedance sensor foils, channels 7-9 show impedance measurements between different impedance sensor foils and channel 10 shows temperature measurements over time.

4.3.2 Chapter discussion

A major limitation of the B-13 cell line is that it is of rat origin, which restricts the predictive value of research results for humans, and implies some differences in metabolic enzymes.[111,113,184] To solve this problem, introduction of human genes into the B-13 cells was attempted,[121] which opens the opportunity to generate cell lines with human characteristics to be used in *in vitro* models. To meet clinical requirements, generation of a cell line of human origin with similar characteristics is desirable for provision of human-typical functions and high clinical safety. If successful, the possibility of generating great quantities of liver cells at low costs within short time would meet the high demand of cells required for extracorporeal liver support.

The H-14 cell line, provided by the group of Professor Matthew Wright, University of Newcastle, was derived from a human pancreatic ductal adenocarcinoma cell line (HPAC). HPAC are sensitive to glucocorticoid treatment inducing trans-differentiation to hepatic cells as previously described for the B-13 cell line. The trans-differentiation of the cell line into a liver-like phenotype was improved by genetic encoding of transcription factors, which have been reported to be involved in the process of trans-differentiation (HNF-1, HNF-3α, HNF-3β, HNF-4, C/EBPα, C/EBPβ),[185–187] resulting in the generation of the humanized H-14 cell line. H-14 cells showed successful culture performance using small-scale bioreactors (data not shown) encouraging their usage in up-scaled clinical grade bioreactors.

The scalable 3D four-compartment bioreactor technology used at the Charité group in Berlin enables adaptation of the culture system for individual fields of application.[149] In contrast to conventional 2D cultures, the flexible size of the 3D bioreactor system facilitates the generation of large cell masses, as shown for mouse embryonic stem cells.[188] Furthermore, the option of periodic cell harvesting allows cell expansion in a highly controlled environment generating sufficient cell numbers for *in vitro* or clinical application.[151] Thus, the technology is of interest for cell cultivation at a large scale for extracorporeal liver support therapy.

Based on experiments using non-invasive online sensors (oxygen, ammonia and impedance) in an 8 ml analytical-scale bioreactor, the methodology was implemented in an up-scaled bioreactor variant for potential use in clinical application. Integration of online sensors was successful except for the online ammonia sensor, which had to be withdrawn due to leakage interfering with the electrical read out device. This issue can be addressed in future experiments by better shielding of electronic components from the liquid part of the sensors and by gluing individual sensor chambers using material which is resistant to dynamic pressure changes located in the bioreactor perfusion.

The culture performance of humanized H-14 cells in the clinical-scale bioreactor, showing promising results in 2 ml small-scale bioreactor cultures, indicates a decrease in cell number and/or viability during culture. Increased LDH release of the first four days followed by a decline to basal levels indicates cell stress due to enzymatic cell harvesting prior to cell inoculation. In addition, cell damage may occur as a result of low cell attachment in the cell compartment. Decreasing energy metabolism as shown by glucose consumption and lactate production rates indicates that significant proliferation did not occur in the bioreactor. This was confirmed by the results of impedance measurement showing no signal increase, which is expected when cells proliferate. Online measurement of oxygen concentrations in the culture perfusate showed similar results. The application of 30 mmol/l APAP induces a temporary increase in ammonia and glucose production followed by a sharp decrease indicating

cell damage. Toxic stress was also detected via impedance monitoring showing a slight increase of signals after drug exposition.

A potential reason for the rather low performance of the cells can be seen in the low cell number used in relation to the cell compartment volume. Since the number of cells inoculated was lower than that used for primary human liver cell culture, where a cell number of approx. 1.4×10^{10} is proposed,[89,148] the cell density of H-14 cells used in the clinical-scale bioreactor was probably not sufficient to enable efficient cell proliferation. To gain the needed larger cell numbers for the clinical-scale bioreactor, labour- and material-intensive 2D cell expansion is required. To solve this issue, multi-layer culture flasks (e.g. cell factory, Thermo Scientific) or small-scale variants of the bioreactor technology in combination with periodic cell harvesting could be used to facilitate cell expansion.[151] The absence of a stronger effect caused by toxic drug exposure as observed in 8 ml B-13/H bioreactor cultures can be attributed to the lower cell density in the clinical scale BAL. Furthermore, the vertical arrangement of impedance sensor foils in the clinical-scale bioreactor, which was necessary due to short length of the sensor foils, could have had a negative effect of cell attachment on the sensor foils, which is essential to impedance measurement. Horizontal alignment of impedance sensor foils in 8 ml analytical-scale bioreactor simplified cell attachment. In order to improve cell attachment, the use of larger sensor foils and arrangement in a way favouring cell adhesion would be an option.

In conclusion, the results of the pilot study performed in this thesis show that the generated cell line H-14 can be cultured and shows metabolic activity in the 3D bioreactor system. The low level of cell activity observed could be due to an insufficient cell density in the pilot experiment. The utilization of non-invasive sensors integrated in the bioreactor system requires additional work. The results obtained encourage further labour to achieve the goal of making available a suitable human cell source in large numbers for extracorporeal liver support approaches.

5 Conclusions and perspectives

Extracorporeal liver support systems are under investigation as a temporary therapy in acute or acute-on chronic liver failure. In order to provide a safe, cost-effective, functional system for extracorporeal liver support, a suitable cell source and methods for quality assessment during clinical sessions are required.

In this thesis successful culture and trans-differentiation of B-13 cells into functional hepatocyte-like B-13/H cells was shown in a 3D high-density bioreactor system. B-13/H bioreactor cultures showed a tendency to improve liver-like functions in prolonged culture. To provide a human cell source for clinical use, culturing genetically modified HPAC (e.g. H-14) in an up-scaled four-compartment bioreactor provides a promising option, if sufficient functionality and achievement of required cell numbers can be achieved. Online impedance measurement (Fraunhofer IBMT) was shown to be a safe, sensitive, label-free and non-invasive method to monitor culture conditions in 3D high-density bioreactor cultures. The technology was successfully used for detecting drug-induced cell damage in 3D bioreactor cultures. Furthermore, online measurement of oxygen and pH using optical-chemical sensors (PreSens-Precision Sensing GmbH) provided additional information on bioreactor cell culture and allowed closely controlled culture performance. The integration of an online ammonia sensor (CEA-Leti-France) showed acceptable correlation to offline ammonia values, but further improvement of the method with regard to sensitivity, sterility, signal shielding and sensor leakage is required. Based on the results, a procedure for culture prediction and decision-making conceived for bio-artificial liver support in a clinical setting was established.

These results highlight the potential of pancreas-derived cell lines, such as B-13/H or human H-14 cells, in combination with the 3D bioreactor system and online sensor technologies to provide a liver culture model for *in vitro* and clinical application. For example, the model can be used to perform studies on hepatic drug toxicity and metabolism, enabling various modes of substance application and regular sample taking with the option to connect automated analytic devices. The integration of online sensor technologies can be used for non-invasive monitoring of the culture state and the cell behaviour in such studies. The prospective of 3D culture systems to investigate more precisely questions of pathogenesis and of disease processes in the body offers the opportunity to better translate research results into clinical applications.

Figures

Tables

Formulas

References

1. Williams, R. Global challenges in liver disease. *Hepatology* **44,** 521–526 (2006).
2. Blachier, M., Leleu, H., Peck-Radosavljevic, M., Valla, D.-C. & Roudot-Thoraval, F. The burden of liver disease in Europe: a review of available epidemiological data. *J. Hepatol.* **58,** 593–608 (2013).
3. Bosch, F. X., Ribes, J., Díaz, M. & Cléries, R. Primary liver cancer: Worldwide incidence and trends. in *Gastroenterology* **127,** S5–S16 (2004).
4. Yu, M. C. & Yuan, J. M. Environmental factors and risk for hepatocellular carcinoma. *Gastroenterology* **127,** S72–78 (2004).
5. Zatoński, W. A. *et al.* Liver cirrhosis mortality in Europe, with special attention to Central and Eastern Europe. *Eur. Addict. Res.* **16,** 193–201 (2010).
6. Mann, R. E., Smart, R. G. & Govoni, R. The epidemiology of alcoholic liver disease. *Alcohol Res. Health* **27,** 209–219 (2003).
7. Rehm, J. *et al.* Alcohol as a risk factor for liver cirrhosis: A systematic review and meta-analysis. *Drug Alcohol Rev.* **29,** 437–445 (2010).
8. Bedogni, G. *et al.* Incidence and natural course of fatty liver in the general population: The dionysos study. *Hepatology* **46,** 1387–1391 (2007).
9. Dugum, M. & McCullough, A. Diagnosis and Management of Alcoholic Liver Disease. *J. Clin. Transl. Hepatol.* **3,** 109–116 (2015).
10. Rehm, J., Samokhvalov, A. V. & Shield, K. D. Global burden of alcoholic liver diseases. *J. Hepatol.* **59,** 160–168 (2013).
11. Mota, A., Areias, J. & Cardoso, M. F. Chronic liver disease and cirrhosis among patients with hepatitis B virus infection in northern Portugal with reference to the viral genotypes. *J. Med. Virol.* **83,** 71–77 (2011).
12. Hatzakis, A. *et al.* The state of hepatitis B and C in Europe: Report from the hepatitis B and C summit conference. *J. Viral Hepat.* **18,** 1–16 (2011).
13. European Liver Patients Association. *Report on Hepatitis Patient Self-Help in Europe by the European Liver Patients Association (ELPA)*. (2010). at <http://www.hepbcppa.org/wp-content/uploads/2011/11/Report-on-Patient-Self-Help.pdf>
14. Patel, N. *et al.* Hepatic decompensation/serious adverse events in post-liver transplantation recipients on sofosbuvir for recurrent hepatitis C virus. *World J. Gastroenterol.* **22,** 2844–2854 (2016).
15. Wilder, J. M. & Muir, A. J. Strategies for treating chronic HCV infection in patients with cirrhosis: latest evidence and clinical outcomes. *Ther. Adv. Chronic Dis.* **6,** 314–327 (2015).
16. Zhang, X. Direct anti-HCV agents. *Acta Pharm. Sin. B* **6,** 26–31 (2016).
17. Rizzetto, M. Hepatitis D: Thirty years after. *J. Hepatol.* **50,** 1043–1050 (2009).
18. Romeo, R. *et al.* A 28-year study of the course of hepatitis Delta infection: a risk factor for cirrhosis and hepatocellular carcinoma. *Gastroenterology* **136,** 1629–1638 (2009).
19. FitzSimons, D., Hendrickx, G., Vorsters, A. & Van Damme, P. Hepatitis A and E: Update on prevention and epidemiology. in *Vaccine* **28,** 583–588 (2010).
20. Smith, B. W. & Adams, L. A. Non-alcoholic fatty liver disease. *Crit. Rev. Clin. Lab. Sci.* **48,** 97–113 (2011).

21. Schattenberg, J. M. Nicht-alkoholische Fettleber (NAFLD) und nicht-alkoholische Steatohepatitis (NASH): Pathophysiologie und Ernährungsaspekte. *Ernährungs Umschau* M92–M100 (2015).
22. Radu, C. *et al.* Prevalence and associated risk factors of non-alcoholic fatty liver disease in hospitalized patients. *J. Gastrointestin. Liver Dis.* **17,** 255–260 (2008).
23. Smith, B. W. & Adams, L. A. Nonalcoholic fatty liver disease and diabetes mellitus: pathogenesis and treatment. *Nat. Rev. Endocrinol.* **7,** 456–465 (2011).
24. Angulo, P. GI epidemiology: nonalcoholic fatty liver disease. *Aliment. Pharmacol. Ther.* **25,** 883–889 (2007).
25. Cowan, M. L. *et al.* The increasing hospital disease burden of haemochromatosis in England. *Aliment. Pharmacol. Ther.* **31,** 247–252 (2010).
26. Gerlach, J. C., Zeilinger, K. & Patzer Ii, J. F. Bioartificial liver systems: why, what, whither? *Regen. Med.* **3,** 575–595 (2008).
27. Starzl, T. E. *et al.* Homotransplantation of the liver in humnans. *Surg. Gynecol. Obstet.* **117,** 659–76 (1963).
28. Crossan, C. *et al.* Cost-effectiveness of non-invasive methods for assessment and monitoring of liver fibrosis and cirrhosis in patients with chronic liver disease: systematic review and economic evaluation. *Health Technol. Assess.* **19,** 1–409, v–vi (2015).
29. Pascher, A., Nebrig, M. & Neuhaus, P. Irreversible liver failure: treatment by transplantation: part 3 of a series on liver cirrhosis. *Dtsch. Arztebl. Int.* **110,** 167–173 (2013).
30. Riordan, S. M. & Williams, R. Perspectives on liver failure: Past and future. *Seminars in Liver Disease* **28,** 137–141 (2008).
31. Chistiakov, D. A. Liver regenerative medicine: Advances and challenges. *Cells Tissues Organs* **196,** 291–312 (2012).
32. Hauboldt, R. H., Hanson, S. G. & Bernstein, G. R. 2008 U.S. organ and tissue transplant cost estimate and discussion. *Milliman Res. Rep.* **April,** 1–17 (2008).
33. Bentley, T. S. & Hanson, S. G. 2014 U.S. organ and tissue transplant cost estimates and discussion. *Milliman Res. Rep.* **December,** 1–16 (2014).
34. Bengmark, S. Curcumin, an atoxic antioxidant and natural NFkappaB, cyclooxygenase-2, lipooxygenase, and inducible nitric oxide synthase inhibitor: a shield against acute and chronic diseases. *JPEN. J. Parenter. Enteral Nutr.* **30,** 45–51 (2006).
35. Wang, Y. *et al.* Current development of bioreactors for extracorporeal bioartificial liver (Review). *Biointerphases* **5,** FA116–FA131 (2010).
36. Stutchfield, B. M., Simpson, K. & Wigmore, S. J. Systematic review and meta-analysis of survival following extracorporeal liver support. *Br. J. Surg.* **98,** 623–631 (2011).
37. Bañares, R., Catalina, M.-V. & Vaquero, J. Liver support systems: will they ever reach prime time? *Curr. Gastroenterol. Rep.* **15,** 312 (2013).
38. Carpentier, B., Gautier, A. & Legallais, C. Artificial and bioartificial liver devices: present and future. *Gut* **58,** 1690–1702 (2009).
39. Court, F. G., Wemyss-Holden, S. A., Dennison, A. R. & Maddern, G. J. Bioartificial liver support devices: Historical perspectives. *ANZ Journal of Surgery* **73,** 739–748 (2003).
40. Kiley, J. E., Welch, H. F., Pender, J. C. & Welch, C. S. Removal of blood ammonia by hemodialysis. *Proc. Soc. Exp. Biol. Med.* **91,** 489–90 (1956).
41. Patzer 2nd, J. F. Thermodynamic considerations in solid adsorption of bound solutes for patient support in liver failure. *Artif. Organs* **32,** 499–508 (2008).

42. Saliba, F. The Molecular Adsorbent Recirculating System (MARS) in the intensive care unit: a rescue therapy for patients with hepatic failure. *Crit. Care* **10,** 118 (2006).
43. Mitzner, S., Klammt, S., Stange, J. & Schmidt, R. Albumin regeneration in liver support-comparison of different methods. *Ther. Apher. Dial.* **10,** 108–117 (2006).
44. Stange, J. *et al.* Liver support by extracorporeal blood purification: A clinical observation. *Liver Transplant.* **6,** 603–613 (2000).
45. Pless, G. Artificial and bioartificial liver support. *Organogenesis* **3,** 20–24 (2007).
46. Palsson, R. & Niles, J. L. Regional citrate anticoagulation in continuous venovenous hemofiltration in critically ill patients with a high risk of bleeding. *Kidney Int* **55,** 1991–1997 (1999).
47. Bouchard, J. & Madore, F. Role of citrate and other methods of anticoagulation in patients with severe liver failure requiring continuous renal replacement therapy. *NDT Plus* **2,** 11–19 (2009).
48. Patzer 2nd, J. F., Safta, S. A. & Miller, R. H. Slow continuous ultrafiltration with bound solute dialysis. *ASAIO J* **52,** 47–58 (2006).
49. Kreymann, B., Seige, M., Schweigart, U., Kopp, K. F. & Classen, M. Albumin dialysis: Effective removal of copper in a patient with Fulminant wilson disease and successful bridging to liver transplantation: A new possibility for the elimination of protein-bound toxins. *J. Hepatol.* **31,** 1080–1085 (1999).
50. Santoro, A. *et al.* Prometheus System: A Technological Support in Liver Failure. *Transplant. Proc.* **38,** 1078–1082 (2006).
51. Rademacher, S., Oppert, M. & Jörres, A. Artificial extracorporeal liver support therapy in patients with severe liver failure. *Expert Rev. Gastroenterol. Hepatol.* **5,** 591–599 (2011).
52. Bernal, W., Lee, W. M., Wendon, J., Larsen, F. S. & Williams, R. Acute liver failure: A curable disease by 2024? *Journal of Hepatology* **62,** S112–S120 (2015).
53. Sen, S., Mookerjee, R. P., Davies, N. A., Williams, R. & Jalan, R. Review article: the Molecular Adsorbents Recirculating System (MARS) in liver failure. *Aliment. Pharmacol. Ther.* **16,** 32–38 (2002).
54. Sen, S., Jalan, R. & Williams, R. Liver failure: Basis of benefit of therapy with the molecular adsorbents recirculating system. *Int. J. Biochem. Cell Biol.* **35,** 1306–1311 (2003).
55. Collins, K. L., Roberts, E. A., Adeli, K., Bohn, D. & Harvey, E. A. Single pass albumin dialysis (SPAD) in fulminant Wilsonian liver failure: A case report. *Pediatr. Nephrol.* **23,** 1013–1016 (2008).
56. Heemann, U. *et al.* Albumin dialysis in cirrhosis with superimposed acute liver injury: a prospective, controlled study. *Hepatology* **36,** 949–958 (2002).
57. Mitzner, S. R. *et al.* Improvement of Hepatorenal SyndromeWith Extracorporeal Albumin Dialysis MARS: Results of a Prospective, Randomized, Controlled Clinical Trial. *Liver Transplant.* **6,** 277–286 (2000).
58. Peszynski, P. *et al.* Albumin dialysis: single pass vs. recirculation (MARS). *Liver* **22,** 40–42 (2002).
59. Mitzner, S. R. *et al.* Extracorporeal detoxification using the molecular adsorbent recirculating system for critically ill patients with liver failure. *J. Am. Soc. Nephrol.* **12,** S75–S82 (2001).
60. Sauer, I. M. *et al.* In Vitro Comparison of the Molecular Adsorbent Recirculation System (MARS) and Single-pass Albumin Dialysis (SPAD). *Hepatology* **39,**

1408–1414 (2004).
61. Sen, S. *et al.* Pathophysiological effects of albumin dialysis in acute-on-chronic liver failure: A randomized controlled study. *Liver Transplant.* **10,** 1109–1119 (2004).
62. Stange, J., Hassanein, T. I., Mehta, R., Mitzner, S. R. & Bartlett, R. H. The molecular adsorbents recycling system as a liver support system based on albumin dialysis: A summary of preclinical investigations, prospective, randomized, controlled clinical trial, and clinical experience from 19 centers. *Artif. Organs* **26,** 103–110 (2002).
63. Patzer, J. Principles of bound solute dialysis. *Ther. Apher. Dial.* **10,** 118–124 (2006).
64. Falkenhagen, D. *et al.* Fractionated plasma separation and adsorption system: A novel system for blood purification to remove albumin bound substances. *Artif. Organs* **23,** 81–86 (1999).
65. Rifai, K. *et al.* Prometheus(R) - A new extracorporeal system for the treatment of liver failure. *J. Hepatol.* **39,** 984–990 (2003).
66. Rifai, K. *et al.* Removal selectivity of prometheus: A new extracorporeal liver support device. *World J. Gastroenterol.* **12,** 940–944 (2006).
67. Kramer, L. *et al.* Successful treatment of refractory cerebral oedema in ecstasy/cocaine-induced fulminant hepatic failure using a new high-efficacy liver detoxification device (FPSA-Prometheus). *Wien. Klin. Wochenschr.* **115,** 599–603 (2003).
68. Krisper, P. *et al.* In vivo quantification of liver dialysis: Comparison of albumin dialysis and fractionated plasma separation. *J. Hepatol.* **43,** 451–457 (2005).
69. Vaquero, J., Chung, C., Cahill, M. E. & Blei, A. T. Pathogenesis of hepatic encephalopathy in acute liver failure. *Semin. Liver Dis.* **23,** 259–269 (2003).
70. Evenepoel, P. *et al.* Prometheus versus molecular adsorbents recirculating system: Comparison of efficiency in two different liver detoxification devices. *Artif. Organs* **30,** 276–284 (2006).
71. Kribben, A. *et al.* Effects of fractionated plasma separation and adsorption on survival in patients with acute-on-chronic liver failure. *Gastroenterology* **142,** 782–789.e3 (2012).
72. Bañares, R. *et al.* Extracorporeal albumin dialysis with the molecular adsorbent recirculating system in acute-on-chronic liver failure: The RELIEF trial. *Hepatology* **57,** 1153–1162 (2013).
73. Stauber, R. E. & Krisper, P. MARS and Prometheus in Acute-on-Chronic Liver Failure : Toxin Elimination and Outcome. *Transplantationsmedizin* **22,** 333–338 (2010).
74. Stange, J. Extracorporeal liver support. *Organogenesis* **71,** 64–73 (2011).
75. Tsiaoussis, J., Newsome, P. N., Nelson, L. J., Hayes, P. C. & Plevris, J. N. Which hepatocyte will it be? hepatocyte choice for bioartificial liver support systems. *Liver Transplant.* **7,** 2–10 (2001).
76. Wallace, K., Fairhall, E. A., Charlton, K. A. & Wright, M. C. AR42J-B-13 cell: An expandable progenitor to generate an unlimited supply of functional hepatocytes. *Toxicology* **278,** 277–287 (2010).
77. Hoffmann, S. A. *et al.* Analysis of drug metabolism activities in a miniaturized liver cell bioreactor for use in pharmacological studies. *Biotechnol. Bioeng.* **109,** 3172–3181 (2012).
78. Padgham, C. R. *et al.* Alteration of transcription factor mRNAs during the isolation and culture of rat hepatocytes suggests the activation of a proliferative

mode underlies their de-differentiation. *Biochem. Biophys. Res. Commun.* **197,** 599–605 (1993).
79. Jakubowski, A. *et al.* TWEAK induces liver progenitor cell proliferation. *J. Clin. Invest.* **115,** 2330–2340 (2005).
80. Erker, L. & Grompe, M. Signaling networks in hepatic oval cell activation. *Stem Cell Research* **1,** 90–102 (2007).
81. Scheving, L. A., Stevenson, M. C., Zhang, X. & Russell, W. E. Cultured rat hepatocytes upregulate Akt and ERK in an ErbB-2-dependent manner. *Am J Physiol Gastrointest Liver Physiol* **295,** G322–331 (2008).
82. Rozga, J. *et al.* Development of a hybrid bioartificial liver. *Ann Surg* **217,** 502–509 (1993).
83. Gerlach, J. C. *et al.* Extracorporeal liver support : Porcine or human cell based systems ? *Int. J. Artif. Organs* **25,** 1013–1018 (2002).
84. Stockmann, H. B., Hiemstra, C. A., Marquet, R. L. & IJzermans, J. N. Extracorporeal perfusion for the treatment of acute liver failure. *Ann. Surg.* **231,** 460–70 (2000).
85. Harrison, S. *et al.* An efficient method for producing alpha(1,3)-galactosyltransferase gene knockout pigs. *Cloning Stem Cells* **6,** 327–331 (2004).
86. Irgang, M. *et al.* Porcine endogenous retroviruses: No infection in patients treated with a bioreactor based on porcine liver cells. *J. Clin. Virol.* **28,** 141–154 (2003).
87. Di Nicuolo, G. *et al.* No evidence of in vitro and in vivo porcine endogenous retrovirus infection after plasmapheresis through the AMC-bioartificial liver. *Xenotransplantation* **12,** 286–292 (2005).
88. Van De Kerkhove, M. P., Hoekstra, R., Chamuleau, R. A. F. M. & van Gulik, T. M. Clinical application of bioartificial liver support systems. *Ann. Surg.* **240,** 216–230 (2004).
89. Gerlach, J. C. *et al.* Use of primary human liver cells originating from discarded grafts in a bioreactor for liver support therapy and the prospects of culturing adult liver stem cells in bioreactors: a morphologic study. *Transplantation* **76,** 781–786 (2003).
90. Ellis, A. J. *et al.* Pilot-controlled trial of the extracorporeal liver assist device in acute liver failure. *Hepatology* **24,** 1446–1451 (1996).
91. Poyck, P. P. *et al.* In vitro comparison of two bioartificial liver support systems: MELS CellModule and AMC BAL. *Int. J. Artif. Organs* **30,** 183–191 (2007).
92. Allen, J. W., Hassanein, T. & Bhatia, S. N. Advances in bioartificial liver devices. *Hepatology* **34,** 447–455 (2001).
93. Millis, J. M. *et al.* Initial experience with the modified extracorporeal liver-assist device for patients with fulminant hepatic failure: system modifications and clinical impact. *Transplantation* **74,** 1735–1746 (2002).
94. Mavri-Damelin, D. *et al.* Cells for bioartificial liver devices: The human hepatoma-derived cell line C3A produces urea but does not detoxify ammonia. *Biotechnol. Bioeng.* **99,** 644–651 (2008).
95. Gripon, P. *et al.* Infection of a human hepatoma cell line by hepatitis B virus. *Proc. Natl. Acad. Sci. U. S. A.* **99,** 15655–15660 (2002).
96. Andersson, T. B., Kanebratt, K. P. & Kenna, J. G. The HepaRG cell line: a unique in vitro tool for understanding drug metabolism and toxicology in human. *Expert Opin. Drug Metab. Toxicol.* **8,** 909–920 (2012).
97. Lübberstedt, M. *et al.* HepaRG human hepatic cell line utility as a surrogate for primary human hepatocytes in drug metabolism assessment in vitro. *J. Pharmacol. Toxicol. Methods* **63,** 59–68 (2011).

98. Nibourg, G. A. A. *et al.* Increased hepatic functionality of the human hepatoma cell lineHepaRG cultured in the AMC bioreactor. *Int. J. Biochem. Cell Biol.* **45,** 1860–1868 (2013).
99. Darnell, M. *et al.* Cytochrome P450-dependent metabolism in HepaRG cells cultured in a dynamic three-dimensional bioreactor. *Drug Metab. Dispos.* **39,** 1131–1138 (2011).
100. Takayama, K. *et al.* Generation of metabolically functioning hepatocytes from human pluripotent stem cells by FOXA2 and HNF1α transduction. *J. Hepatol.* **57,** 628–636 (2012).
101. Zhang, Z. *et al.* Generation, characterization and potential therapeutic applications of mature and functional hepatocytes from stem cells. *J. Cell. Physiol.* **228,** 298–305 (2013).
102. De Freitas Souza, B. S. *et al.* Current status of stem cell therapy for liver diseases. *Cell Transplantation* **18,** 1261–1279 (2009).
103. Lemaigre, F. & Zaret, K. S. Liver development update: New embryo models, cell lineage control, and morphogenesis. *Current Opinion in Genetics and Development* **14,** 582–590 (2004).
104. Zaret, K. S. & Grompe, M. Generation and regeneration of cells of the liver and pancreas. *Science* **322,** 1490–1494 (2008).
105. Yeldandi, A. V *et al.* Coexpression of glutamine synthetase and carbamoylphosphate synthage I genes in pancreatic hepatocytes of rat. *Proc. Natl. Acad. Sci. U. S. A.* **87,** 881–885 (1990).
106. Waalkes, M. P., Cherian, M. G., Ward, J. M. & Goyer, R. A. Immunohistochemical evidence of high concentrations of metallothionein in pancreatic hepatocytes induced by cadmium in rats. *Toxicol. Pathol.* **20,** 323–326 (1992).
107. Krakowski, M. L. *et al.* Pancreatic Expression of Keratinocyte Growth Factor Leads to Differentiation of Islet Hepatocytes and Proliferation of Duct Cells. *Am. J. Pathol.* **154,** 683–691 (1999).
108. Lardon, J. *et al.* Plasticity in the adult rat pancreas: transdifferentiation of exocrine to hepatocyte-like cells in primary culture. *Hepatology* **39,** 1499–1507 (2004).
109. Munck, A., Guyre, P. M. & Holbrook, N. J. Physiological functions of glucocorticoids in stress and their relations to pharmacological actions. *Endocr Rev* **5,** 25–44 (1984).
110. Kotelevtsev, Y. *et al.* 11Beta-Hydroxysteroid Dehydrogenase Type 1 Knockout Mice Show Attenuated Glucocorticoid-Inducible Responses and Resist Hyperglycemia on Obesity or Stress. *Proc. Natl. Acad. Sci. U. S. A.* **94,** 14924–14929 (1997).
111. Wallace, K., Marek, C. J., Currie, R. A. & Wright, M. C. Exocrine pancreas trans-differentiation to hepatocytes-A physiological response to elevated glucocorticoid in vivo. *J. Steroid Biochem. Mol. Biol.* **116,** 76–85 (2009).
112. Wallace, K., Flecknell, P. A., Burt, A. D. & Wright, M. C. Disrupted pancreatic exocrine differentiation and malabsorption in response to chronic elevated systemic glucocorticoid. *Am. J. Pathol.* **177,** 1225–1232 (2010).
113. Fairhall, E. A. *et al.* Adult human exocrine pancreas differentiation to hepatocytes – potential source of a human hepatocyte progenitor for use in toxicology research. *Toxicol. Res. (Camb).* **2,** 80–87 (2013).
114. Wallace, K., Marek, C. J., Hoppler, S. & Wright, M. C. Glucocorticoid-dependent transdifferentiation of pancreatic progenitor cells into hepatocytes is

dependent on transient suppression of WNT signalling. *J. Cell Sci.* **123,** 2103–2110 (2010).
115. Thompson, M. D. & Monga, S. P. S. WNT/beta-catenin signaling in liver health and disease. *Hepatology* **45,** 1298–1305 (2007).
116. Burke, Z. D. *et al.* Liver Zonation Occurs Through a β-Catenin-Dependent, c-Myc-Independent Mechanism. *Gastroenterology* **136,** 2316–2324.e1–3 (2009).
117. Tosh, D., Shen, C. N. & Slack, J. M. W. Differentiated properties of hepatocytes induced from pancreatic cells. *Hepatology* **36,** 534–543 (2002).
118. Fairhall, E. A. *et al.* The B-13 hepatocyte progenitor cell resists pluripotency induction and differentiation to non-hepatocyte cells. *Toxicol. Res. (Camb).* **2,** 308–320 (2013).
119. Shen, C. N., Slack, J. M. W. & Tosh, D. Molecular basis of transdifferentiation of pancreas to liver. *Nat. c* **2,** 879–887 (2000).
120. Marek, C. J., Cameron, G. A., Elrick, L. J., Hawksworth, G. M. & Wright, M. C. Generation of hepatocytes expressing functional cytochromes P450 from a pancreatic progenitor cell line in vitro. *Biochem. J.* **370,** 763–769 (2003).
121. Probert, P. M. E. *et al.* Utility of B-13 progenitor-derived hepatocytes in hepatotoxicity and genotoxicity studies. *Toxicol. Sci.* **137,** 350–370 (2014).
122. Swift, B., Pfeifer, N. D. & Brouwer, K. L. R. Sandwich-cultured hepatocytes: an in vitro model to evaluate hepatobiliary transporter-based drug interactions and hepatotoxicity. *Drug Metab. Rev.* **42,** 446–471 (2010).
123. Decaens, C., Durand, M., Grosse, B. & Cassio, D. Which in vitro models could be best used to study hepatocyte polarity? *Biol. Cell* **100,** 387–398 (2008).
124. Rhee, S. Fibroblasts in three dimensional matrices: cell migration and matrix remodeling. *Exp. Mol. Med.* **41,** 858–865 (2009).
125. Schyschka, L. *et al.* Hepatic 3D cultures but not 2D cultures preserve specific transporter activity for acetaminophen-induced hepatotoxicity. *Arch. Toxicol.* **87,** 1581–1593 (2013).
126. Abbott, A. Cell culture: biology's new dimension. *Nature* **424,** 870–2 (2003).
127. Cukierman, E., Pankov, R. & Yamada, K. M. Cell interactions with three-dimensional matrices. *Current Opinion in Cell Biology* **14,** 633–639 (2002).
128. Morsiani, E. *et al.* Biologic liver support: optimal cell source and mass. *Int. J. Artif. Organs* **25,** 985–93 (2002).
129. Kelly, J. H. & Sussman, N. L. The hepatix extracorporeal liver assist device in the treatment of fulminant hepatic failure. *Asaio J* **40,** 83–85 (1994).
130. Erro, E. *et al.* Bioengineering the liver: scale-up and cool chain delivery of the liver cell biomass for clinical targeting in a bioartificial liver support system. *Biores. Open Access* **2,** 1–11 (2013).
131. Allen, J. W. & Bhatia, S. N. Improving the next generation of bioartificial liver devices. *Seminars in Cell and Developmental Biology* **13,** 447–454 (2002).
132. Zeilinger, K. *et al.* [Liver cell culture in bioreactors for in vitro drug studies as an alternative to animal testing]. *ALTEX* **17,** 3–10 (2000).
133. Sussman, N. L. *et al.* Reversal of fulminant hepatic failure using an extracorporeal liver assist device. *Hepatology* **16,** 60–65 (1992).
134. Sussman, N. L., Gislason, G. T., Conlin, C. A. & Kelly, J. H. The Hepatix extracorporeal liver assist device: initial clinical experience. *Artif. Organs* **18,** 390–6 (1994).
135. Patzer, J. F. *et al.* Novel bioartificial liver support system: Preclinical evaluation. in *Annals of the New York Academy of Sciences* **875,** 340–352 (1999).
136. Mazariegos, G. V *et al.* Safety observations in phase I clinical evaluation of the

Excorp Medical Bioartificial Liver Support System after the first four patients. *ASAIO J.* **47,** 471–475 (2001).
137. Mazariegos, G. V *et al.* First clinical use of a novel bioartificial liver support system (BLSS). *Am. J. Transplant* **2,** 260–266 (2002).
138. Watanabe, F. D. *et al.* Clinical experience with a bioartificial liver in the treatment of severe liver failure. A phase I clinical trial. *Ann. Surg.* **225,** 484–491; discussion 491–494 (1997).
139. Demetriou, A. A. *et al.* Prospective, Randomized, Multicenter, Controlled Trial of a Bioartificial Liver in Treating Acute Liver Failure. *Ann. Surg.* **239,** 660–670 (2004).
140. Samuel, D. *et al.* Neurological improvement during bioartificial liver sessions in patients with acute liver failure awaiting transplantation. *Transplantation* **73,** 257–264 (2002).
141. Mullon, C. & Pitkin, Z. The HepatAssist® Bioartificial Liver Support System: clinical study and pig hepatocyte process. *Expert Opin. Investig. Drugs* **8,** 229–235 (1999).
142. Sosef, M. N. *et al.* ASSESSMENT OF THE AMC-BIOARTIFICIAL LIVER IN THE ANHEPATIC PIG. *Transplantation* **73,** 204–209 (2002).
143. Van De Kerkhove, M. P. *et al.* Phase I clinical trial with the AMC-bioartificial liver. *Int. J. Artif. Organs* **25,** 950–959 (2002).
144. Gerlach, J. C. Development of a hybrid liver support system: A review. *International Journal of Artificial Organs* **19,** 645–654 (1996).
145. Sauer, I. M. *et al.* Clinical extracorporeal hybrid liver support - Phase I study with primary porcine liver cells. *Xenotransplantation* **10,** 460–469 (2003).
146. Sauer, I. M. *et al.* Extracorporeal liver support based on primary human liver cells and albumin dialysis - Treatment of a patient with primary graft non-function. *J. Hepatol.* **39,** 649–653 (2003).
147. Zeilinger, K. *et al.* Time course of primary liver cell reorganization in three-dimensional high-density bioreactors for extracorporeal liver support: an immunohistochemical and ultrastructural study. *Tissue Eng.* **10,** 1113–1124 (2004).
148. Schmelzer, E. *et al.* Effect of human patient plasma ex vivo treatment on gene expression and progenitor cell activation of primary human liver cells in multi-compartment 3D perfusion bioreactors for extra-corporeal liver support. *Biotechnol. Bioeng.* **103,** 817–827 (2009).
149. Zeilinger, K. *et al.* Scaling down of a clinical three-dimensional perfusion multicompartment hollow fiber liver bioreactor developed for extracorporeal liver support to an analytical scale device useful for hepatic pharmacological in vitro studies. *Tissue Eng. Part C. Methods* **17,** 549–556 (2011).
150. Lübberstedt, M. *et al.* Serum-free culture of primary human hepatocytes in a miniaturized hollow-fibre membrane bioreactor for pharmacological in vitro studies. *J. Tissue Eng. Regen. Med.* **9,** 1017–1026 (2015).
151. Knöspel, F., Freyer, N., Stecklum, M., Gerlach, J. C. & Zeilinger, K. Periodic Harvesting of Embryonic Stem Cells from a Hollow-Fiber Membrane Based Four-Compartment Bioreactor. *Biotechnol. Prog.* **32,** 141–151 (2015).
152. Raschzok, N. *et al.* Imaging of primary human hepatocytes performed with micron-sized iron oxide particles and clinical magnetic resonance tomography. *J. Cell. Mol. Med.* **12,** 1384–1394 (2008).
153. Pless, G. *et al.* Evaluation of primary human liver cells in bioreactor cultures for extracorporeal liver support on the basis of urea production. *Artif. Organs* **30,**

686–694 (2006).
154. Gerlach, J. C. *et al.* Lidocaine/monoethylglycinexylidide test, galactose elimination test, and sorbitol elimination test for metabolic assessment of liver cell bioreactors. *Artif. Organs* **34,** 462–72 (2010).
155. Santoro, R., Krause, C., Martin, I. & Wendt, D. On-line monitoring of oxygen as a non-destructive method to quantify cells in engineered 3D tissue constructs. *J. Tissue Eng. Regen. Med.* **6,** 696–701 (2012).
156. Lei, K. F., Wu, M. H., Hsu, C. W. & Chen, Y. D. Real-time and non-invasive impedimetric monitoring of cell proliferation and chemosensitivity in a perfusion 3D cell culture microfluidic chip. *Biosens. Bioelectron.* **51,** 16–21 (2014).
157. Sharma, R., Blackburn, T., Hu, W., Wiltberger, K. & Velev, O. D. On-chip microelectrode impedance analysis of mammalian cell viability during biomanufacturing. *Biomicrofluidics* **8,** 54108 (2014).
158. Ehret, R. *et al.* Monitoring of cellular behaviour by impedance measurements on interdigitated electrode structures. *Biosens. Bioelectron.* **12,** 29–41 (1997).
159. Peyre, L. *et al.* High-content screening imaging and real-time cellular impedance monitoring for the assessment of chemical ' s bio-activation with regards hepatotoxicity. *Toxicol. Vitr.* **29,** 1916–1931 (2015).
160. Witkowski, P. T. *et al.* Cellular impedance measurement as a new tool for poxvirus titration, antibody neutralization testing and evaluation of antiviral substances. *Biochem. Biophys. Res. Commun.* **401,** 37–41 (2010).
161. Ramasamy, S., Bennet, D. & Kim, S. Drug and bioactive molecule screening based on a bioelectrical impedance cell culture platform. *International Journal of Nanomedicine* **9,** 5789–5809 (2014).
162. Atienza, J. M. *et al.* Dynamic and label-free cell-based assays using the real-time cell electronic sensing system. *Assay Drug Dev. Technol.* **4,** 597–607 (2006).
163. Tang, W., Song, H., Cai, W. & Shen, X. Real Time Monitoring of Inhibition of Adipogenesis and Angiogenesis by (-)-Epigallocatechin-3-Gallate in 3T3-L1 Adipocytes and Human Umbilical Vein Endothelial Cells. *Nutrients* **7,** 8871–8886 (2015).
164. Urcan, E. *et al.* 300_Urcan_xCellignece_2010. *Dent. Mater.* **26,** 51–58 (2010).
165. Quereda, J. J. *et al.* Validation of xCELLigence real-time cell analyzer to assess compatibility in xenotransplantation with pig-to-baboon model. *Transplant. Proc.* **42,** 3239–3243 (2010).
166. Lei, K. F., Huang, C. H. & Tsang, N. M. Impedimetric quantification of cells encapsulated in hydrogel cultured in a paper-based microchamber. *Talanta* **147,** 628–633 (2016).
167. Lei, K. F., Wu, M. H., Hsu, C. W. & Chen, Y. D. Electrical impedance determination of cancer cell viability in a 3-Dimensional cell culture microfluidic chip. *Int. J. Electrochem. Sci.* **7,** 12817–12828 (2012).
168. Canali, C. *et al.* An impedance method for spatial sensing of 3D cell constructs--towards applications in tissue engineering. *Analyst* **140,** 6079–6088 (2015).
169. Knobeloch, D. *et al.* Human hepatocytes: isolation, culture, and quality procedures. *Methods Mol. Biol.* **806,** 99–120 (2012).
170. Pfeiffer, E. *et al.* Featured Article: Isolation, characterization, and cultivation of human hepatocytes and non-parenchymal liver cells. *Exp. Biol. Med. (Maywood).* **240,** 645–56 (2015).
171. Borisov, S. M., Neurauter, G., Schroeder, C., Klimant, I. & Wolfbeis, O. S. Modified dual lifetime referencing method for simultaneous optical determination and sensing of two analytes. *Appl. Spectrosc.* **60,** 1167–1173

(2006).
172. Fairhall, E. A. Hepatocyte generation from pancreatic acinar cell lines. *PhD thesis Newcastle Univ. Fac. Med. Sci. Inst. Cell. Med.* 1–228 (2013). at <https://theses.ncl.ac.uk/dspace/handle/10443/2375>
173. Probert, P. M. E. *et al.* An expandable donor-free supply of functional hepatocytes for toxicology. *Toxicol. Res.* **4,** 203–222 (2015).
174. Stachelscheid, H. *et al.* Teratoma formation of human embryonic stem cells in three-dimensional perfusion culture bioreactors. *J. Tissue Eng. Regen. Med.* **7,** 729–741 (2013).
175. Hoekstra, R. *et al.* The HepaRG cell line is suitable for bioartificial liver application. *Int. J. Biochem. Cell Biol.* **43,** 1483–1489 (2011).
176. Richter, M. *et al.* Pancreatic progenitor-derived hepatocytes are viable and functional in a 3D high density bioreactor culture system. *Toxicol. Res. (Camb).* **5,** 278–290 (2016).
177. Mew, N. A. *et al.* Effects of a single dose of N-carbamylglutamate on the rate of ureagenesis. *Mol. Genet. Metab.* **98,** 325–330 (2009).
178. Meredith, C., Scott, M. P., Renwick, A. B., Price, R. J. & Lake, B. G. Studies on the induction of rat hepatic CYP1A, CYP2B, CYP3A and CYP4A subfamily form mRNAs in vivo and in vitro using precision-cut rat liver slices. *Xenobiotica.* **33,** 511–527 (2003).
179. Thangavel, C., Dhir, R. N., Volgin, D. V. & Shapiro, B. H. Sex-dependent expression of CYP2C11 in spleen, thymus and bone marrow regulated by growth hormone. *Biochem. Pharmacol.* **74,** 1476–1484 (2007).
180. Mottino, A.-D. & Catania, V.-A. Hepatic drug transporters and nuclear receptors: regulation by therapeutic agents. *World J Gastroenterol* **14,** 7068–7074 (2008).
181. Ratra, G. S., Cottrell, S. & Powell, C. J. Effects of induction and inhibition of cytochromes P450 on the hepatotoxicity of methapyrilene. *Toxicol. Sci.* **46,** 185–96 (1998).
182. Laine, J. E., Auriola, S., Pasanen, M. & Juvonen, R. O. Acetaminophen bioactivation by human cytochrome P450 enzymes and animal microsomes. *Xenobiotica.* **39,** 11–21 (2009).
183. Rodríguez, A. J. *et al.* A fiber optic ammonia sensor using a universal pH indicator. *Sensors (Basel).* **14,** 4060–4073 (2014).
184. Stanger, B. Z. & Hebrok, M. Control of cell identity in pancreas development and regeneration. *Gastroenterology* **144,** 1170–1179 (2013).
185. Dabeva, M. D., Hurston, E., Shafritz, D. A. & Bessin, M. Transcription Factor and Liver-Specific mRNA Expression in Facultative Epithelial Porgenitor Cells of Liver and Pancreas. *Am. J. Pathol.* **147,** 1633–1648 (1995).
186. Rao, M. S., Yukawa, M., Omori, M., Thorgeirsson, S. S. & Reddy, J. K. Expression of transcription factors and stem cell factor precedes hepatocyte differentiation in rat pancreas. *Gene Expr.* **6,** 15–22 (1996).
187. Huang, P. *et al.* Induction of functional hepatocyte-like cells from mouse fibroblasts by defined factors. *Nature* **475,** 386–389 (2011).
188. Gerlach, J. C. *et al.* Interwoven four-compartment capillary membrane technology for three-dimensional perfusion with decentralized mass exchange to scale up embryonic stem cell culture. *Cells Tissues Organs* **192,** 39–49 (2010).

List of Publications

Knöspel, F., Jacobs, F., Freyer, N., Damm, G., De Bondt, A., Van Den Wyngaert, I., Snoeys, J., Monshouwer, M., **Richter, M.**, Strahl, N., Seehofer, D., Zeilinger, K. *In vitro* model for hepatotoxicity studies based on primary human hepatocyte cultivation in a perfused 3D bioreactor system. Int. J. Mol. Sci. 2016, 17 (**4**), pii:E584, DOI: 10.3390/ijms17040584; http://www.mdpi.com/1422-0067/17/4/584.

Richter, M., Fairhall, E.A., Hoffmann, S.A., Tröbs, S., Knöspel, F., Probert, P.M.E., Oakley, F., Stroux, A., Wright, M.C., Zeilinger, K. Pancreatic progenitor-derived hepatocytes are viable and functional in a 3D high density bioreactor culture system. Toxicol. Res. 2016, 5 (**1**), 278-290, DOI: 10.1039/C5TX00187K; http://pubs.rsc.org/en/Content/ArticleLanding/2016/TX/C5TX00187K#!divAbstract.

Fairhall, E.A., Charles, M.A., Wallace, K., Schwab, C.J., Harrison, C.J., **Richter, M.**, Hoffmann, S.A., Charlton, K.A., Zeilinger, K., Wright, M.C. The B-13 hepatocyte progenitor cell resists pluripotency induction and differentiation to non-hepatocyte cells. Toxicol. Res. 2013, 2(**5**), 308-320, DOI: 10.1039/C3TX50030F; http://pubs.rsc.org/en/content/articlelanding/2013/tx/c3tx50030f#!divAbstract.

Miller, L., **Richter, M.**, Hapke, C., Nitsche, A. Genomic expression libraries for the identification of cross-reactive orthopoxvirus antigens. PLoS One 2011, 6(**7**), e21950, DOI:10.1371/journal.pone.0021950;
http://journals.plos.org/plosone/article?id=10.1371/journal.pone.0021950.

Conference and workshop participation

Richter, M., Tröbs, S., Cosnier, M-L., Schuck, H., Freyer, N., Schubert, F., Wright, M.C., Zeilinger, K. Integration of multi-parametric sensor systems in bioartificial liver support system. 41st Annual Congress of the European Society for Artificial Organs (ESAO), September 17-20 2014, Rom, Italy (Oral presentation).

Richter, M., Fairhall E.A., Hoffmann, S.A., Schubert, F., Wright, M.C., Zeilinger, K. Hepatic trans-differentiation of pancreatic hepatocyte-progenitor cells (B-13) in a 3D high-density culture system. German Association for the study of the Liver (GASL), January 24-25 2014, Tübingen, Germany (Oral presentation).

Richter, M., Fairhall, E.A., Hoffmann, S.A., Frühwald, J., Wright, M.C., Zeilinger, K. Dexamethasone induced hepatic differentiation of rat pancreatic progenitor cells (B-13) in a 3D multi-compartment bioreactor system. European Association for the study of the liver (EASL), April 24-28 2013, Amsterdam, Netherland (Poster).

Richter, M., Ertel, C., Hoffmann, S.A., Lübberstedt, M., Müller-Vieira, U., Biemel, K., Schulz, A., Damm, G., Nüssler, A.K., Zeilinger, K. Bioreactor system suitable for *in vitro* studies on hepatic metabolism and cell re-organization. German Conference on Bioinformatics; Satellite Workshop Organ-oriented System Biology, September 19. 2012, Jena, Germany (Oral presentation).

Richter, M., Hoffmann, S.A., Ertel, C., Müller-Vieira, U., Biemel, K., Damm, G., Nüssler, A.K., Zeilinger, K. Characterization of the time course of re-organization of primary human liver cells in a miniaturized 3D bioractor system. Conference on Systems Biology of Mammalian Cells (SBMC), July 9-11 2012, Leipzig, Germany (Poster).